2009

Dosimetric evaluation of a delivery verification and dose reconstruction method for helical tomotherapy

Ricky Hesston
Louisiana State University and Agricultural and Mechanical College

DOSIMETRIC EVALUATION OF A DELIVERY VERIFICATION AND DOSE RECONSTRUCTION METHOD FOR HELICAL TOMOTHERAPY

A Thesis

Submitted to the Graduate Faculty of the
Louisiana State University and
Agricultural and Mechanical College
in partial fulfillment of the
requirements for the Degree of
Master of Science

in

The Department of Physics and Astronomy

by
Ricky Hesston
B.S., Indiana University, 1999
May 2009

ACKNOWLEDGEMENTS

I would like to thank the following members of on my advisory committee: Dr. John Gibbons, my advisor and mentor, for his guidance and knowledge in relation to my thesis topic; Dr. Kenneth Hogstrom for giving me the opportunity to continue my education and providing different perspective and views on the thesis; Dr. Kenneth Matthews for educating me on the topic of imaging, providing assistant throughout my graduate study and especially for the exciting and fun-filled house parties; Dr. Sheldon Johnson for his professional perspective in the clinical aspect of the project and Dr. Phillip Sprunger for his non-bias opinions and suggestions throughout the process.

I would like to thank Mary Bird Perkins Cancer Center for allowing the use of their equipments, the support from their staffs and luxurious student offices. This work is made possible by the support of TomoTherapy Inc. and their research and development team. I would especially like to thank Tim Chapman, Quan Chen, Ken Ruchala and Gustavo Olivera for their involvement in responding to my feedbacks and providing updates to the software used in this study.

I dedicate this work to my family and friends for their love and support throughout my graduate study.

TABLE OF CONTENTS

LIST OF TABLES

LIST OF FIGURES

ABSTRACT

Purpose: To determine the dosimetric accuracy of a dose reconstruction method used for verification of helical tomotherapy delivery for three different clinical sites.

Methods and Materials: A delivery verification and dose reconstruction method has been applied to helical tomotherapy treatment plans of three different treatment sites (head & neck, prostate and lung). Treatment plans were generated on a cylindrical measurement phantom (TomoPhantom) using contours, prescriptions and planning objectives taken from clinical patient plans of the three sites. Film and ion chamber measurements were made for each plan with and without intentional changes in the machine output [-4% to 4%] or leaf open times [-30 ms to +30 ms] to the planned delivery.

A TomoTherapy delivery verification tool uses pulse-by-pulse machine CT detector and transmission ion chamber data, extracted at the conclusion of each delivery, to determine the incident energy fluence delivered for each projection. Dose reconstruction was calculated by simulating the delivered energy fluence onto the planning CT. The reconstructed doses were compared with both the measured and planned dose distributions.

Results: Measured dose variations for repeated daily deliveries were small, typically within 2%. Greatest differences between the measured dose and planned dose occurred when intentional changes in leaf open times (±30 ms) were made to the delivery. Measured doses from all deliveries were well predicted by the dose reconstruction method, which demonstrated agreement for point doses to within 2%. The dose reconstruction method also demonstrated acceptable agreement with the film dose measurements for all three plans. Comparison of film versus reconstructed dose for all cases showed that over 90% of a selected region of interest had a gamma index of less than 1.

Conclusion: The method of dose reconstruction based on machine detector data can account for daily variations in the delivered dose due to machine error. Dosimetric accuracy for the method is acceptable within clinical standards.

CHAPTER 1. INTRODUCTION

1.1 Background and Significance

1.1.1 Goals and Advances in Radiation Therapy

The goal of radiation therapy is to deliver as much dose as necessary to destroy cancerous cells while minimizing or limiting the dose to normal healthy tissues. It begins at the treatment planning stage where planning target volume (PTV) and organs at risk (OARs) are defined[1, 2] on a treatment planning CT image dataset of a patient taken while in treatment position. The PTV covers the gross tumor volume (GTV) with additional margin to account for microscopic cancer, effects of organ and patient movements, radiation beam inaccuracy and set-up uncertainty (Figure 1). OARs are normal healthy tissues near the PTV that have set tolerances for radiation dose and are the limiting factors during treatment planning. Dose objectives for PTVs and OARs are influenced by the overall treatment objective (curative or palliative). Once PTV and OARs have been determined, the next step is to determine which modality of treatment is best suited to achieve the goal of a favorable outcome for the patient. This includes the method of treatment (brachytherapy, external beam, intra-operative, etc.), the type of radiation (photons, electrons, protons, etc.) and energy selection.

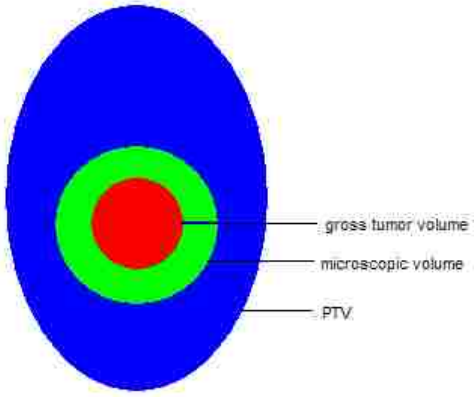

Figure 1. Illustration of PTV (blue) coverage that includes the GTV (red), microscopic extension (green) and setup error

One of the latest advances in radiation delivery is intensity modulated radiation therapy (IMRT). IMRT is a treatment delivery method that uses optimized non-uniform or modulated beam intensities to deliver a highly conformal dose distribution within a patient.[3, 4] The benefit of this method is the ability to escalate dose to cancerous cells while decreasing the maximum dose to the surrounding normal tissues. The result is higher tumor control probabilities and/or lower normal tissue complication probabilities. However, these advantages assume that the patient's anatomy is in the same position at the time of treatment as they were during the treatment planning CT. If the tumor were to shift or change size or shape from the planned image during treatment delivery, it may not receive the planned radiation dose coverage. Furthermore, a normal tissue adjacent to the tumor could receive too much dose.

The different ways to deliver an IMRT treatment may be divided into gantry static (i.e., multiple field originating from different fixed positions) and gantry dynamic delivery techniques. Gantry static techniques typically achieve beam modulation through the use of multi-leaf collimator (MLC), although compensator filters or beam scanning are sometimes used. MLC leaf positions are adjusted during the treatment to define field shapes or segments. Gantry static MLC techniques may be further divided into segmental (SMLC), where no radiation is delivered during leaf movement or dynamic (DMLC), where radiation is delivered during leaf movement. Gantry dynamic techniques include intensity modulated arc therapy (IMAT) and serial and helical tomotherapy. Tomotherapy delivery systems use a binary MLC where the leaf positions are either open or closed at any point in time during the treatment.

The importance that IMRT places on the reproducibility of patient's position has motivated developments in image-guided radiation therapy (IGRT). The basis of IGRT is to take an image of the patient immediately prior to or during the treatment to verify and adjust (if

necessary) the patient's position so that he/she is in the same position as the time the planning image was taken. Obtaining the image in the treatment room can be done by using ultrasound[5], planar x-rays[6], kilovoltage CT (kVCT)[7, 8] or a megavoltage CT (MVCT)[9].

1.2 TomoTherapy

1.2.1 Introduction to the Hi·Art Delivery System

The TomoTherapy Hi·Art delivery system is one of the latest advancement in radiotherapy that is capable of both a helical IMRT delivery and a MVCT IGRT imaging system within the same unit (Figure 2).[10] The radiation source used for both treatment and imaging is a linear accelerator (linac) with nominal photon beam energies of 6 MV and 3.5 MV, respectively. The linac rotates on a slip-ring gantry about a fixed axis located 85 cm from the source. The field width in the longitudinal direction is defined by a pair of collimating jaws that have an adjustable range of 0.6-5.0 cm at the axis of rotation. The field length in the lateral direction is defined by a 64-leaf binary MLC. Each leaf of the MLC has a projected width of 6.25 mm at 85 cm from the source which allow for a field length ranging from 0-40 cm, depending on the number of open leaves.

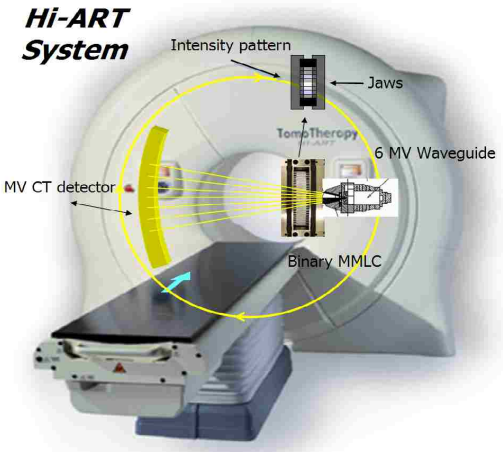

Figure 2. TomoTherapy Hi·ART delivery system

The imaging detectors for TomoTherapy consist of 738 gas-filled xenon ion chambers aligned in an arc located on the opposite side of the gantry from the radiation source (Figure 2). Due to the maximum field length, the MVCT image is limited to a 40 cm field of view (FOV) instead of the standard 50 cm FOV in a conventional CT. Of the 738 detector channels, only the

central 640 records exit beam data. The radiation emitted through each open leaf will expose approximately 7 exit detectors. Detector data are recorded at a rate of 300 pulses per second.

Helical treatment is delivered by moving the couch through the rotating gantry at a constant speed. The distance the couch moves per gantry rotation is equal to the selected field width times a user-selected pitch. In the treatment planning process, each rotation is divided into 51 projections, or beams incident from fixed, equally-spaced (approximately every 7°) gantry angles. In a typical treatment plan, there may be up to several thousand projections, depending on the length of the PTV(s) and the selected pitch. IMRT delivery is achieved by optimizing the time each of the 64 leaves remains open per projection in the treatment planning process.

1.2.2 Delivery Subsystem

During treatment, the delivery subsystem software components assist in reading, translating, and transferring data. One component in particular, the Data Acquisition System (DAS), translate photon counts from the transmission monitor chambers (located between the beam source and collimating jaws) and exit detectors into raw detector data. TomoTherapy stores this data defining the machine state over time in the form of sinograms. A number of different sinograms are used within the planning and delivery systems, of which a few are defined here:[11]

- Leaf control sinogram: The planned leaf open time versus projection number per delivery. It has a matrix of 64 by the number of projections (N_{proj}) for the treatment plan. The values within this sinogram are fractions of leaf open time per projection.
- Treatment detector sinogram: The number of counts per pulse (300 pulses/sec) for the centrally located 640 detectors (out of the 738) and the 3 monitor chambers. This

sinogram is a matrix of 643 (first 640 are exit CT detector data, last 3 are output data) × (300 pulses/sec × delivery time [sec]).

- Delivery Verification (DV) sinogram: The computed effective leaf open time versus projection number of a delivered treatment based on the treatment detector sinogram.

The matrix size and value range for each cell are the same as the leaf control sinogram. It is important to note that there is a leaf control sinogram file for each scheduled fraction within a plan. Therefore, a plan that has 38 fractions will have 38 leaf control sinogram files.

1.2.3 Image-guided Radiation Therapy (IGRT)

IGRT on TomoTherapy is achieved by initially taking an MVCT scan of the patient in treatment position prior to a treatment delivery. The MVCT image is overlaid with the planned image to allow for manual or auto registration. If a shift is needed to align patient into the planned position, the TomoTherapy Hi·Art system can automatically shift the couch laterally, longitudinally and vertically. Tilt misalignment in the sagittal plane cannot be corrected by the system. However, tilt misalignment in the axial plane can be corrected for by offsetting the delivery angle accordingly.

As mentioned in section 1.2.2, during treatment delivery, the DAS records exit detector data from the same detectors used for imaging. This data can be used to detect errors in treatment delivery based on leaf opening time[12] and output.[13]

1.3 Delivery Verification and Dose Reconstruction

1.3.1 Deviations Associated with Treatment Delivery

Although IGRT can be beneficial in properly positioning the patient, it does not correct for changes in the patient anatomy throughout treatment. Changes to patient anatomy can affect the delivered dose in two ways. First, the radiation transmission through the patient will be

altered if the patient changes shape over the course of treatment. This effect may be due to the patient gaining or losing weight or through tumor shrinkage during the course of treatment. Second, the radiation dose to the PTV and/or OAR structures may change if they are deformed relative to their shape at the time of treatment planning.

In addition to changes in patient anatomy, deviations from the planned incident radiation fluence will also affect the administered dose. Minor deviations (i.e., within machine tolerance) in machine output will change the delivered dose to the patient. Although IGRT may be used to determine patient anatomical changes, it does not account for deviations from the planned delivery associated with the machine.

If daily changes to the delivered dose can be accounted for, the patient's plan can be modified during the course of treatment. The process is commonly known as "adaptive radiotherapy" within the field of practice.[14]

1.3.2 Methods to Account for Deviated Treatment Delivery

Within the TomoTherapy Hi-Art system, a number of methods to correct for changes in delivered dose have been proposed and/or implemented. In TomoTherapy Planned Adaptive (PA™) program, the effect of changes to patient anatomy is accounted for by re-computing the radiation dose on the daily MVCT taken prior to treatment. This process has been described by Langen et al.[15] Because the MVCT image dataset is smaller (e.g., 40 cm field of view) than the planning kVCT image dataset (e.g., typically 50 cm), a composite or merged image dataset of the MVCT and the kVCT is created for the dose recomputation. For the merged image, the kVCT covers all the image area where the MVCT did not cover relative to the planning image.

Since an MVCT image will be used for dose computation, it is imperative that the image value-to-density table (IVDT) applied to the MVCT image corresponds to a similar density as

the planning kVCT image for the same structure. The determination and constancy of IVDTs for the Hi-Art system has been discussed by Langen et al.[15]

Although the dose may be recomputed on the daily MVCT image, the clinical impact of these variations is difficult to quantify unless contour changes in the PTV(s) and OAR(s) have been accounted. The process of registering a daily treatment image to the planning CT that account for internal anatomical changes is known as deformable registration.[16] Once the new PTV and OAR have been registered, the cumulative dose to the structures can be recomputed by applying the planned delivery parameters (machine parameters such as output dose rate, leaf open sequence, gantry & couch speed and beam field size) onto the registered image. This dose can then be compared to the planned dose to determine whether a new plan is necessary to compensate for dose differences in the PTV and OAR. Lu et al.[16] discussed the use of deformable registration for TomoTherapy Hi-Art planning systems.

To account for delivery deviations during treatment, it is necessary to include changes in machine parameters which affect the delivered dose. This process is sometimes referred to as delivery verification (DV).[11] Kapatoes et al described a technique where the incident energy fluence ($\boldsymbol{\Psi}$) can be determined by multiplying the treatment exit-detector signal ($\boldsymbol{s}$) by the inverse of a measured transfer matrix ($\boldsymbol{D}$).

$$\boldsymbol{\Psi} = \boldsymbol{D}^{-1} \cdot \boldsymbol{s} \qquad (1)$$

With the incident energy fluence from Eq. (1) and an IGRT image, dose may be calculated with actual, rather than planned, delivery parameters. The incorporation of actual (verified) delivery parameters into the dose calculation on the daily IGRT image is known as dose reconstruction (DR)[17]. Implementing DV and DR into adaptive planning should improve the evaluation of treatment delivery for patients undergoing IMRT which could lead to improved clinical outcome.

1.4 Delivery Verification for TomoTherapy

1.4.1 General Concerns

Unlike conventional linear accelerator, TomoTherapy does not deliver a plan according to the planned monitor units (MUs) which is related to radiation dose. Instead, the delivery is governed by treatment time that assumes a constant beam output, similar to that of traditional Co-60 therapy unit (uses an isotope as source of radiation). For the Hi·Art system, the delivered dose can deviate from the planned dose since TomoTherapy's beam output are allowed to vary throughout a treatment delivery by up to 5% over a 5 second interval without interlocking the machine.[18] An illustration of this output variation as seen from a sample patient treatment delivery is shown in Figure 3, which displays the normalized signals obtained from the three transmission monitor chambers versus projection number. Notice that the variation is cyclical with rotation (51 projections per rotation) and also show a long term drift.

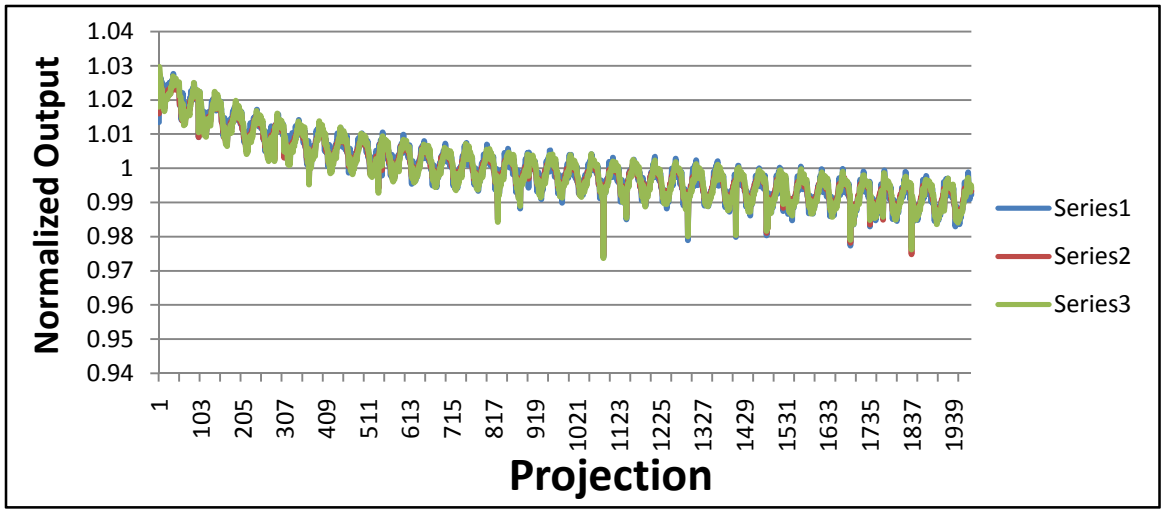

Figure 3. Normalized output reading from the three transmission monitor chamber during a typical patient treatment delivery on TomoTherapy

Output deviation may also be due to differences between the planned and actual leaf open times that are a result of mechanical issues of the 64 leaves and/or their controlling components.

In the Hi-Art system, the machine delivery tolerance is set to stop treatment if there are four instances where an individual leaf's open time is different by more than 32 ms from the planned leaf opening time. Differences less than this value may affect the delivered dose without interlocking the machine.

TomoTherapy stores transmission monitor chambers and exit detector data for each individual treatment delivery in the form of a treatment detector sinogram (defined previously). The number of counts per pulse recorded by each exit detector is dependent on whether the leaves are opened or closed, the beam's radiological path length through all structures (e.g., patient, couch, etc.) between the source and the exit detector, and the beam output. Determination of the energy fluence as a function of off-axis position is possible but requires knowledge of the patient position and the transmission characteristics of the beam through the patient.[17] However, if we assume that the beam's profile remains constant during delivery, then changes in the energy fluence rate through each leaf would be proportional to the signal of the transmission monitor chambers. For each projection, the total energy fluence that is emitted through each leaf would then be proportional to the amount of time each leaf remains open.

1.4.2 TomoTherapy DVPA software program

TomoTherapy has developed a delivery verification planned adaptive (DVPA^{TM}) program that can reconstruct the dose based on the DV sinogram and MVCT image data. The algorithm used for dose calculation in DVPA is the same as that used within the TomoTherapy treatment planning system (TPS) and assumes a constant beam output for dose calculation. To account for beam output variations during delivery in the reconstructed dose calculation, DVPA adjusts each measured leaf open time per projection by the percentage of the difference between

measured beam output and planned beam output over the period of that projection. The adjusted leaf open time is defined as the effective leaf open time.

The energy fluence emitted though an open MLC leaf irradiates approximately 7 exit detectors. Leaf open time per projection for each leaf is determined in DVPA by taking the average full width-half max (FWHM) of the 5 central detectors' (of the 7) signal profile (Figure 4). Thus, the delivered energy fluence can be determine by scaling the beam's intensity up or down based on the measured output data and use the rise and fall times of the exit detector signals to determine the leaf open times.[12]

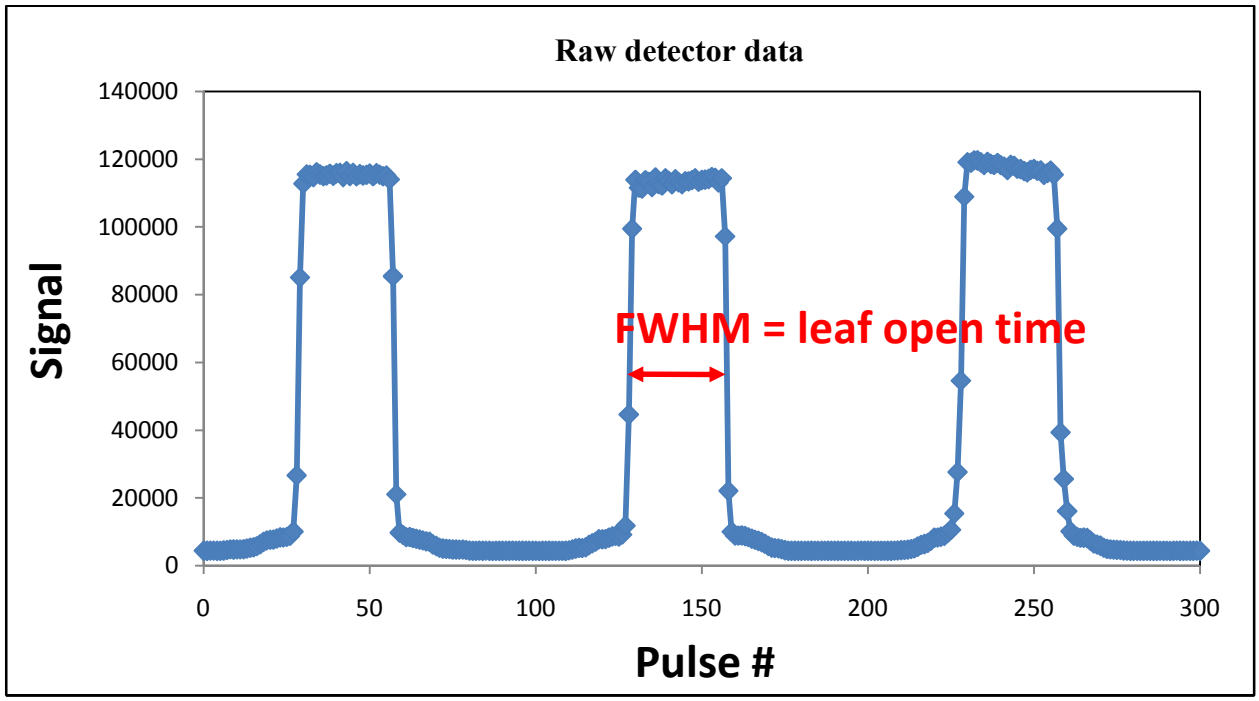

Figure 4. Signal reading from one exit detector over 300 pulses

Once DVPA determines the effective leaf open time for all projections of a delivery, it creates the DV sinogram. The energy fluence throughout the delivery is derived from the DV sinogram and the planned beam output. A reconstructed dose is then computed by applying the energy fluence onto the MVCT image taken for the delivered plan. Figure 5 illustrates the path that begins with the acquired exit detector data and ends with the reconstructed dose.

For this study, we will apply DV and DR method for helical tomotherapy delivery to 3 simulated patient plans (head & neck, prostate and lung) applied to a single phantom image dataset. Each plan will be delivered with and without intentionally-introduced offsets (within machine delivery interlocks limit). Comparison between the reconstructed and measured dose will determine how well the method can account for typical variations of machine performance.

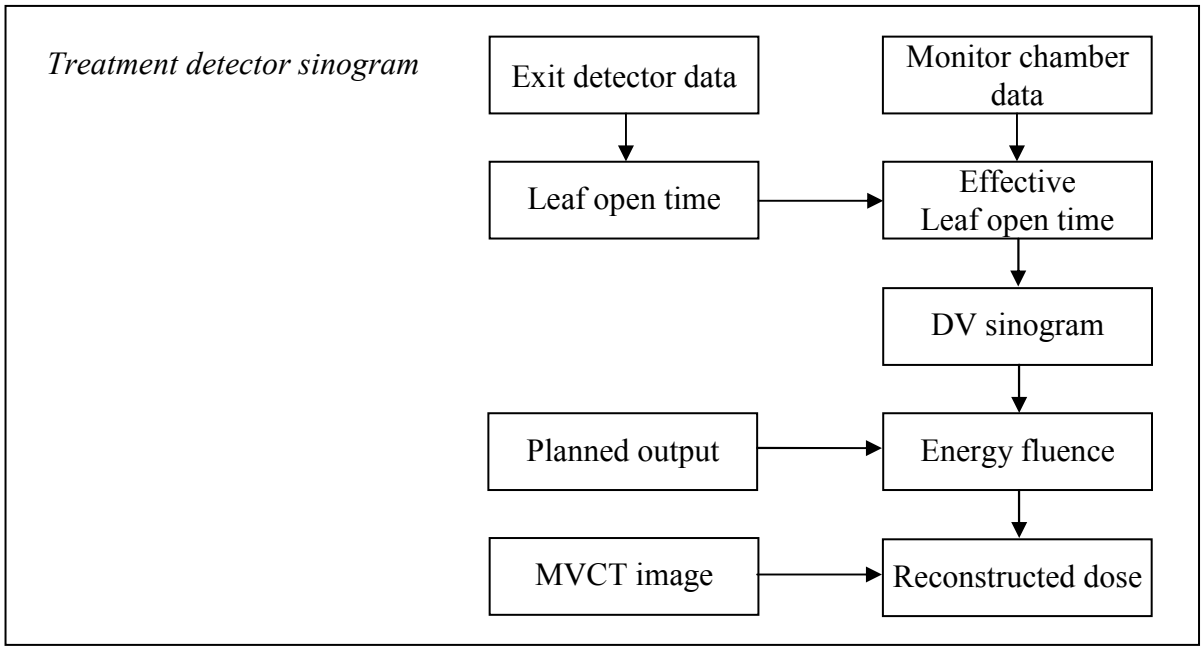

Figure 5. Block diagram of DV and DR for TomoTherapy

1.5 Hypothesis and Specific Aims

1.5.1 Hypothesis

Comparison of measured and reconstructed doses (based on TomoTherapy DVPA software) for head and neck, prostate and lung plans delivered to the TomoPhantom with and without intentional delivery errors will demonstrate:

(a) agreement within 2% for a point in a high dose, low gradient region

(b) a gamma index < 1 for 90% of the points within a selected two dimensional region

1.5.2 Specific Aims

1. Create three different TomoTherapy treatment plans on the TomoPhantom. Generate plans using PTV and OAR contours extracted from clinical treatment plans for a head & neck (H&N), prostate and lung, and placed on the TomoPhantom. Optimize plans using standard clinical protocols.
2. Deliver, measure and extract the exit detector data for each plan
   a. multiple times on different days (to account for statistical fluctuation)
   b. with intentional adjustment to machine's output
   c. with intentional leaf opening time error (to determine the significance of leaf opening time error within the set tolerance of the delivery system)
3. Compute the reconstructed dose on DVPA software using the treatment detector sinogram.
4. Compare the measured dose with the original planned dose and the reconstructed dose calculated. Compare both point dose (ion chamber) and relative dose (film) results.

CHAPTER 2. METHODS AND MATERIALS

2.1 Aim 1: Generate Treatment Plans

2.1.1 TomoTherapy TomoPhantom

Plans for this study were generated on the TomoTherapy-provided cylindrical measurement phantom, or TomoPhantom™ (TomoTherapy Inc.) (Figure 6). The two halves of the TomoPhantom combine to create a cylinder with dimensions of 30 cm in diameter and 18 cm in length. The material of the homogeneous phantom consists of Virtual Water™ with a density of 1.024 gram per cm^3.[19] Along one diameter on the side of the phantom, there are 28 6.3-mm diameter cylindrical slots aligned parallel to the cylinder axis and separated by 1 cm from their centers to allow for point dose measurements using ionization chambers (Figure 7). There are virtual water plugs for the slots that don't have a detector. Relative dose distribution measurements may be achieved by placing a radiographic film between the 2 halves of the phantom.

Figure 6. Photo of the TomoPhantom with the two halves apart

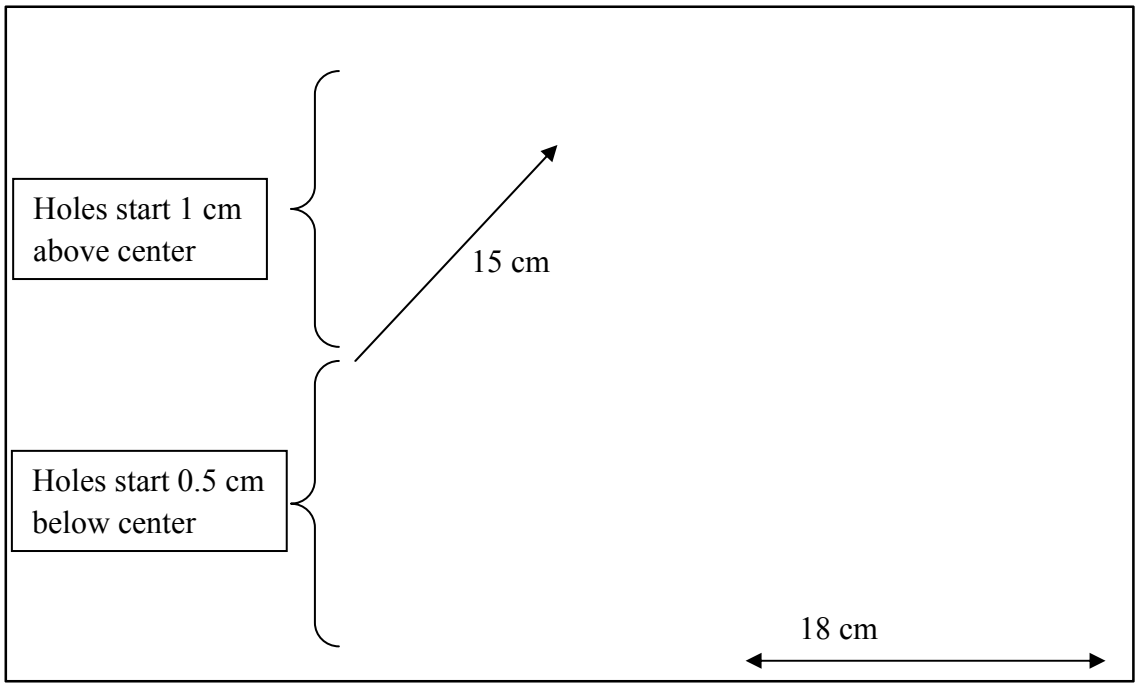

Figure 7. Axial and sagittal (central cut) view of the TomoPhantom

2.1.2 Scanning and Transferring the Image of the TomoPhantom

The TomoPhantom was scanned on the GE Lightspeed RT CT scanner available at Mary Bird Perkins Cancer Center. Orientation of the phantom was set such that the circular volume is in the axial plane with the cylindrical slots lined up vertically during scan. The scanning parameters were set as the following:

- Helical scan
- 50 cm diameter field of view
- 512×512 axial pixel resolution
- 2.5 mm longitudinal spacing
- 83 slices = 20.75 cm
- 120 kVp beam energy

After obtaining an image dataset of the TomoPhantom, the same image dataset was sent to the TomoTherapy Research TPS three separate times to create three different treatment plans. Each time, the name of the image dataset was changed to create and identify the three different plans ("DV STUDY – H/N", "DV STUDY – PROSTATE" and "DV STUDY – LUNG").

The image dataset was also sent once to Pinnacle[3] TPS for the purpose of creating a structure set for each plan. Since the phantom is not anthropomorphic, a virtual structure set for each plan was obtained by copying a patient's structure set with disease sites corresponding to those studied here. Figures 8 and 9 illustrate the copying of contours from a patient plan to the TomoPhantom for the lung case. Figure 8 shows axial, coronal and sagittal slices through a patient's CT dataset. The target volume and critical structures have been contoured and are displayed by colored lines on the CT images. The structure sets was copied to the phantom image dataset as seen in Figure 9.

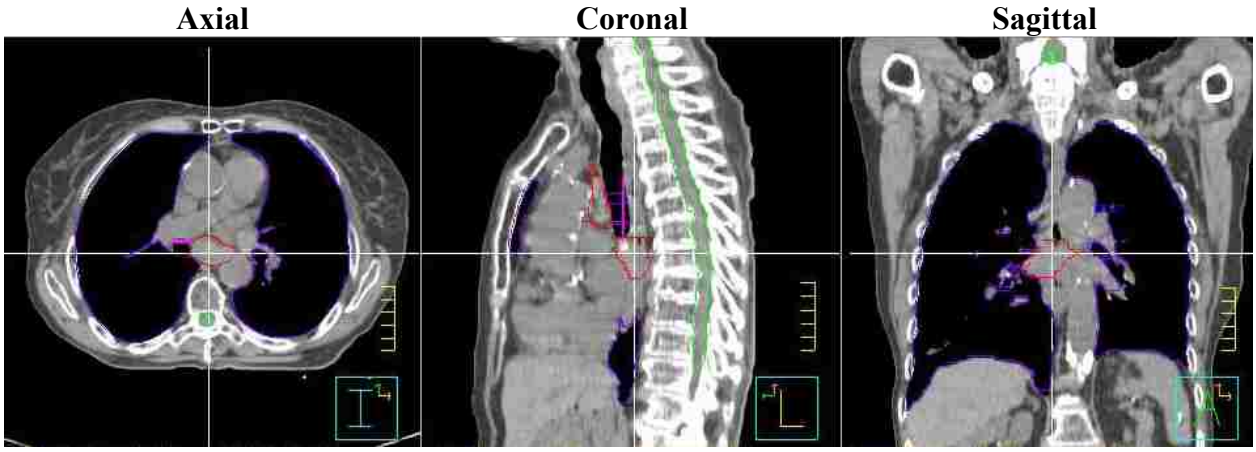

Figure 8. Contours of lung patient with target volume in red

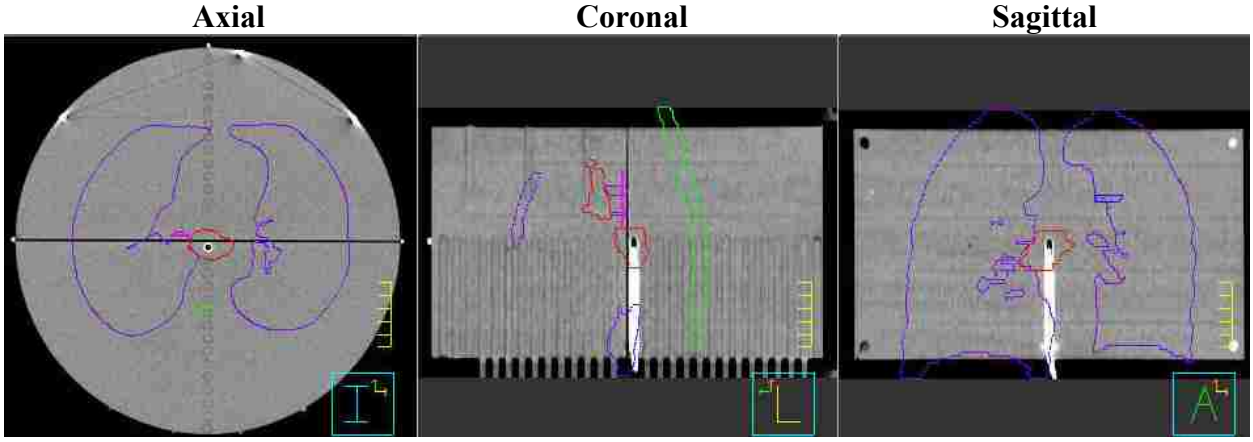

Figure 9. Contours of lung patient copied onto the TomoPhantom

2.1.3 Treatment Planning

Copying of the contours for each plan in Pinnacle^3 TPS required adding a patient image dataset corresponding to the disease site into the plan's list of images. The patient's image dataset was set as the secondary image while the TomoPhantom image dataset was set as the primary image. Importing of the patient's structure set was done separately within each plan and was assigned to the patient's image dataset initially. The patient's image dataset (with the structure set) was then fused with the TomoPhantom image dataset. This allowed displaying and shifting of the structure set position relative to the TomoPhantom. The structure set was shifted such that the center of the target volume covered the active measurement volume of the ionization chamber (see Figure 9). The structure set was then assigned to the TomoPhantom's image dataset and exported to the TomoTherapy Research TPS.

Image data that were imported into TomoTherapy Research TPS were down-sampled to 256×256 axial pixel resolution. Planning parameters (jaw size setting, pitch, prescription dose on PTVs and dose tolerances for OARs) for each plan used standard clinical protocols in use at MBPCC and are shown in Table 1. Treatment delivery was set to 2 Gy per fraction to simulate patient treatment. Figure 10 shows an overview for the generation of the plans.

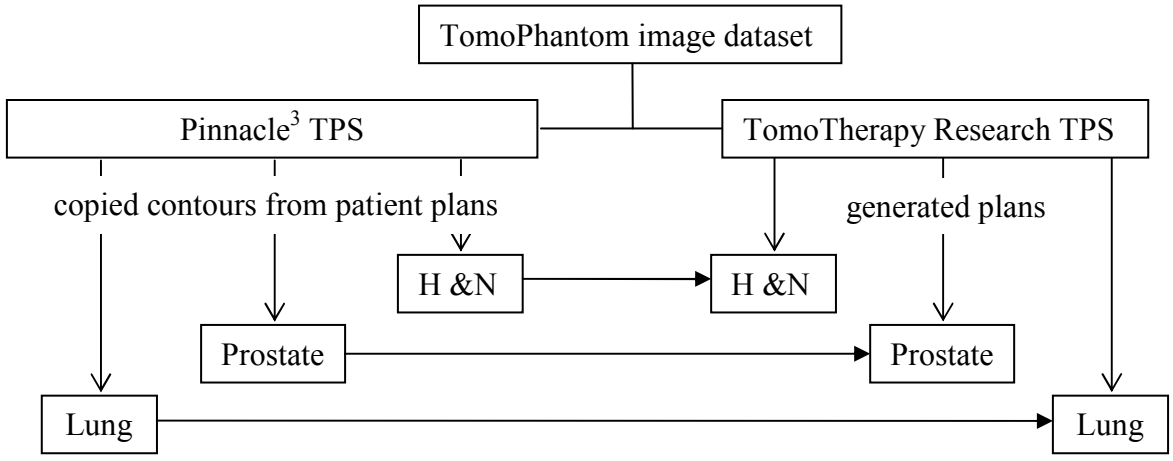

Figure 10. Block diagram showing how the treatment plans were created.

Table 1. Planning parameters and dose tolerance [dose @ % volume] for critical structures

		DV STUDY H&N	DV STUDY PROTSTATE	DV STUDY LUNG
	Prescription @ 95% volume of PTV	72 Gy	76 Gy	58 Gy
	Jaw Width	2.54 cm	2.54 cm	2.54 cm
	Pitch	0.287	0.287	0.287
	Dose Grid	Fine	Fine	Fine
	Optimization Mode	Beamlet	Beamlet	Beamlet
	Modulation Factor	4	4	3
Dose Tolerance	Spinal Cord	39 Gy @ 100%		2 Gy @ 50% (max 52 Gy)
	Lung			5 Gy @ 50% (max 60 Gy)
	Lt Femur		45 Gy @ 1% (max 45 Gy)	
	Rt Femur		45 Gy @ 1% (max 45 Gy)	
	Bladder		40 Gy @ 50% (max 76 Gy)	
	Rectum/Anus		40 Gy @ 35% (max 76 Gy)	
	Brain	54 Gy @ 100%		
	Lt parotid	26 Gy @ 50% (max 60 Gy)		

Plans were optimized using beamlet mode with a modulation factor of 3.0 and 4.0 (see Table 1). Settings for the importance of PTV were initially set 3 times more than the avoidance structures. Penalties for all structures were initially set to 1. The procedure used for adjusting penalties during optimization followed the standard recommended procedure from TomoTherapy. Changes in penalties were made after every 12 iterations and to only those structures that did not yet meet the plan objectives as outline in Table 1. The total number of iterations for each plan had approximately 120 iterations. Although the plan quality was not of interest for this study, the final plans were made to resemble typical clinical plans. Each plan was then archived and transferred onto the delivery system data server for delivery.

2.2 Aim 2: Delivery of Treatment Plans

2.2.1 Measurement Setup

Prior to the delivery of each plan, an MVCT scan was taken of the TomoPhantom to verify and adjust alignment, if necessary. To prevent exposure to the film before the planned delivery, no film was placed in the phantom during scan. Measurements were collected using an ionization chamber (Model A1SL Exradin Miniature Shonka Thimble Chamber), with a collecting volume of 0.057 cm^3, placed in one of the cylindrical slots of the TomoPhantom and an Extended Dose Range 2 (EDR2) radiographic Kodak film placed in between the two halves of the phantom (Figure 11). The electrometer (Keithley Model 614) used to take readings from the ionization chamber had a bias voltage setting of -300V with a maximum leakage rate of 0.01 nC/minute.

The prostate and lung plans were delivered with the phantom orientation as seen in Figure 10a. For the H&N plan, the phantom was rotated 90° counterclockwise (Figure 10b) so that the ionization chamber could be within the plan's PTV.

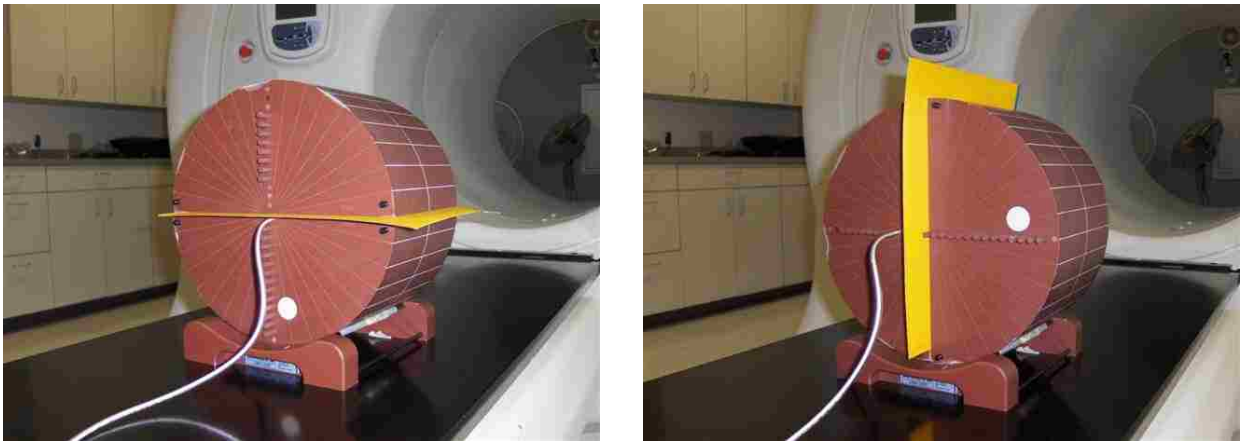

(a) **(b)**

Figure 11. Film measurement in the (a) coronal plane and (b) sagittal plane

2.2.2 Treatment Delivery

Each plan was delivered twice per day and repeated over several days to account for statistical fluctuations. For each delivery, measurements for each plan consisted of two ion chamber readings and one film exposure. The temperature and pressure were recorded at the time of measurements to correct for the ion chamber calibration value (P_{TP}).

Conversion of the ion chamber's electrometer reading (M_{raw}) to measured dose (D_M) followed the AAPM TG-51 protocol[20] given by equation 2.

$$D_M = M_{raw} P_{ion} P_{TP} P_{elec} P_{pol} k_Q N_{D,w}^{60Co} \quad (2)$$

P_{ion}: ion recombination correction

P_{TP}: temperature & pressure correction

P_{elec}: electrometer calibration factor [C/reading]

P_{pol}: chamber polarity effects

k_Q: beam quality conversion factor

$N_{D,w}^{60Co}$: ionization chamber calibration factor [Gy/C]

Values of P_{ion} (1.004) and P_{pol} (1.000) had previously been determined for this chamber following TG-51 protocol. The value of k_Q (0.996) was obtained using the procedure recommended by Thomas et al.[21] The calibration factor for both the ionization chamber ($N_{D,w}^{60Co}$) and the electrometer (P_{elec}) had been obtained within the past 2 years from an Accredited Dosimetry Calibration Laboratory (ADCL).

A calibration film was exposed on each day that measurements were made in order to convert the chemical response due to radiation exposure of the film to the dose deposited. The calibration film consists of 8 rectangular regions that were exposed to a range of radiation exposures (Figure 12a)[22] from a Varian 21EX linear accelerator using the same nominal beam

energy (6 MV) as the TomoTherapy Hi·Art delivery system. The calibration film was placed at 100 cm source-to-axis distance with 10 cm of buildup and 5 cm of backscatter using a Plastic Water phantom® (Computerized Imaging Reference Systems Inc., 2428 Almeda Ave. Suite 316, Norfolk, VA 23513). A typical calibration curve is shown in Figure 12b.

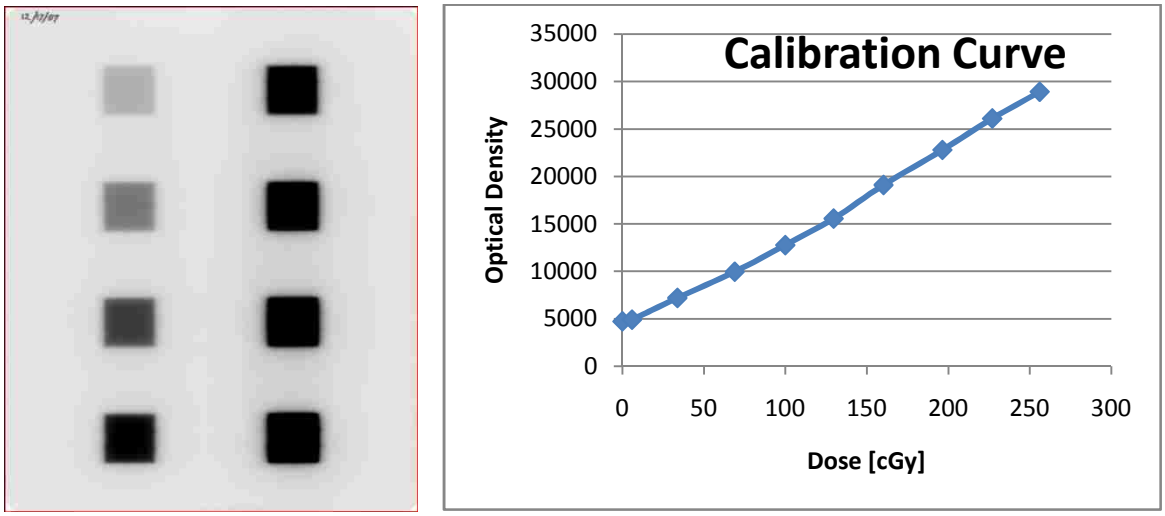

(a) (b)

Figure 12. (a) Scanned image of calibration film after exposure and processing and (b) a typical calibration curve

The average optical density value within a small rectangular region (~3×3 cm) for each of the exposed area was obtained from the scanned image. Dose delivered to the exposed area corresponds to a measured dose that had been made using an ionization chamber placed within the same region under the same setup. All exposed films were processed 24 hours after delivery (due to variations in dose response within 1 hour of exposure)[23] and were scanned using a Vidar DosimetryPro Advantage film digitizer (VIDAR Systems Corporation, 365 Herndon Parkway, Herndon, VA 20170). The films were scanned with a resolution of 71 pixels per inch at 16 bit.

In addition to the standard treatment deliveries, each plan was delivered with the output or leaf open times intentionally adjusted away from their baseline value. Adjustments in output were made by varying the voltage setting of the pulse forming network (pfn) at the treatment

console prior to delivery. Pfn voltage settings were adjusted to vary the output by approximately 0.5 - 4% per delivery in either directions. Output variations of more than 4% will trigger an interlock and stop the delivery.

Adjustments in leaf open times were made by modifying the leaf control sinogram files. A separate leaf control sinogram file is created for every scheduled treatment and is accessible in a patient plan archive. In each patient's archive folder, unique identifiers (UID) are given to most of the filenames in the archive directory (e.g., "1.2.826.01.3680043.2.200.2136569166.-142.83541.763.sin"). All UIDs are indexed within a single plan's extensible markup language (xml) file, which is also located under the archive directory. The xml file for each plan was opened using a text editor program (e.g., Notepad). Within the xml file, the leaf control sinogram files UID were listed next to the tag "sinogramDataFile" associated with each date of planned treatment delivery. These numbers were recorded in order to access the sinogram files for this study.

For each patient plan, twelve leaf control sinogram files were modified. A tracking record was kept that associated the modified file with the scheduled delivery date. The file contained a matrix of N_{proj} by 64 floating point numbers ranging in value from 0 to 1.0, where N_{proj} is the number of projections for the treatment. These data represent the fraction of time the leaves remain open for each projection. The sinogram files were written in binary (little-endian) format and were read and byte swapped using a software program called "Transform" (version 3.4, Fortner Software LLC). The matrix data were then copied onto an Excel spreadsheet to modify the leaf open times.

The time equivalent (Δt) for each matrix value was determined by multiplying the value by the projection period (equation 3). The projection period was determined by dividing the

gantry period (given on the plan printout) by the number of projections per rotation (stated previously as 51).

$$matrix\ value = \frac{\Delta t\ [msec]}{\text{projection period}\ [msec]} = \frac{\Delta t\ [msec]}{\frac{\text{gantry period}\ [msec]}{\#\ \text{of projection/rotation}}} \quad (3)$$

The modified matrix data were byte swapped using in-house software, and then copied back onto the Transform program to save it with the proper file name extension. With the modified leaf control sinogram files placed within the archived directory, the plans were retrieved back into the database of the TPS to allow for plan deliveries on the Hi·Art delivery system.

The TomoTherapy Hi·Art delivery system gives a fault and stops treatment when leaf open time errors of ≥ 32 milliseconds (msec) for 4 instances are detected. Intentional leaf open time errors were introduced which were close to but within these limits, in order to test the limits of the correction software. The leaf open times were adjusted for all the leaves by approximately ±10 and ±30 msec (actual adjustment time is dependent on the value from equation 3). Then only the center leaf (since most tomotherapy treatments position the target at isocenter) or the leaf that contributes the most to the target was adjusted by approximately ±10 and ±30 msec to determine the effect on dose delivery. For modified leaf open time values that are greater than 1.0 or less than 0.0, we set them to 1.0 or 0.0 since values outside the range of 0 and 1 are not deliverable.

2.3 Aim 3: Dose Reconstruction Using Detector Data

Treatment delivery data were immediately extracted after each delivery, since these data were erased whenever a new procedure was loaded for delivery. The detector data contain signal information from the centrally located 640 (out of 738) xenon exit detectors and the three monitor chambers located between the x-ray source and MLC (Figure 13). The data was

acquired for every pulse of the linac, which operates at a frequency of 300 pulses per second in treatment mode.

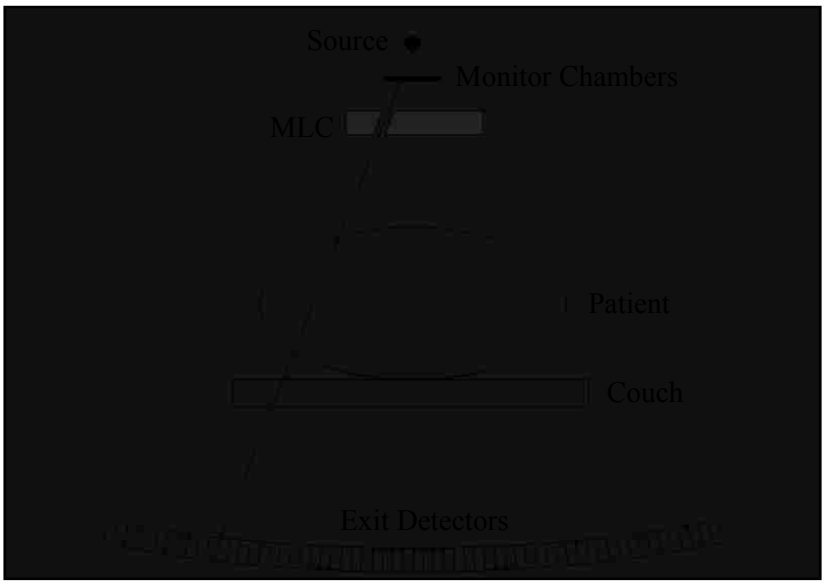

Figure 13. Locations of monitor chambers and exit detectors

The extracted detector data files were transferred to the TomoTherapy Research TPS. These data were read in by the DVPA software to determine the DV sinogram based on variations in machine output and/or leaf open times during treatment delivery. The DVPA software is capable of creating a DV sinogram by considering either factor individually or combined.

As described in section 1.4.2, the DVPA software scales each measured leaf open time by the percent difference between measured and planned beam output over the period of the projection. At the time of the initial beam commissioning, output was adjusted to deliver 900 cGy per minute for a static beam of 40 × 6 cm field size, to a depth of 1.5 cm at the isocenter of the machine. After this adjustment was complete, the average digital signal/pulse of each monitor chamber (MU1) was stored on the DVPA software. The current value for MU1 on the system at Mary Bird Perkins is 16003 counts per pulse. For each leaf, the planned beam output

at any projection is found by multiplying this value by the number of pulses the leaf was opened. The measured output is obtained by summing the counts from MU1 over the same pulses.

If variations in leaf open time relative to the planned treatment are considered in determining the DV sinogram, then the FWHM of the exit detector array signal is used to determine the actual leaf open time. At 300 pulses per second, the time between pulses is approximately 3 msec, which is small compared to typical leaf open times of 200 msec from planned treatment deliveries studied in this work.

Figures 14a, 14b and 15 are screenshots from the DVPA software program which display sample DV sinograms using each factor individually and the combined factors, respectively. The three sinograms represents partial view of the leaf control sinogram for the planned, reconstructed (DV sinogram) and their difference. The horizontal axis is the leaf number and the vertical axis is the projection number. Each cycle in the sinogram represents one rotation of the gantry. Each point in the sinogram matrix represents leaf open time for a specific leaf in unit of second with the brighter colors having longer open times (red being the longest and black meaning closed leaf). The machine output during delivery, determined from the monitor chamber data, is shown as the oscillating purple line.

For all three figures, locations of the crosshair are the same to show how DVPA account variations in machine output and leaf open time separately and their combined contribution to the final DV sinogram. The verification histogram on the right side of Figures 14 and 15 shows the leaf open time differences for fraction of active leaf states. Notice how variations in leaf open time contribute to differences between the planned and reconstructed sinograms more so than machine output variations.

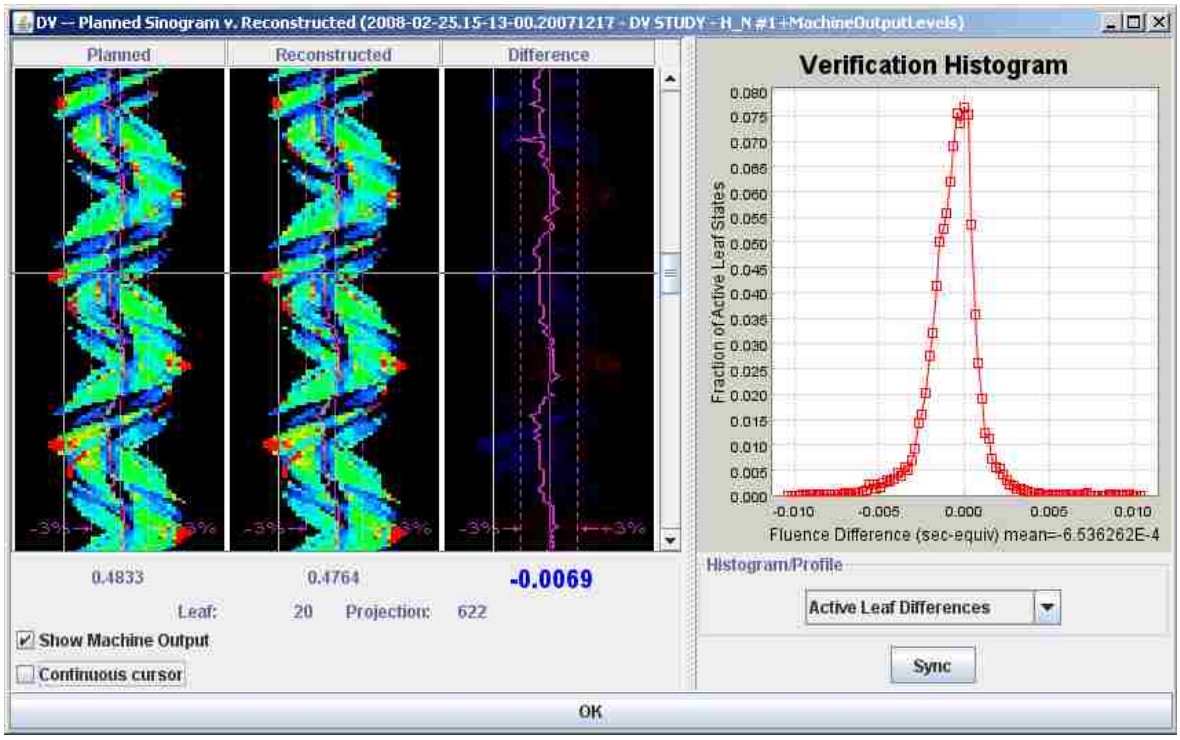

(a)

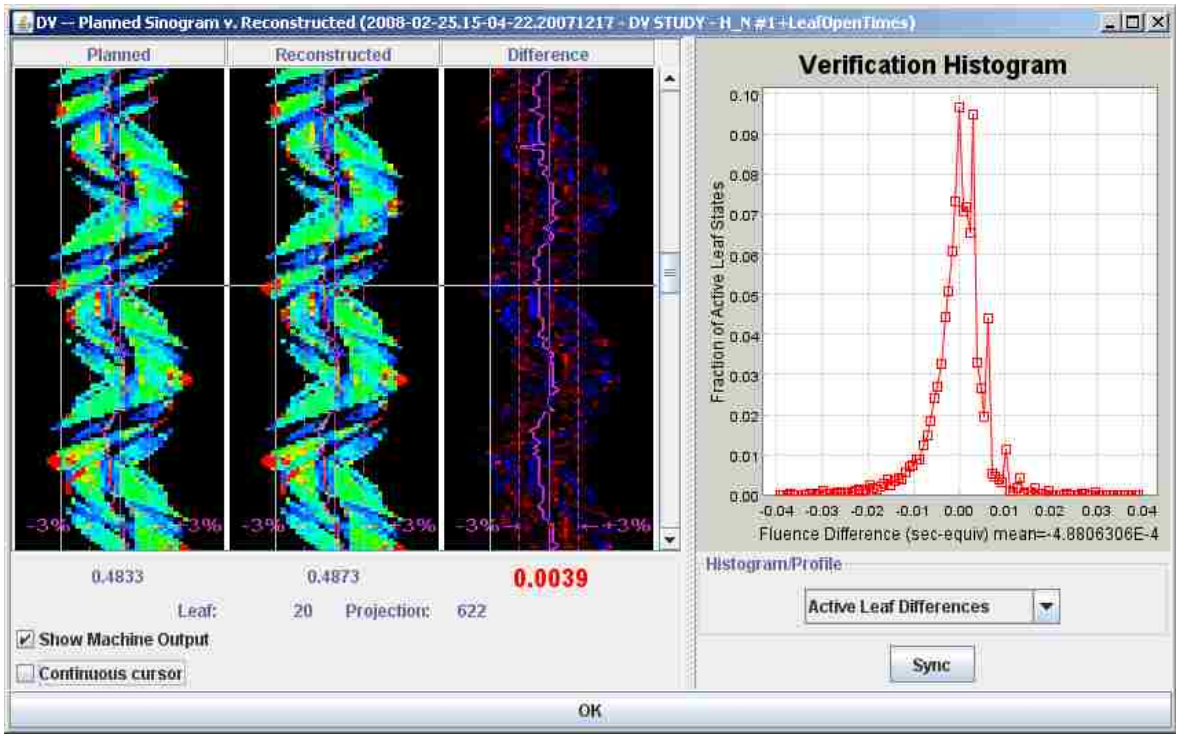

(b)

Figure 14. Comparison of the planned sinogram and reconstructed sinogram based on (a) machine output and (b) leaf opening time.

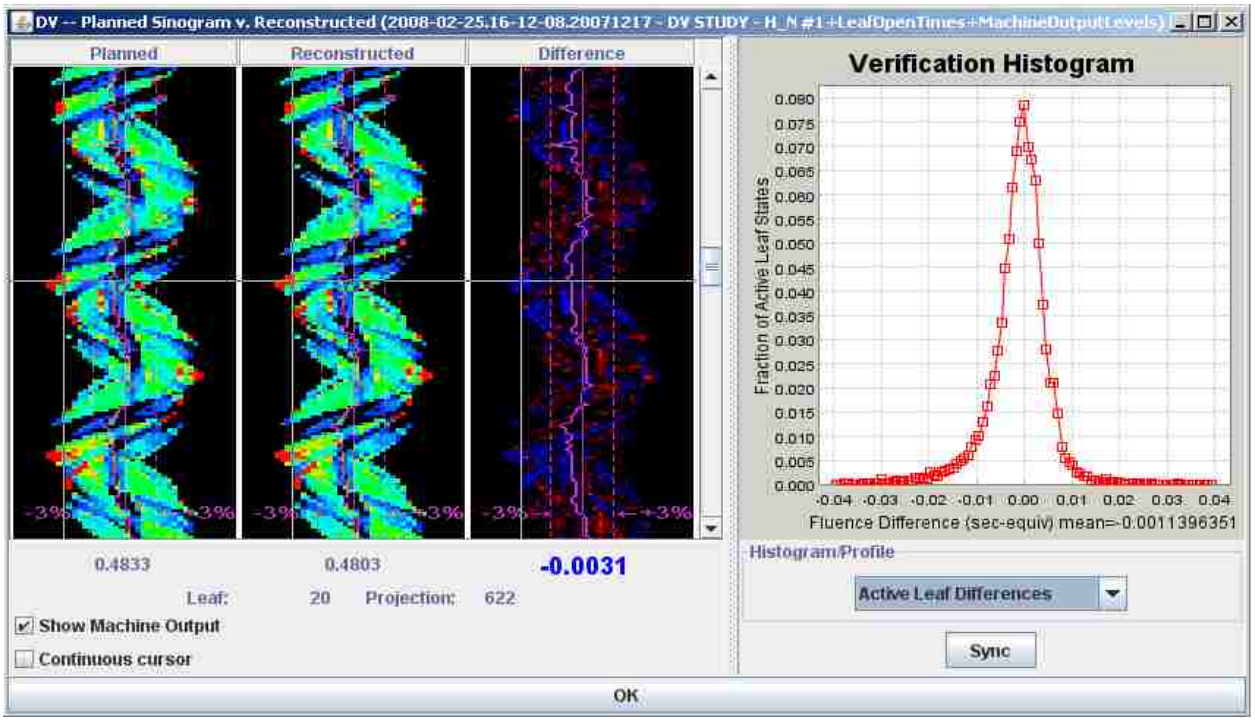

Figure 15. Comparison of the planned sinogram and reconstructed sinogram based on both leaf opening time and machine output.

DR in the DVPA software is computed based on a leaf control sinogram and an image dataset. For leaf control sinogram, DVPA allows the option to either use the planned or DV sinogram. For the image dataset, DVPA allows the option to either use the planned/reference image dataset or to use an MVCT image dataset taken immediately prior to treatment. If an MVCT image dataset is chosen, then a different IVDT is required, since the relationship between CT number and density is changed. Although this is beneficial for a patient with daily setup changes, it is not required for a phantom. Therefore, all reconstructed doses for this study were computed using the reference image and the corresponding DV sinogram with the dose grid set to fine. The reference image dataset was chosen over the MVCT image dataset to omit any density differences, therefore, image dependency on the reconstructed dose relative to the planned dose.

To confirm that the dose algorithm in DVPA is the same as the TPS, a DR was computed on the unmodified H&N plan using the reference image and the planned sinogram. The result showed that there was no difference in the dose distribution between the planned and reconstructed.

2.4 Aim 4: Dose Comparison of Measurements Versus Reconstructed

After DVPA dose reconstruction calculations were performed, the calculated point doses (at the location of the ion chamber) and the planar dose distributions (at the location of the film plane) were extracted from the system for comparison with measurement results. These comparisons were made using the quality assurance tools available on the DVPA software and on the planning station application on the TomoTherapy Research TPS.

The calculated point doses used in comparing with the measured data were chosen to be at the center of the ion chamber's active volume. The dose grid point in the calculated dose matrix closest to this location was selected. In the DVPA software, point dose values from the planned and reconstructed dose distributions are displayed to the thousandth decimal and are in units of gray.

Standard deviations for both the measured and calculated point doses were determined using equation 4. If both the measured or calculated dose for each scheduled delivery have the exact same value, then the standard deviation was set to half of the last significant digit (e.g., 2.07 Gy will have $\sigma = \pm 0.005$).

$$\sigma = \sqrt{\frac{1}{N}\sum_{i=1}^{N}(x_i - \overline{x})^2} \quad (4)$$

N: Number of measurements

x_i: Measured data

Calculation for the differences between measured and reconstructed doses used equation 5. The sum of their standard deviations is taken as the square root of the sum of their square (equation 6).

$$\partial = \frac{D_M - D_R}{D_M} \tag{5}$$

$$\sigma_{sum} = \sqrt{\sigma_m^2 + \sigma_r^2} \tag{6}$$

Evaluation of the film measurements were done within the TomoTherapy Research TPS. It provides a Delivery Quality Assurance (DQA) analysis tool where the DQA plan and measured dose distributions are overlaid for comparisons in one dimension (dose profiles) and/or two dimensions (isodose or gamma index distributions). The DQA plan simulates the planned treatment on a measurement phantom for dose delivery verification. Dose in the DQA plan contains the composite dose from all treatment fractions. In order to compare film measurements with the reconstructed dose distributions computed by DVPA, a DQA plan was created for each patient plan. The dose file created in the DQA plan was then replaced with a reconstructed dose file.

Reconstructed dose files have an ".img" filename extension and are the same dimension and file size as the planned and DQA dose files. All dose files are accessible under the patient archive directory. Identifying a reconstructed dose file to the corresponding treatment delivery was done by associating the date and time it was computed on the DVPA planning system to the date and time that is associated with a filename within the xml file. The same was done for the DQA dose file.

Before replacing the DQA dose file with a reconstructed dose file, each reconstructed dose was scaled up by a factor equal to the total number of fractions for the planned treatment. This is due to the fact that the DQA analysis tool scales the calculated dose down to one fraction

for comparison with the measured data (film), which were measured from a single fraction delivery. Replacement of the DQA dose file with the reconstructed dose file was made by renaming the reconstructed dose file to the DQA's filename. The archive was then retrieved back into the TomoTherapy Research TPS. This step was repeated for every reconstructed dose used to compare with the corresponding measured film data.

Film dosimetry evaluation for this study uses a technique that gives a quantitative analysis of the dose distributions between measured and computed data, also known as gamma index distibution.[24] This technique is a composition of two types of comparisons: 1) dose difference in regions of low dose gradient and 2) distance-to-agreement (DTA) in region of high dose gradients. The latter is used because small spatial error in high dose gradient regions could result in large dose difference. Determination of a pass or fail gamma index is dependent on the conditions set in the parameters for dose difference and DTA tolerances. Independent of the conditions, a gamma index of ≤ 1 is considered passing using equation 7. Figure 16 is a graphical illustration of the gamma index that visually defines the variables used in equations 7 and 8. The surface of the elliptical sphere, which is dependent on the values of the dose difference and the DTA tolerances, represents a gamma value of 1.

$$\gamma(r_m) = \min\{\Gamma(r_m, r_c)\}\forall\{r_c\} \tag{7}$$

where

$$\Gamma(r_m, r_c) = \sqrt{\frac{r^2(r_m,r_c)}{\Delta d_M^2} + \frac{\delta^2(r_m,r_c)}{\Delta D_M^2}} \tag{8}$$

r: distance between r_m and r_c

r_m: measured point

r_c: calculated point

δ: dose difference between doses at r_m and r_c

d_M: DTA tolerance

D_M: dose tolerance

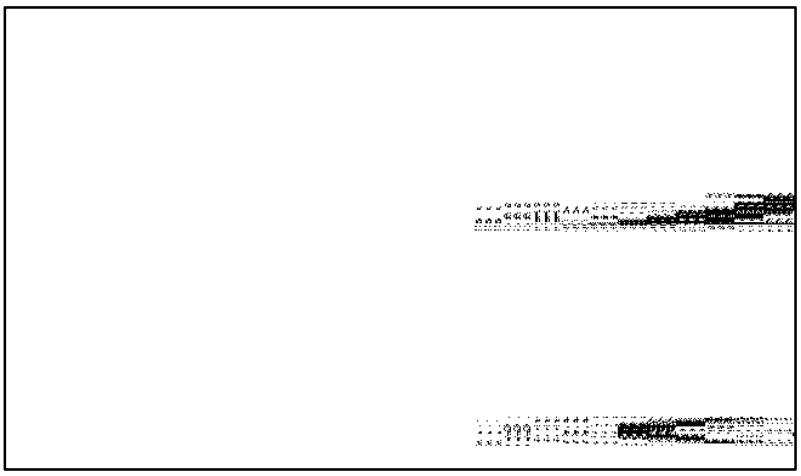

Figure 16. Graphical illustration of the gamma index distribution

This study uses TomoTherapy Planning Station Alpha6, which provides a histogram of the gamma index within a selected region of interest. A maximum region of interest was chosen while keeping the borders at least 2 cm from the phantom edges to avoid markings on the edge of the film used for registration. The regions selected for all film analysis of the same study were consistent to within 0.5 mm (see Figure 17). The standard conditions used for the gamma index were: d_M = 3 mm, D_M = 3% of max dose.

Analysis of film measurements were made after scaling the film dose distributions based on the ionization chamber measurements. It was assumed that the ratio of doses to an arbitrary point on the film (D_{film}) to the ion chamber (D_{ic}) should be the same for the measurement ($_m$) and the reconstructed ($_r$) plan. The film point was selected to be in a low dose gradient region, as close as possible to the ion chamber point. The film dose was scaled by the following scaling factor:

$$Scaling\ factor = \frac{D_{ic,m}}{D_{film,m}} \cdot \frac{D_{film,r}}{D_{ic,r}} \quad (9)$$

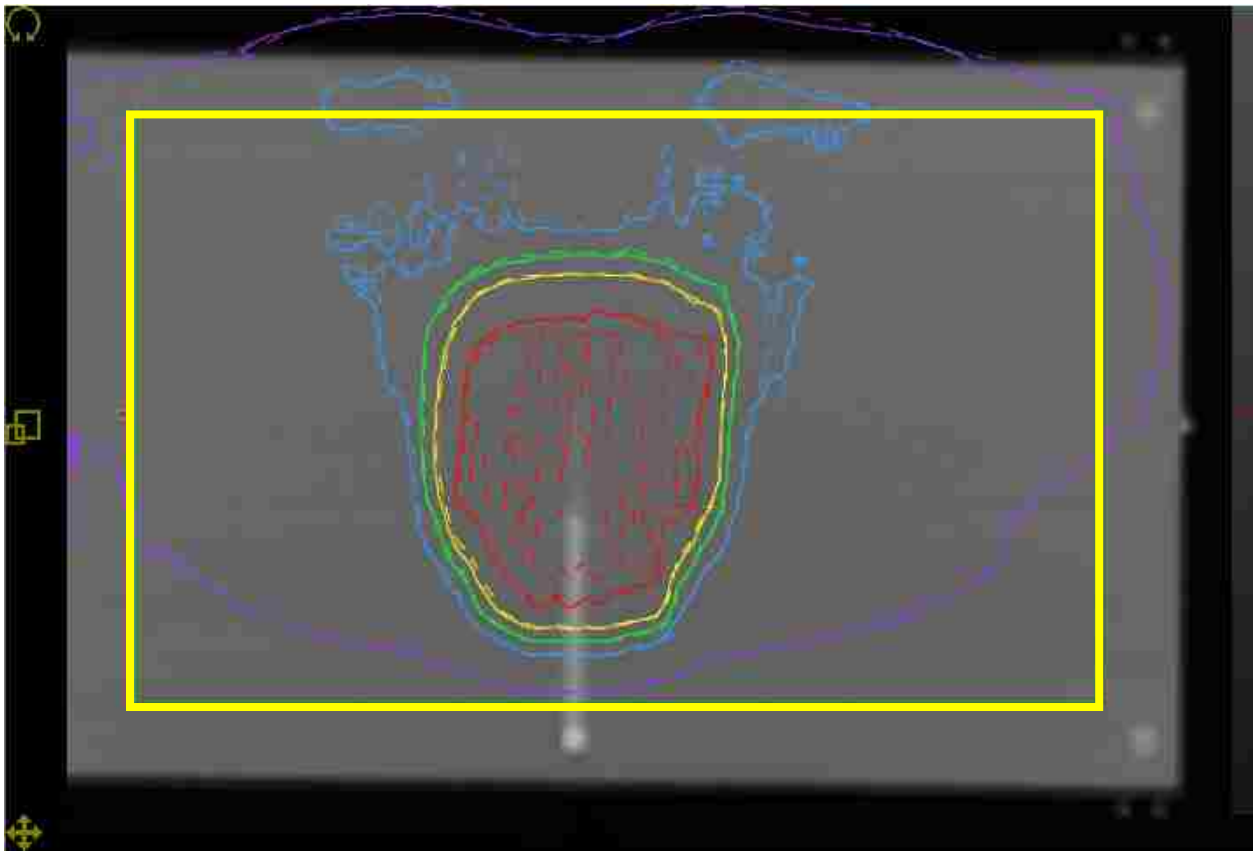

Figure 17. Displays a screenshot of the film analysis program of the TomoTherapy TPS. Shown are isodose lines from computed (solid) and measured (dash) dose distributions overlaid on a reconstructed coronal slice of the measurement phantom. The yellow rectangle shows the ROI selected for this study.

CHAPTER 3. RESULTS AND DISCUSSION

3.1 Aim 1: Generate Treatment Plans

Contours for each of the three plans were copied from a patient plan that corresponded to their treatment site. Treatment planning parameters were set to simulate typical patient plans using standard clinical protocols in use at MBPCC. Figures 18, 20 and 22 show the optimized dose distributions from three different views (axial, coronal and sagittal) of the H&N, prostate and lung plans, respectively. Figures 19, 21 and 23 show the dose volume histograms (DVH) of the H&N, prostate and lung plans, respectively. Despite being optimized on a cylindrical phantom, the dose distributions for each plan are similar to clinical plan results. Dose within the PTVs have a high dose/low gradient which help reduce errors associated with misalignment of ionization chamber during measurements. Dose to the critical structures for the three plans are below standard clinical tolerances.

Since all plans simulated those of clinical patient plans, parameters which affect delivery errors (gantry rotational speed, couch speed and leaf opening time) are likely to be close to clinical values. All plans were also fractionated so that each treatment delivery will deliver a dose of 2 Gy to the PTV.

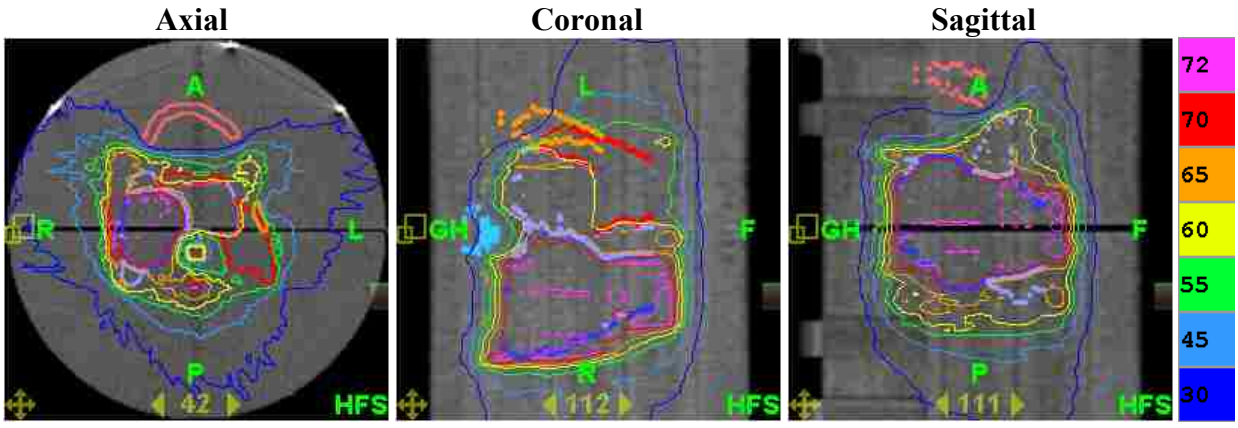

Figure 18. Dose distribution (isodose values are in Gy) of the H&N plan

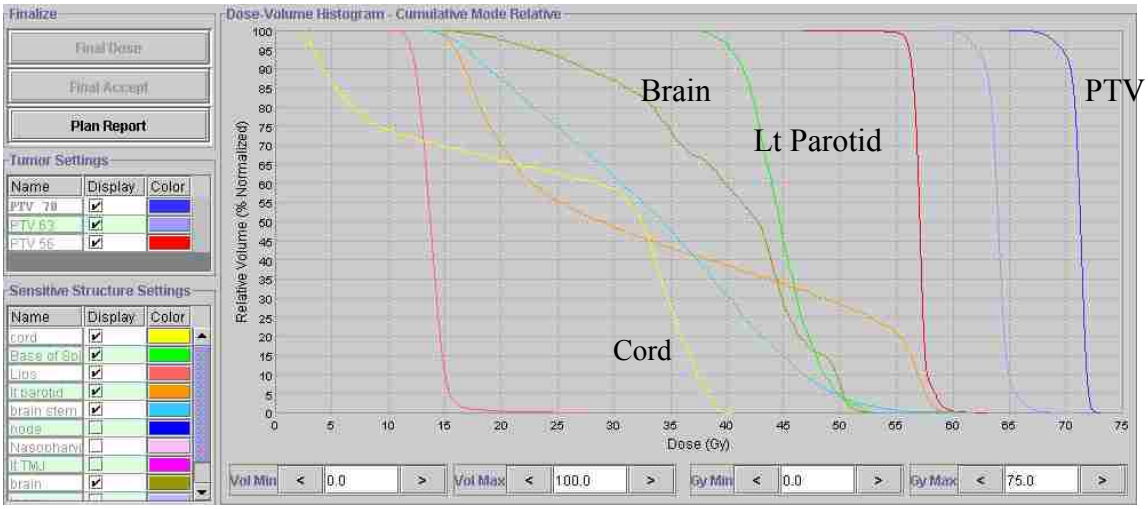

Figure 19. DVH of the H&N plan

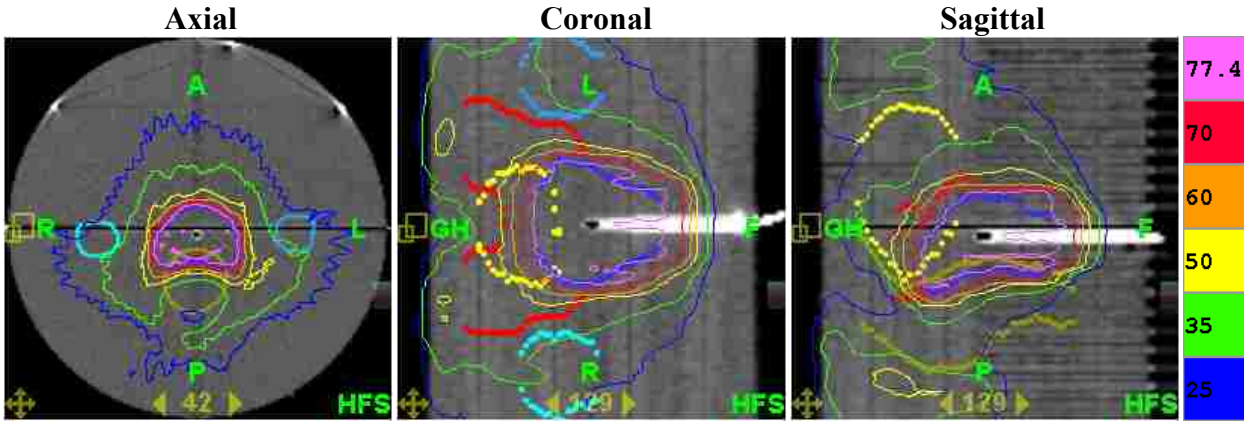

Figure 20. Dose distribution of the prostate plan

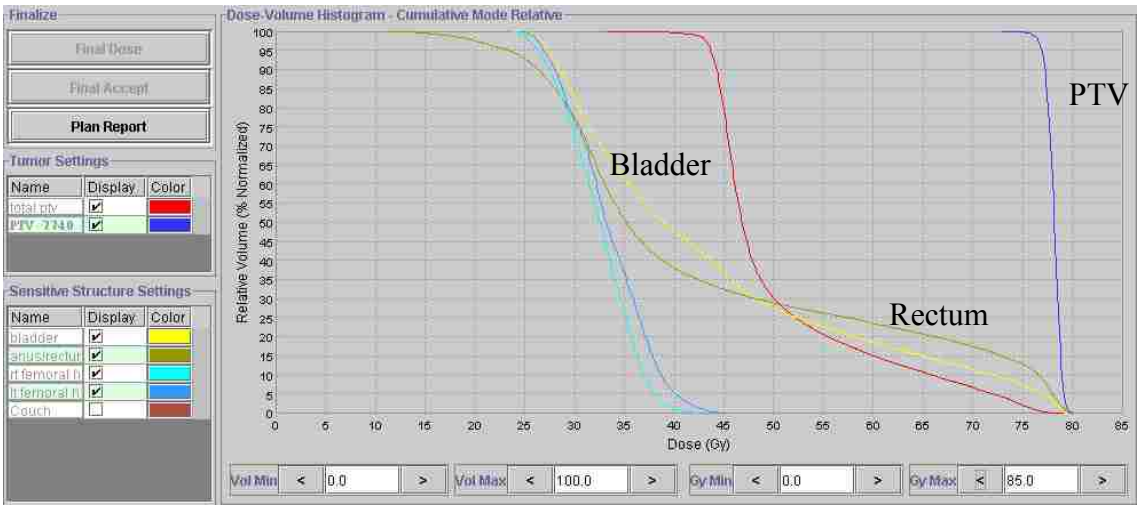

Figure 21. DVH of the prostate plan

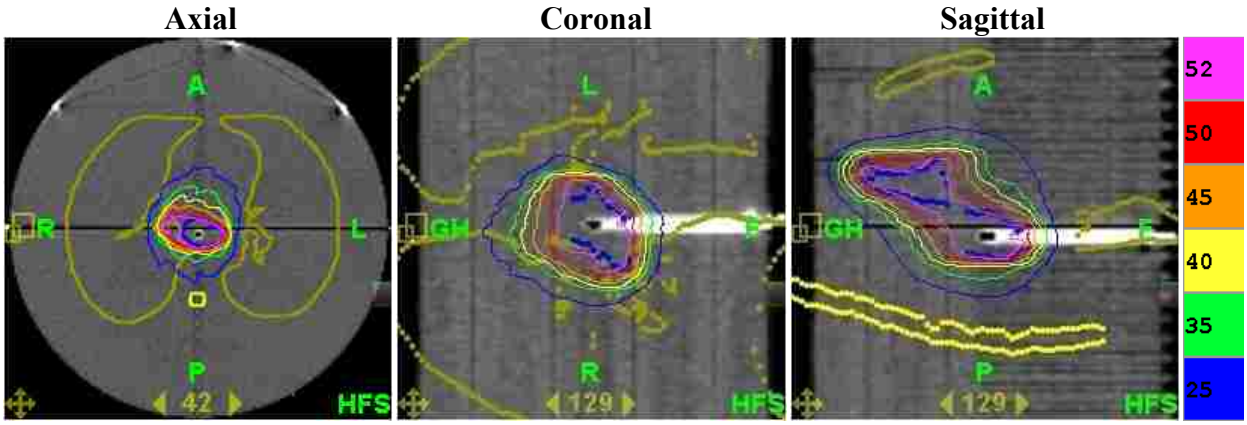

Figure 22. Dose distribution of the lung plan

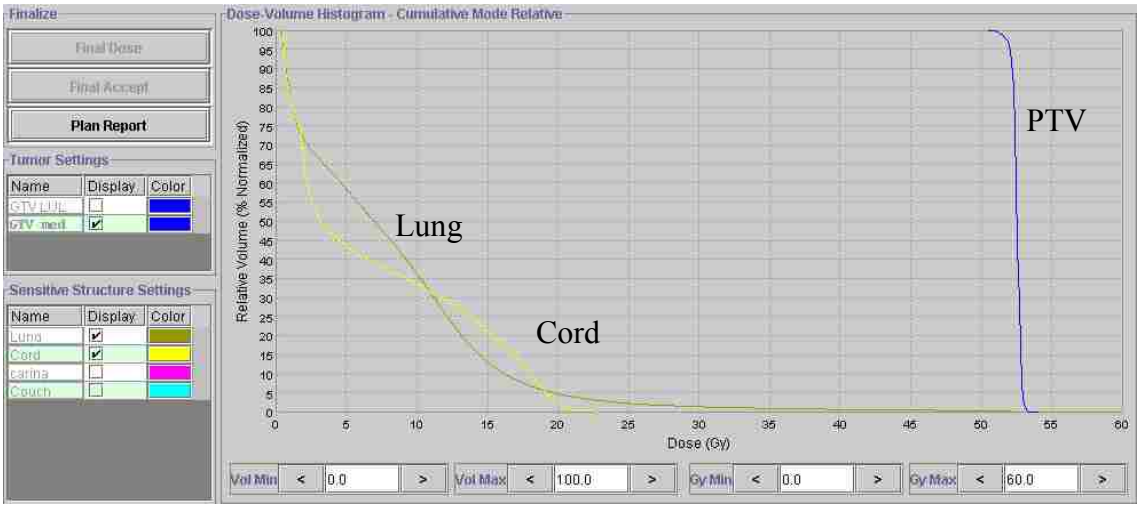

Figure 23. DVH of the lung plan

3.2 Aim 2: Delivery and Measurements of Treatment Plans

Measured data from the delivery of the H&N, prostate and lung plans are shown in Tables 2, 3 and 4, respectively. Film data are not shown here but will be discuss in section 3.4.2. The planned dose at the point of measurement for the H&N, prostate and lung plans are 2.037 Gy, 2.063 Gy and 2.022 Gy, respectively. Each delivery procedure was measured twice per day and is separated in the tables by highlights. Temperature and pressure readings were taken at the end of each delivery. The calibration factors of the electrometer and ion chamber were also recorded. Deliveries made without intentional changes to the planned are labeled 'Normal'.

Deliveries made with intentional offsets to the output are labeled as 'Δpfn' along with the voltage difference from the machine's current value. Calculations for the measured dose used Equation 2 (c.f., section 2.2.2).

Table 2. Ion chamber measurements for the H&N plan (planned dose = 2.037 Gy)

Delivered Plan (H&N)	Reading	Temp. (°C)	Pressure [mmHg]	Electrometer Cal. [C/Rdg]	Chamber Cal. [Gy/C]	Measured Dose [Gy]
Normal - Day 1	0.384	23.8	765.0	9.87E-09	5.468E+08	**2.071**
Normal - Day 1	0.383	23.8	765.0	9.87E-09	5.468E+08	**2.066**
Normal - Day 2	0.380	23.9	763.0	9.87E-09	5.468E+08	**2.056**
Normal - Day 2	0.380	23.9	763.0	9.87E-09	5.468E+08	**2.056**
Normal - Day 3	0.383	23.4	756.3	9.87E-09	5.468E+08	**2.087**
Normal - Day 3	0.383	23.4	756.3	9.87E-09	5.468E+08	**2.087**
Normal - Day 4	0.381	23.3	769.5	9.87E-09	5.468E+08	**2.040**
Normal - Day 4	0.381	23.3	769.5	9.87E-09	5.468E+08	**2.040**
Normal - Day 5	0.378	23.9	770.0	9.87E-09	5.468E+08	**2.027**
Normal - Day 5	0.379	24.1	770.0	9.87E-09	5.468E+08	**2.033**
Normal - Day 6	0.368	24.1	761.0	1.004E-08	5.468E+08	**2.032**
Normal - Day 6	0.369	24.0	761.0	1.004E-08	5.468E+08	**2.037**
Normal - Day 7	0.372	24.6	763.0	1.004E-08	5.468E+08	**2.052**
Normal - Day 7	0.372	25.0	763.0	1.004E-08	5.468E+08	**2.055**
All leaves -10 ms	0.351	23.9	763.0	9.87E-09	5.468E+08	**1.899**
All leaves -10 ms	0.350	23.9	763.0	9.87E-09	5.468E+08	**1.894**
All leaves +10 ms	0.410	24.4	763.0	9.87E-09	5.468E+08	**2.222**
All leaves +10 ms	0.410	24.4	763.0	9.87E-09	5.468E+08	**2.222**
All leaves -30 ms	0.296	24.3	763.0	1.004E-08	5.468E+08	**1.631**
All leaves -30 ms	0.295	24.8	763.0	1.004E-08	5.468E+08	**1.628**
All leaves +30 ms	0.449	24.8	763.0	1.004E-08	5.468E+08	**2.479**
All leaves +30 ms	0.451	24.6	763.0	1.004E-08	5.468E+08	**2.488**
Leaf #27 -10 ms	0.381	24.5	763.0	9.87E-09	5.468E+08	**2.065**
Leaf #27 -10 ms	0.381	24.5	763.0	9.87E-09	5.468E+08	**2.065**
Leaf #27 +10 ms	0.384	24.6	762.0	9.87E-09	5.468E+08	**2.085**
Leaf #27 +10 ms	0.384	24.6	762.0	9.87E-09	5.468E+08	**2.085**
Leaf #33 -10 ms	0.382	24.6	762.0	9.87E-09	5.468E+08	**2.070**
Leaf #33 -10 ms	0.382	24.6	762.0	9.87E-09	5.468E+08	**2.070**
Leaf #33 +10 ms	0.384	24.6	761.0	9.87E-09	5.468E+08	**2.088**
Leaf #33 +10 ms	0.384	24.6	761.0	9.87E-09	5.468E+08	**2.088**

Table 3. Ion chamber measurements for the prostate plan (planned dose = 2.063 Gy)

Delivered Plan (Prostate)	Reading	Temp. (°C)	Pressure [mmHg]	Electrometer Cal. [C/Rdg]	Chamber Cal. [Gy/C]	Measured Dose [Gy]
Normal - Day 1	0.380	23.5	761.0	9.87E-09	5.468E+08	**2.059**
Normal - Day 1	0.380	23.8	761.0	9.87E-09	5.468E+08	**2.061**
Normal - Day 2	0.379	23.7	758.0	9.87E-09	5.468E+08	**2.063**
Normal - Day 2	0.378	23.8	758.0	9.87E-09	5.468E+08	**2.059**
Normal - Day 3	0.378	24.3	755.0	9.87E-09	5.468E+08	**2.070**
Normal - Day 3	0.378	24.5	755.0	9.87E-09	5.468E+08	**2.071**
Normal - Day 4	0.375	24.1	754.5	9.87E-09	5.468E+08	**2.050**
Normal - Day 4	0.375	24.2	754.5	9.87E-09	5.468E+08	**2.051**
Normal - Day 5	0.380	24.5	761.0	9.87E-09	5.468E+08	**2.065**
Normal - Day 5	0.380	24.5	761.0	9.87E-09	5.468E+08	**2.065**
Normal - Day 6	0.371	24.0	761.0	1.004E-08	5.468E+08	**2.048**
Normal - Day 7	0.370	24.2	761.0	1.004E-08	5.468E+08	**2.044**
Normal - Day 7	0.373	23.6	762.0	1.004E-08	5.468E+08	**2.053**
Normal - Day 7	0.373	23.8	762.0	1.004E-08	5.468E+08	**2.055**
All leaves -10 ms	0.352	24.0	761.0	9.87E-09	5.468E+08	**1.908**
All leaves -10 ms	0.352	23.8	761.0	9.87E-09	5.468E+08	**1.908**
All leaves +10 ms	0.406	23.8	761.0	9.87E-09	5.468E+08	**2.202**
All leaves +10 ms	0.406	23.8	761.0	9.87E-09	5.468E+08	**2.202**
All leaves -30 ms	0.294	23.8	758.0	9.87E-09	5.468E+08	**1.601**
All leaves -30 ms	0.294	23.9	758.0	9.87E-09	5.468E+08	**1.601**
All leaves +30 ms	0.458	23.9	758.0	9.87E-09	5.468E+08	**2.494**
All leaves +30 ms	0.458	23.9	757.5	9.87E-09	5.468E+08	**2.508**
Leaf #33 -10 ms	0.367	24.3	755.0	9.87E-09	5.468E+08	**2.009**
Leaf #33 -10 ms	0.368	24.3	755.0	9.87E-09	5.468E+08	**2.015**
Leaf #33 +10 ms	0.386	24.3	755.0	9.87E-09	5.468E+08	**2.113**
Leaf #33 +10 ms	0.383	24.8	755.0	9.87E-09	5.468E+08	**2.102**
Leaf #33 -30 ms	0.350	24.5	761.0	9.87E-09	5.468E+08	**1.902**
Leaf #33 -30 ms	0.350	24.5	761.0	9.87E-09	5.468E+08	**1.902**
Leaf #33 +30 ms	0.406	24.7	761.0	9.87E-09	5.468E+08	**2.208**
Leaf #33 +30 ms	0.406	24.7	761.0	9.87E-09	5.468E+08	**2.208**
Δpfn: +0.01 V	0.383	24.4	762.0	9.87E-09	5.468E+08	**2.078**
Δpfn: +0.01 V	0.383	24.4	762.0	9.87E-09	5.468E+08	**2.078**
Δpfn: +0.02 V	0.385	24.5	761.5	9.87E-09	5.468E+08	**2.091**
Δpfn: +0.04 V	0.389	24.5	761.5	9.87E-09	5.468E+08	**2.113**
Δpfn: +0.07 V	0.388	23.9	761.0	1.004E-08	5.468E+08	**2.141**
Δpfn: +0.07 V	0.389	24.2	761.0	1.004E-08	5.468E+08	**2.149**
Δpfn: -0.07 V	0.356	23.9	761.0	1.004E-08	5.468E+08	**1.964**
Δpfn: -0.07 V	0.354	24.2	761.0	1.004E-08	5.468E+08	**1.955**

Table 4. Ion chamber measurements for the lung plan (planned dose = 2.022 Gy)

Delivered Plan (Lung)	Reading	Temp. (°C)	Pressure [mmHg]	Electrometer Cal. [C/Rdg]	Chamber Cal. [Gy/C]	Measured Dose [Gy]
Normal - Day 1	0.363	24.4	761.0	9.87E-09	5.468E+08	**1.972**
Normal - Day 1	0.364	24.4	761.0	9.87E-09	5.468E+08	**1.978**
Normal - Day 2	0.363	23.6	761.0	9.87E-09	5.468E+08	**1.967**
Normal - Day 2	0.363	24.3	761.0	9.87E-09	5.468E+08	**1.972**
Normal - Day 3	0.357	23.8	761.0	1.004E-08	5.468E+08	**1.969**
Normal - Day 3	0.357	23.7	761.0	1.004E-08	5.468E+08	**1.969**
Normal - Day 4	0.358	23.8	762.0	1.004E-08	5.468E+08	**1.972**
Normal - Day 4	0.358	23.8	762.0	1.004E-08	5.468E+08	**1.972**
Normal - Day 5	0.353	24.6	762.0	1.004E-08	5.468E+08	**1.950**
Normal - Day 5	0.353	24.8	762.0	1.004E-08	5.468E+08	**1.951**
All leaves -10ms	0.339	24.6	761.0	9.87E-09	5.468E+08	**1.843**
All leaves -10ms	0.339	24.6	761.0	9.87E-09	5.468E+08	**1.843**
All leaves +10 ms	0.389	24.8	761.0	9.87E-09	5.468E+08	**2.117**
All leaves +10 ms	0.389	24.8	761.0	9.87E-09	5.468E+08	**2.117**
All leaves -30 ms	0.289	24.8	762.0	9.87E-09	5.468E+08	**1.570**
All leaves -30 ms	0.289	24.8	762.0	9.87E-09	5.468E+08	**1.570**
All leaves +30 ms	0.439	24.8	762.0	9.87E-09	5.468E+08	**2.385**
All leaves +30 ms	0.439	24.8	762.0	9.87E-09	5.468E+08	**2.385**
Leaf #32/33 -10 ms	0.343	24.2	761.0	9.87E-09	5.468E+08	**1.862**
Leaf #32/33 -10 ms	0.343	24.2	760.5	9.87E-09	5.468E+08	**1.864**
Leaf #32/33 +10 ms	0.384	24.3	760.0	9.87E-09	5.468E+08	**2.089**
Leaf #32/33 +10 ms	0.384	24.2	760.0	9.87E-09	5.468E+08	**2.088**
Leaf #32/33 -30 ms	0.299	24.3	760.0	9.87E-09	5.468E+08	**1.626**
Leaf #32/33 -30 ms	0.298	24.3	760.0	9.87E-09	5.468E+08	**1.621**
Leaf #32/33 +30 ms	0.429	24.4	760.0	9.87E-09	5.468E+08	**2.334**
Leaf #32/33 +30 ms	0.428	24.2	760.0	9.87E-09	5.468E+08	**2.327**
Δpfn: -0.05 V	0.351	24.3	760.0	9.87E-09	5.468E+08	**1.909**
Δpfn: -0.05 V	0.350	24.3	760.0	9.87E-09	5.468E+08	**1.904**
Δpfn: +0.05 V	0.373	24.0	760.0	9.87E-09	5.468E+08	**2.027**
Δpfn: +0.05 V	0.373	24.2	760.0	9.87E-09	5.468E+08	**2.028**
Δpfn: -0.07 V	0.340	24.3	761.0	1.004E-08	5.468E+08	**1.879**
Δpfn: -0.07 V	0.341	23.9	761.0	1.004E-08	5.468E+08	**1.882**
Δpfn: +0.07 V	0.374	24.1	761.0	1.004E-08	5.468E+08	**2.065**
Δpfn: +0.07 V	0.373	24.1	761.0	1.004E-08	5.468E+08	**2.060**

The measurement results in Tables 2-4 show a wide range of point doses measured near the center of the target volume of each plan. The top portion of each table displays results for treatment plans delivered without any intentional variation in output or leaf open time. In general, these data show little to no variation between doses measured on the same day, although

small differences are seen between doses measured on different days. The minimum and maximum measured doses ranged from (2.03, 2.09) Gy, or (-0.3%, +2.6%) of the planned dose, for the H&N plan; (2.05, 2.07) Gy, or (-0.6%, +0.3%) for the prostate plan, and (1.95, 1.98) Gy, or (-3.6%, -2.1%) for the lung plan. The lung plan had the worst agreement when comparing with the planned dose, although the overall agreement was still within 4%.

The measurement results for leaf open time changes in Tables 2-4 show the largest variation in doses from the planned doses. Results are displayed for a constant increase in all leaf open times for all projections for both an individual leaf, and all 64 leaves. As expected, the differences were largest when all leaf open times were intentionally adjusted by 30 msec. The variation seen for these cases were (-20.0%, +22.2%) for H&N plan, (-22.4%, +21.2%) for the prostate plan, and (-22.4%, +18.2%) for the lung plan.

The magnitude of the changes for the adjustment of one or two leaf open times varied according to treatment plan. For the H&N plan, where either leaf number 27 or 33 were adjusted, the measured doses ranged from (2.07, 2.09) Gy, or (+1.6%, +2.6%) above the plan dose. For the prostate plan, a larger variation was seen when leaf number 33 was adjusted by the same amount, with measured doses ranging from (2.01, 2.11) Gy, or (-2.6%, +2.3%) above the plan dose. This difference may be due to the fact that the H&N target and measurement point are located further away from the tomotherapy axis or rotation, so that individual leaves contribute to the dose at this point for a few projections only. In the H&N case, the measurement was made 4 cm from the axis, while the lung and prostate doses were measured 0.5 cm from the axis. For the lung plan, the two leaves centered on the central axis (number 32 and 33) were varied by both 10 and 30 msec. In this case the variation in measured dose was larger, ranging from (1.86, 2.09) Gy, or (-8.0%, +3.4%).

The intentional changes made to the leaf open times were much larger than those seen in a typical treatment delivery (c.f., Figure 14 from Chapter 2). Nevertheless, these changes test the accuracy of the DVPA program under extreme conditions.

Linac output rates were adjusted for both the lung and prostate treatment deliveries by adjusting the pfn voltage up to ±0.07 volts. These results are also displayed in Tables 3 and 4. In these cases, the measured doses scaled proportional to the pfn voltage, with a slope of approximately 0.65% per unit change in pfn (1 cV). Larger changes in pfn voltage setting (i.e., ±0.08 volts) resulted in the machine interlock.

3.3 Aim 3: Dose Reconstruction Using Detector Data

3.3.1 H&N Plan

Reconstructed doses computed on DVPA use the DV sinogram and the reference image. Figures 24a, 24b and 24c shows the reconstructed (dashed) and planned (solid) isodose lines of the H&N study for the planned, +10 msec offset to center leaf and +10 msec offset to all leaves deliveries, respectively. Figures 25a, 25b and 25c are the corresponding DVHs. As expected, the reconstructed dose from planned delivery of the H&N study matched well with the planned dose (Figures 24a and 25a). However, a slight difference in the dose delivered (~2%) is seen in Figures 24b and 25b due to placing a +10 msec offset to the center leaf for the entire delivery. The reconstructed isodose lines cover a larger volume relative to the planned isodose lines. Adjusting all leaves by +10 msec caused a larger increase in the dose delivered by approximately 8% (Figures 24c and 25c).

Note that Figures 24-25 displays only a portion of the delivered plans made in this study to illustrate the effect of leaf open time errors in the delivered dose.

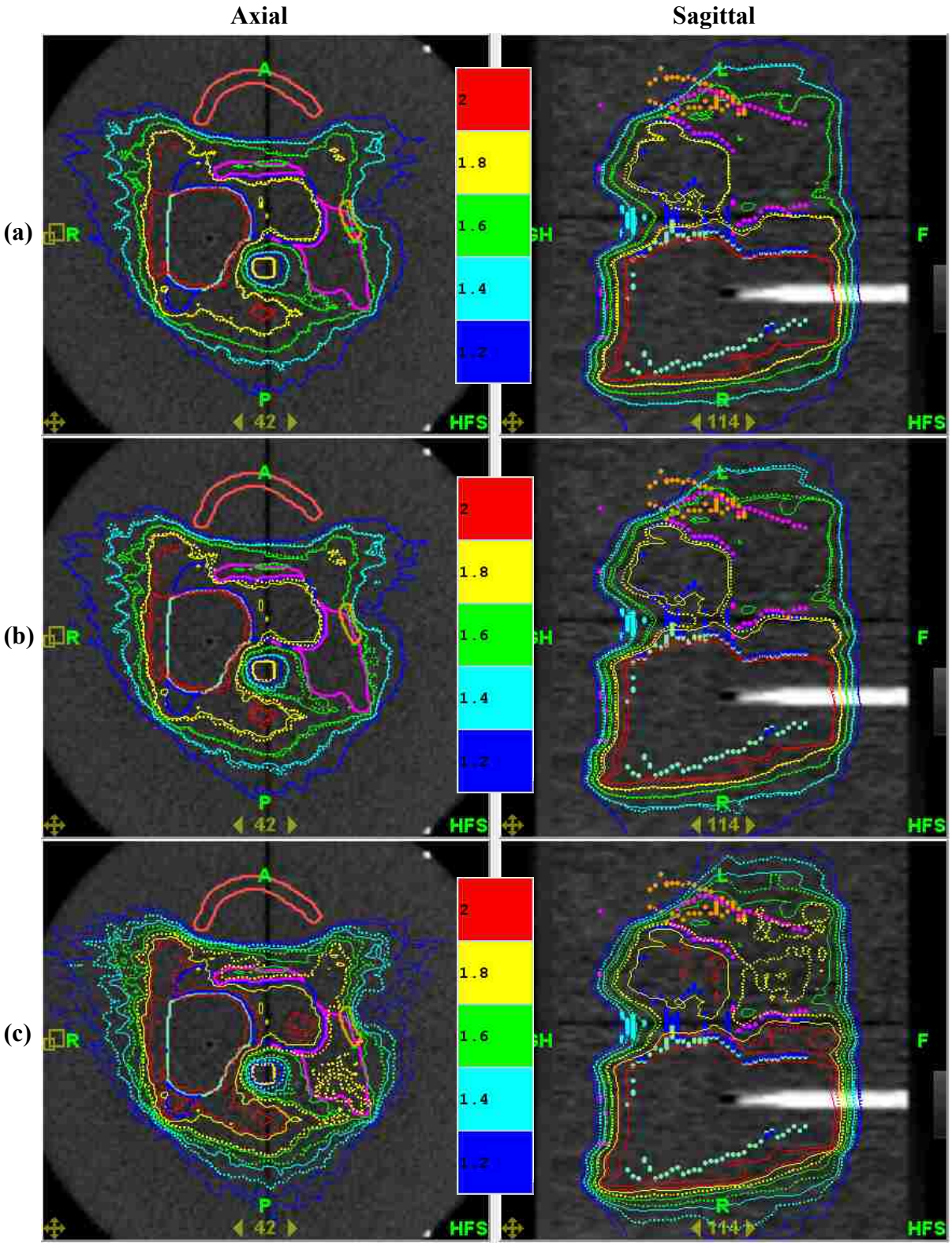

Figure 24. Isodose [Gy] overlay of the planned (solid) and reconstructed (dashed) for (a) planned delivery, (b) +10 msec offset to center leaf delivery and (c) +10 msec offset to all leaves delivery from the H&N study

(a)

(b)

(c)

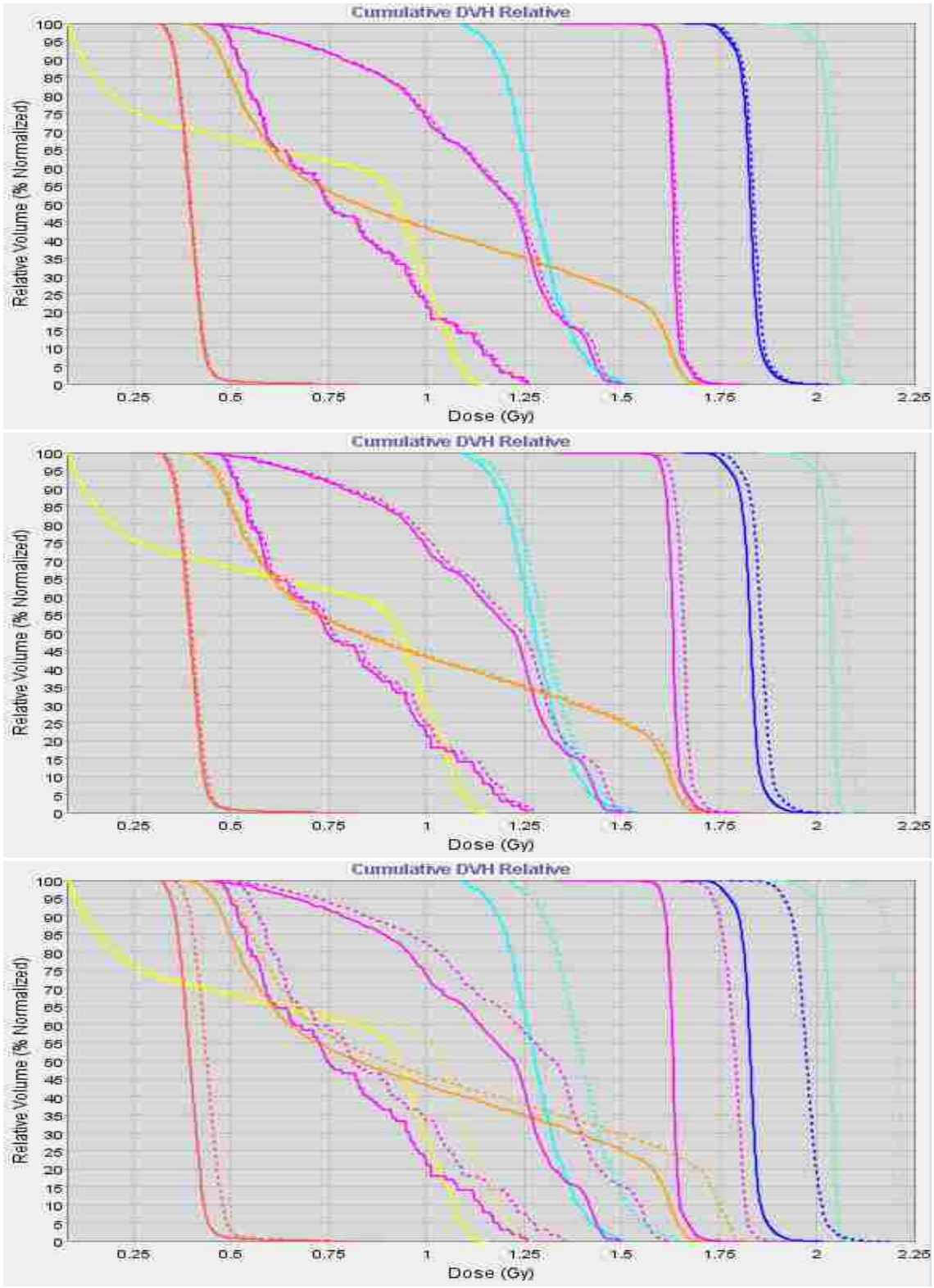

Figure 25. DVH comparison between the planned (solid) and reconstructed (dashed) for (a) planned delivery, (b) +10 msec offset to center leaf delivery and (c) +10 msec offset to all leaves delivery from the H&N study

3.3.2 Prostate Plan

For the prostate study, isodose lines of a reconstructed dose from a planned delivery matched the planned isodose lines (Figure 26a) with their DVHs showing no significant difference (Figure 27a). The delivery with an intentional offset to the center leaf by +30 msec led to an overdose along the central axis of the phantom which is depicted in Figure 26b. Figure 27b displays the corresponding PTV, which was located about the central axis of the machine, receiving an overdose for a portion of its volume. Delivery with a +30 msec offset to all leaves caused an increase in the overall dose delivered by approximately +20% (Figures 26c and 27c). Delivery with a machine output offset of 0.7 V to the pfn (approx. +3.9%) yield to a delivered dose of approximately +4% (Figures 26d and 27d), as expected.

Not all reconstructed doses for the prostate plan are shown, but the results for each agreed accordingly with the different offsets applied to the delivery.

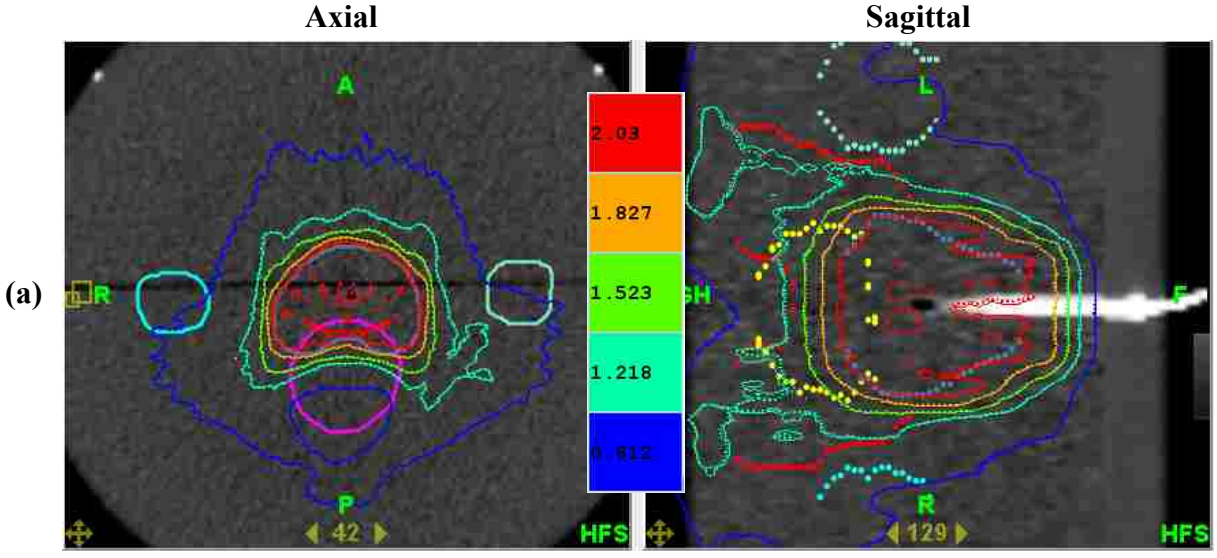

Figure 26. Isodose [Gy] overlay of the planned (solid) and reconstructed (dashed) for (a) planned delivery, (b) +30 msec offset to center leaf delivery, (c) +30 msec offset to all leaves delivery and (d) +0.7 V to the pfn delivery from the prostate study

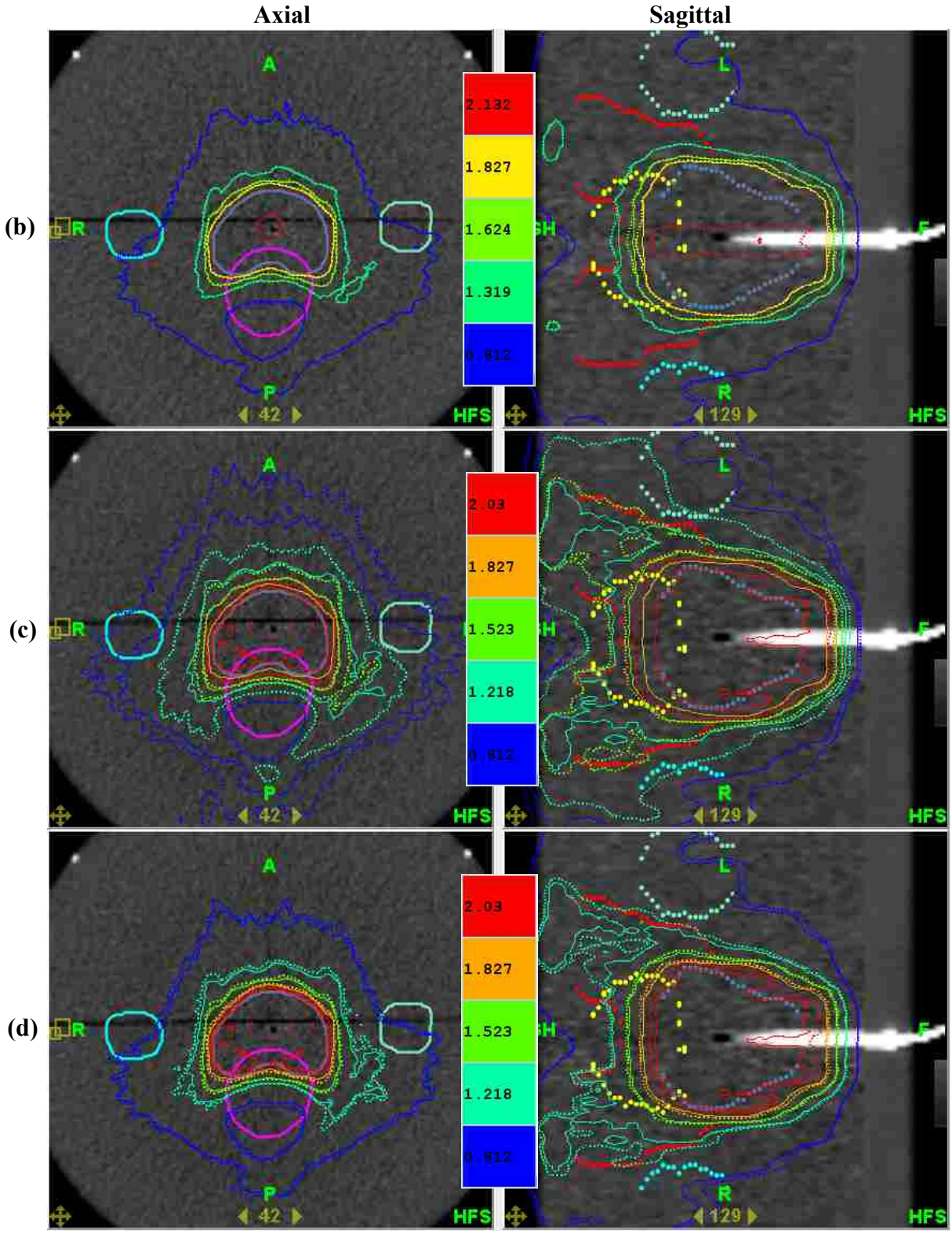

Figure 26 (continued)

(a)

(b)

(c)

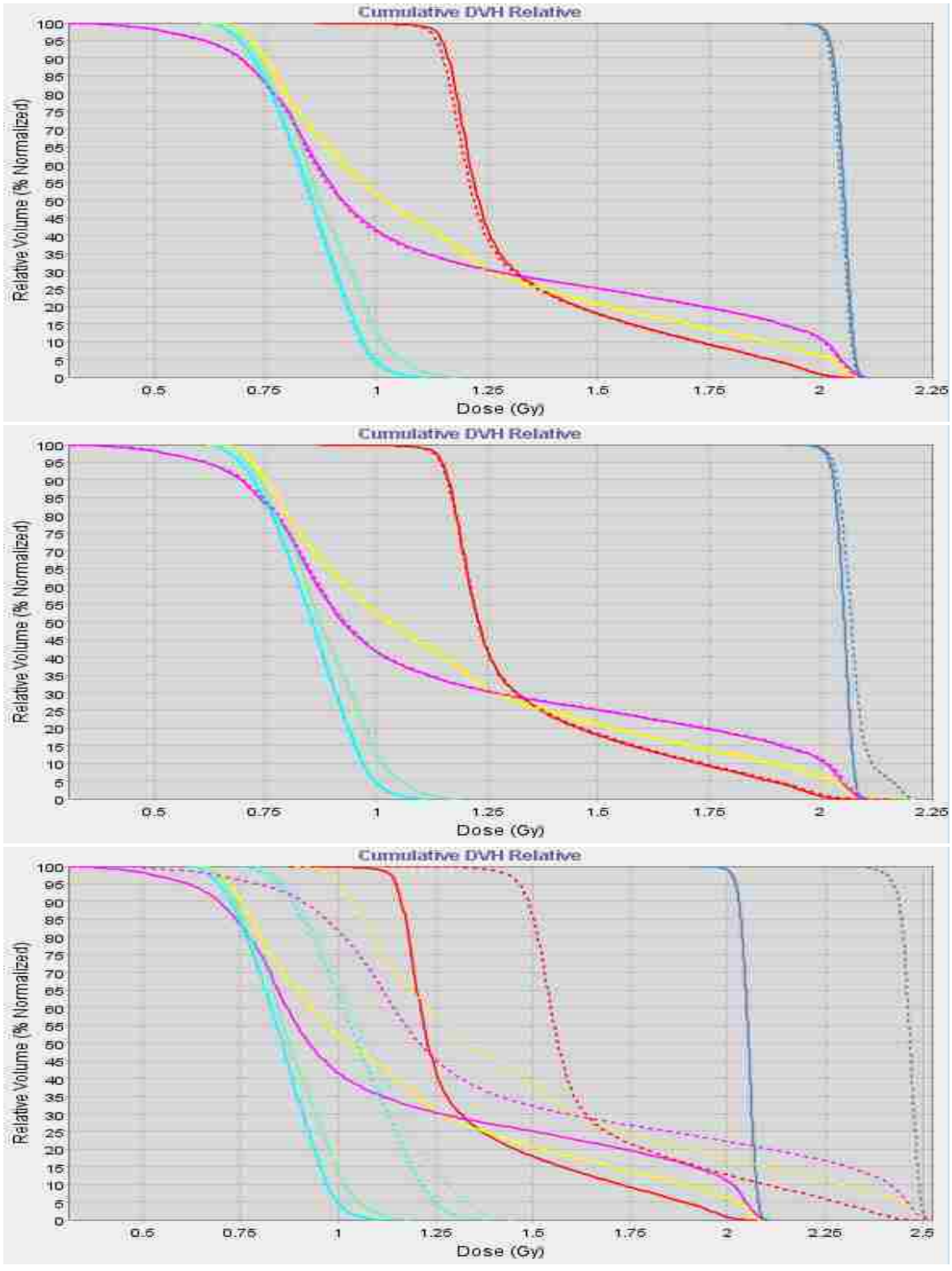

Figure 27. DVH comparison between the planned (solid) and reconstructed (dashed) for (a) planned delivery, (b) +30 msec offset to center leaf delivery, (c) +30 msec offset to all leaves delivery and (d) +0.7 V to the pfn offset delivery from the prostate study

(d)

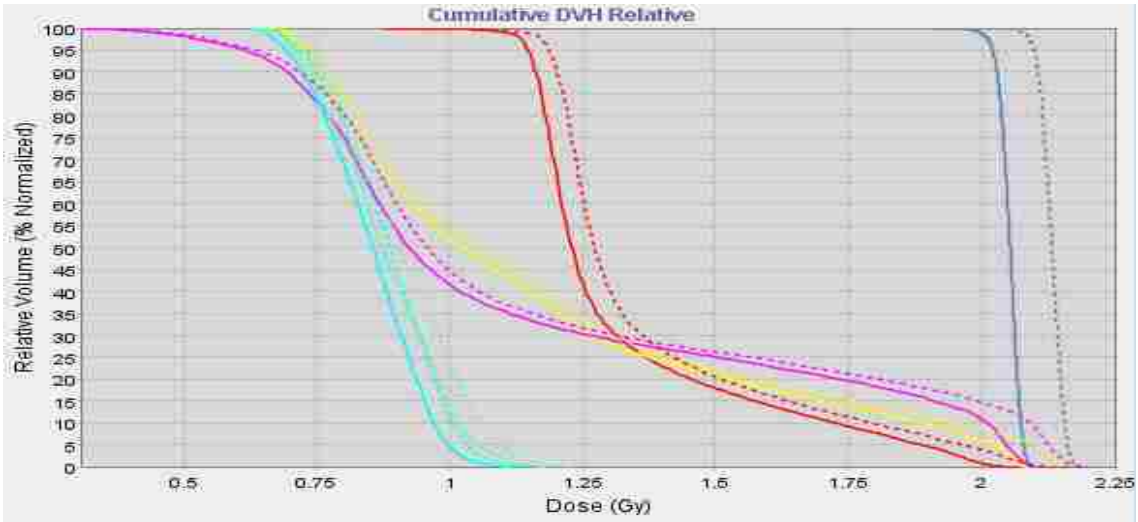

Figure 27 (continued).

3.3.3 Lung Plan

For the lung study, isodose lines of the reconstructed dose from a planned delivery matched the planned isodose lines (Figure 28a) with their DVHs having small differences (Figure 29a). The delivery with an intentional center leaf offset of -30 msec led to a decrease in dose throughout the phantom and especially along the central axis of the phantom (Figure 28b). Compared to the prostate delivery with an intentional center leaf offset of +30 msec, this delivery has a greater effect in the delivered dose due to the PTV having a smaller volume. Therefore, leaf open time errors have a greater contribution to the delivered dose of smaller PTV than to a larger PTV. This is shown when comparing the DVHs of Figures 27b and 29b. For the delivery with an intentional leaf open time offset of -30 msec to all leaves, the delivered dose to the PTV is approximately -22% less than the planned (Figures 28c and 29c).

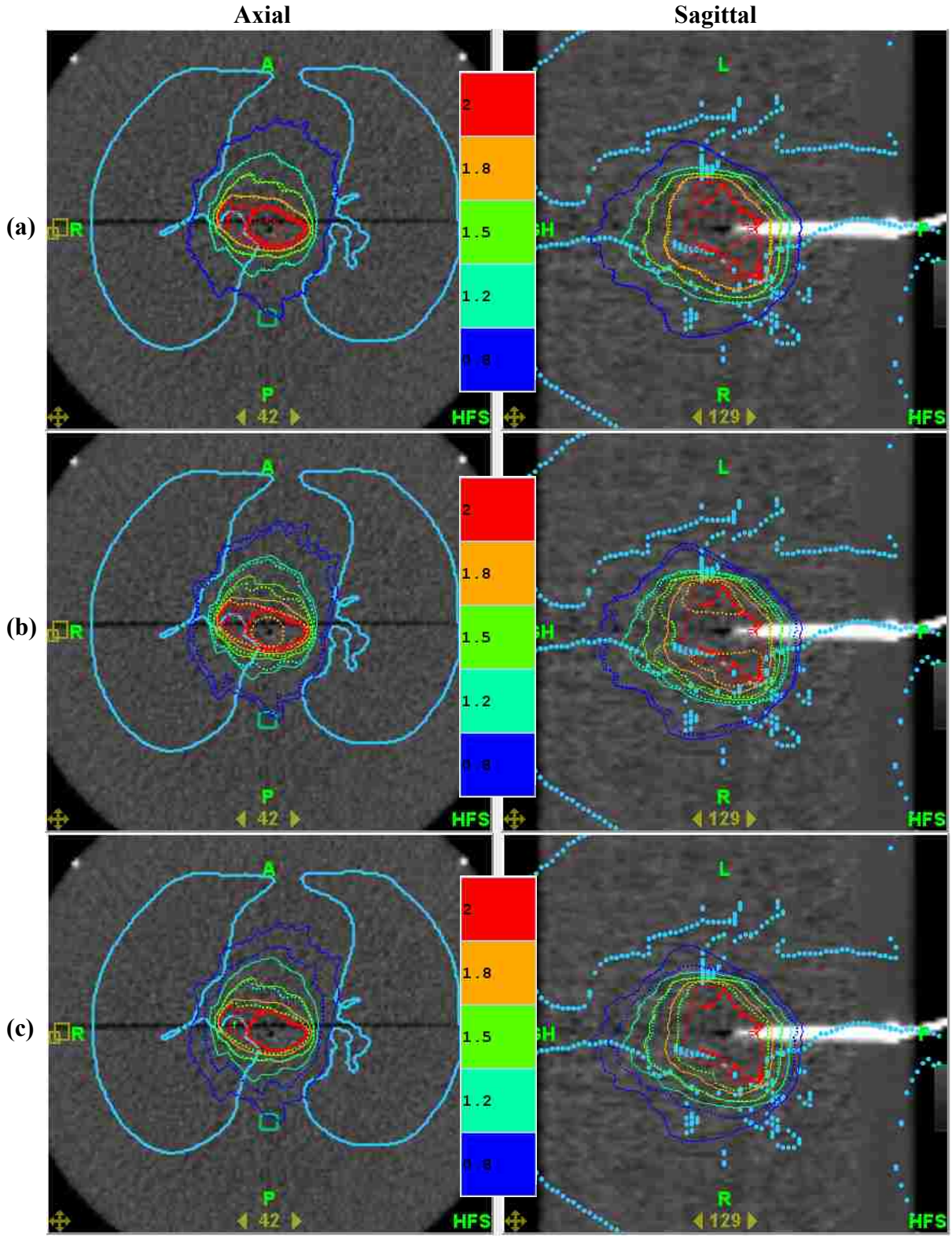

Figure 28. Isodose [Gy] overlay of the planned (solid) and reconstructed (dashed) for (a) planned delivery, (b) -30 msec offset to center leaf delivery and (c) -30 msec offset to all leave delivery from the lung study

(a)

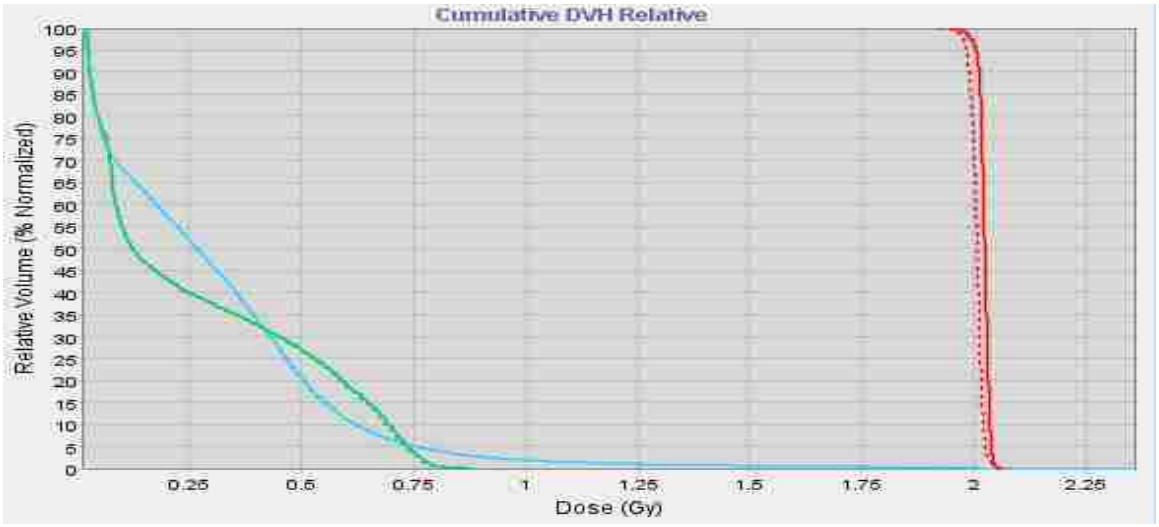

(b)

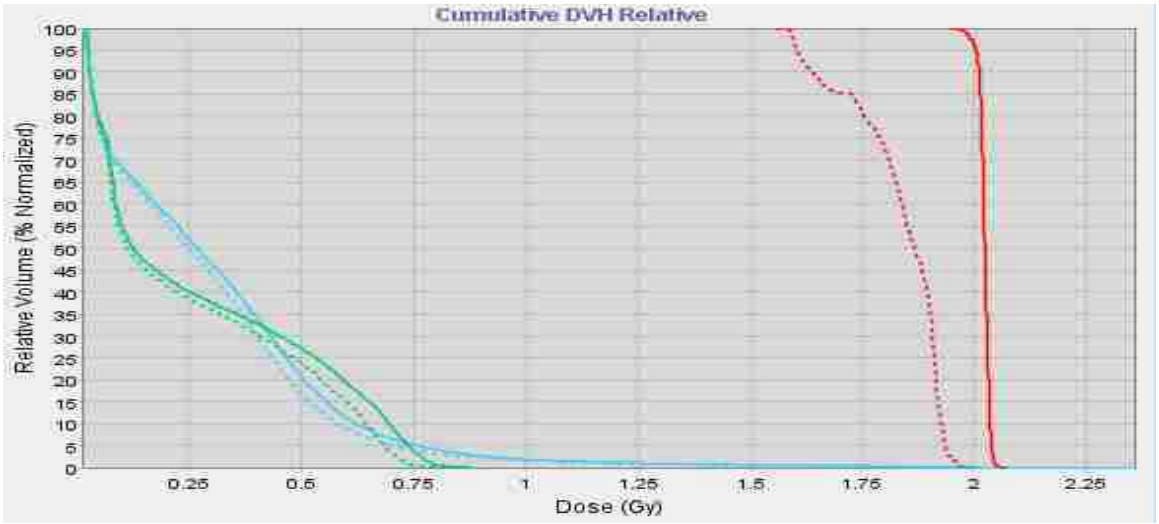

(c)

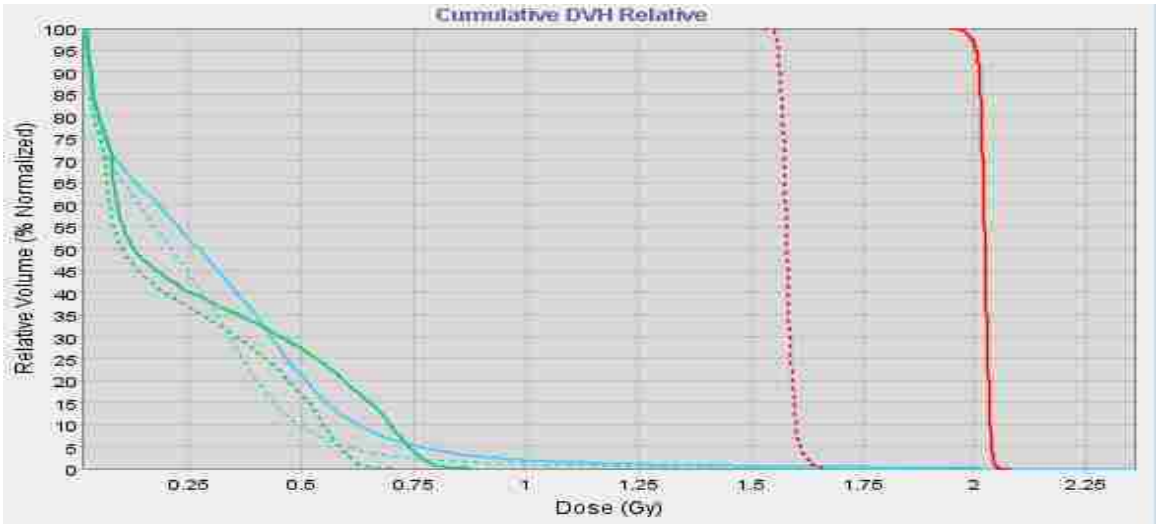

Figure 29. DVH comparison between the planned (solid) and reconstructed (dashed) for (a) planned delivery, (b) -30 msec offset to center leaf delivery and (c) -30 msec offset to all leaves delivery from the lung study

(c)

3.4 Aim 4: Comparison of the Measured Dose Versus Reconstructed Dose

3.4.1 Point Dose Comparison

Daily ion chamber measurements for each plan consisted of two readings. The readings on any given day varied little, and their average value was used for comparison with the model. Comparisons between the average measured dose and average reconstructed (DV) dose from deliveries with no intentional offset of the H&N, prostate and lung plans are shown in Tables 5, 6 and 7, respectively.

Table 5. Point dose comparison between the measured and the DV dose from DVPA for the H&N plan with no offset (planned dose = 2.037 Gy)

Delivered Plan (H&N)	Avg Measured Dose [Gy]	Avg DV Dose [Gy]	Diff.
Normal - Day 1	2.068	2.075	0.3%
Normal - Day 2	2.056	2.058	0.1%
Normal - Day 3	2.087	2.083	-0.2%
Normal - Day 4	2.040	2.040	0.0%
Normal - Day 5	2.030	2.033	0.1%
Normal - Day 6	2.054	2.066	0.6%

Table 6. Point dose comparison between the measured and the DV dose from DVPA for the prostate plan with no offset (planned dose = 2.063 Gy)

Delivered Plan (prostate)	Avg Measured Dose [Gy]	Avg DV Dose [Gy]	Diff.
Normal - Day 1	2.060	2.032	-1.4%
Normal - Day 2	2.061	2.039	-1.0%
Normal - Day 3	2.071	2.044	-1.3%
Normal - Day 4	2.051	2.026	-1.2%
Normal - Day 5	2.065	2.054	-0.5%
Normal - Day 6	2.046	2.051	0.2%
Normal - Day 7	2.054	2.069	0.7%

Table 7. Point dose comparison between the measured and the DV dose from DVPA for the prostate plan with no offset (planned dose = 2.022 Gy)

Delivered Plan (lung)	Avg Measured Dose [Gy]	Avg DV Dose [Gy]	Diff.
Normal - Day 1	1.975	1.958	-0.9%
Normal - Day 2	1.970	1.954	-0.8%
Normal - Day 3	1.969	1.973	0.2%
Normal - Day 4	1.972	1.990	0.9%
Normal - Day 5	1.951	1.970	1.0%

The results show agreement between the DVPA model and the measured dose to within 2% for all cases studied. The slightly lower dose measured for the lung treatment plan was also reproduced by the DVPA software in Table 8.

Table 8. Summary of the mean differences and their standard deviation over all measurements delivered with no intentional offset for each plan

Plan	Mean Diff. (%)	±	σ
H&N	0.12	±	0.34
Prostate	-0.64	±	0.82
Lung	0.08	±	1.66

Figures 30 through 32 displays the statistical variations and comparisons of the measured and reconstructed point dose data relative to the planned point dose for all plans.

Comparisons between measured and reconstructed doses for deliveries with intentional leaf open time errors are shown in Tables 9, 10 and 11. The results show that the DVPA is able to predict the delivered dose to within 2% for all three plans that had variable leaf open time offsets.

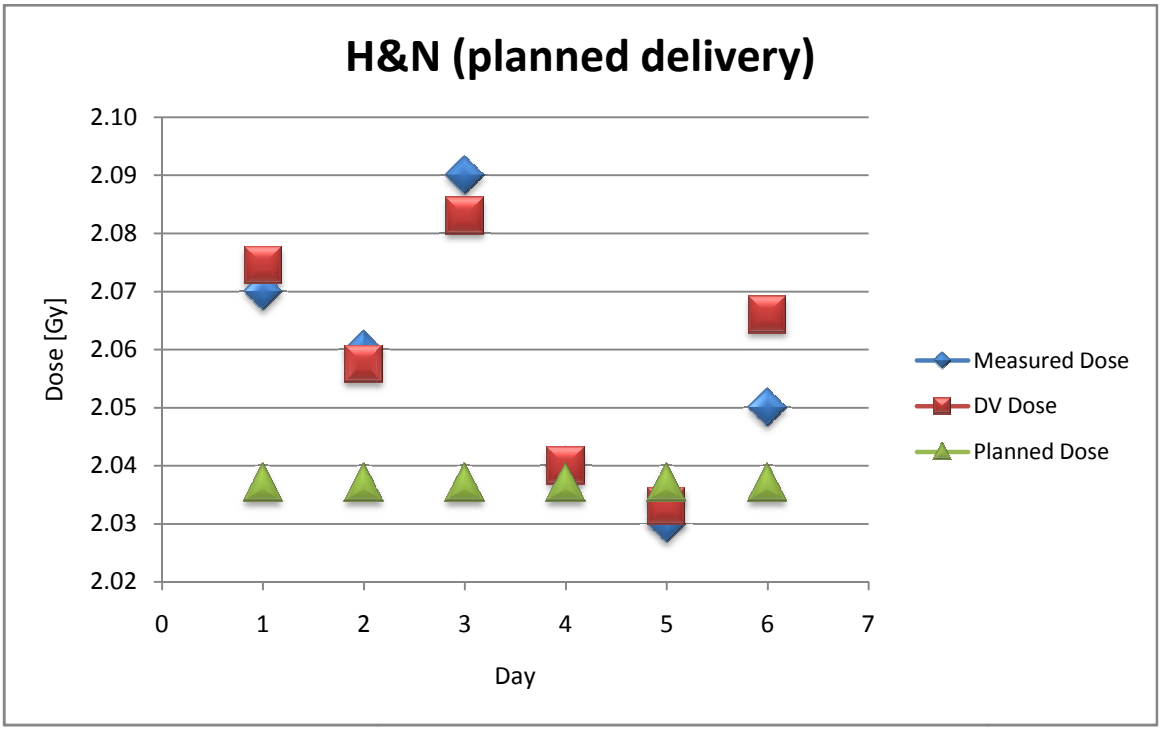

Figure 30. Statistical variations of the measured and reconstructed doses (DV dose) with no intentional offset in the deliveries for the H&N plan

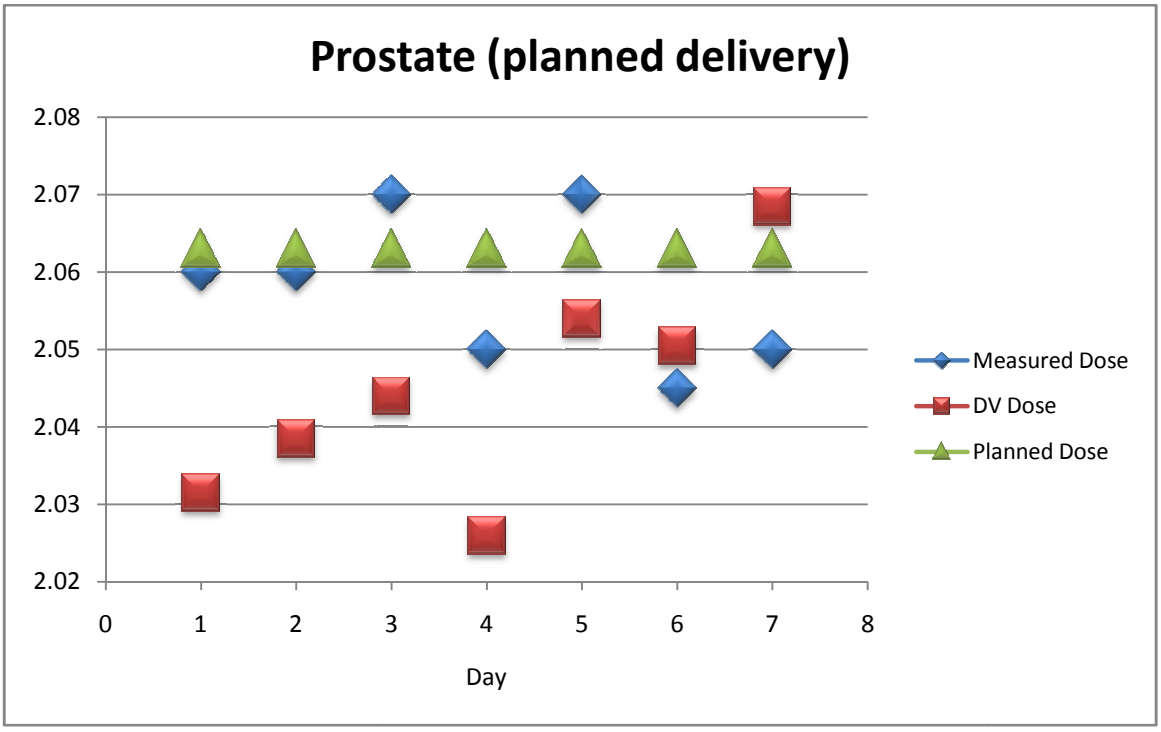

Figure 31. Statistical variations of the measured and reconstructed doses (DV dose) with no intentional offset in the deliveries for the prostate plan

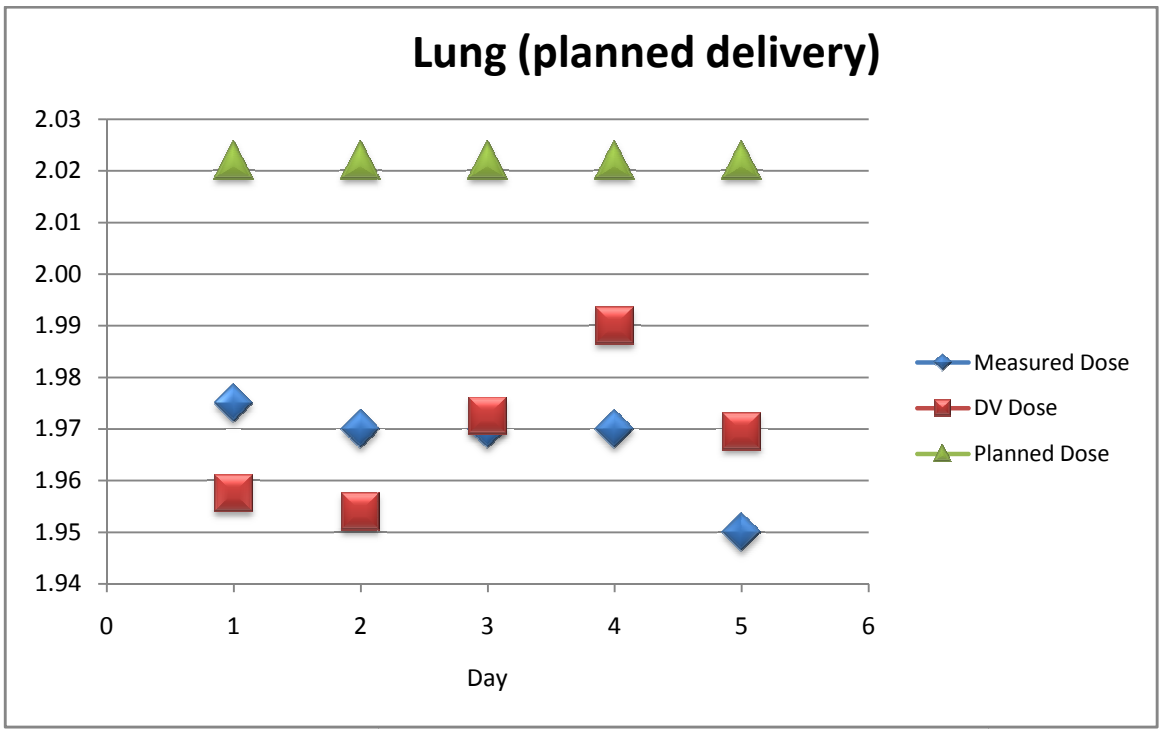

Figure 32. Statistical variations of the measured and reconstructed doses (DV dose) with no intentional offset in the deliveries for the lung plan

Table 9. Point dose comparison between the measured and the reconstructed dose from DVPA for the H&N plan with intentional leaf open time offset (planned dose = 2.037 Gy)

Delivered Plan (H&N)	Avg Measured Dose [Gy]	Avg DV Dose [Gy]	Diff.
All leaves -10 ms	1.90	1.897	0.1%
All leaves +10 ms	2.22	2.215	-0.2%
All leaves -30 ms	1.63	1.643	0.8%
All leaves +30 ms	2.49	2.498	0.5%
Leaf #27 -10 ms	2.07	2.062	-0.4%
Leaf #27 +10 ms	2.09	2.081	-0.5%
Leaf #33 +10 ms	2.09	2.081	-0.4%

Table 10. Point dose comparison between the measured and the reconstructed dose from DVPA for the prostate plan with intentional leaf open time offset (planned dose = 2.063 Gy)

Delivered Plan (Prostate)	Avg Measured Dose [Gy]	Avg DV Dose [Gy]	Diff.
All leaves -10 ms	1.91	1.882	-1.5%
All leaves +10 ms	2.20	2.177	-1.1%
All leaves -30 ms	1.60	1.582	-1.1%
All leaves +30 ms	2.50	2.471	-1.0%
Leaf #33 -10 ms	2.01	1.983	-1.4%
Leaf #33 +10 ms	2.11	2.101	-0.2%
Leaf #33 -30 ms	1.90	1.860	-2.1%
Leaf #33 +30 ms	2.21	2.226	0.7%

Table 11. Point dose comparison between the measured and the reconstructed dose from DVPA for the lung plan with intentional leaf open time offset (planned dose = 2.022 Gy)

Delivered Plan (Lung)	Avg Measured Dose [Gy]	Avg DV Dose [Gy]	Diff.
All leaves -10 ms	1.84	1.832	-0.4%
All leaves +10 ms	2.12	2.098	-1.0%
All leaves -30 ms	1.57	1.567	-0.2%
All leaves +30 ms	2.39	2.367	-1.0%
Leaf #32-33 -10ms	1.86	1.846	-0.8%
Leaf #32-33 +10ms	2.09	2.076	-0.7%
Leaf #32-33 -30ms	1.63	1.599	-1.6%
Leaf #32-33 +30ms	2.33	2.312	-0.8%

Table 12 summarizes the range of dose differences of each plan for intentional leaf open time offsets deliveries versus its reconstructed dose.

Table 12. Summary of the mean differences and their standard deviation over all measurements delivered with intentional leaf open time offset for each plan

Plan	Mean Diff. (%)	±	σ
H&N	0.12	±	0.34
Prostate	-0.64	±	0.82
Lung	0.08	±	1.66

Comparisons between measured and reconstructed doses for deliveries with intentional output errors are shown in Table 13 and 14.

Table 13. Point dose comparison between the measured and the reconstructed dose from DVPA for the prostate plan with intentional output offset (planned dose = 2.063 Gy)

Delivered Plan (Prostate)	Avg Measured Dose [Gy]	Avg DVPA Dose [Gy]	Diff.
Output +0.6%	2.08	2.072	-0.4%
Output +1.1%	2.09	2.085	-0.2%
Output +2.2%	2.11	2.097	-0.6%
Output +3.9%	2.15	2.127	-0.9%
Output -3.9%	1.96	1.969	0.4%

Table 14. Point dose comparison between the measured and the reconstructed dose from DVPA for the prostate plan with intentional output offset (planned dose = 2.022 Gy)

Delivered Plan (Lung)	Avg Measured Dose [Gy]	Avg DVPA Dose [Gy]	Diff.
Output -2.7%	1.91	1.901	-0.2%
Output +2.7%	2.03	2.007	-1.1%
Output +3.9%	2.07	2.048	-0.8%

3.4.2 Dose Distribution Comparison

Quantitative comparisons of distributions between calculated and measured film doses was achieved using the gamma statistic[24] computed on the TomoTherapy TPS Alpha6. Fifty-six films were digitized, converted to dose and read into the TPS in this study. Figure 33a display the gamma between the measured film dose and computed planned dose for a H&N planned delivery. The grayscale shows the background of the film and the color-wash represents the gamma index. Figure 33b is an isodose overlay in unit of Gy for the same dose distributions, where the solid lines represent film dose and the dashed represent planned dose. Figure 34 displays the profiles of the film and planned doses taken along the white crosshair in Figure 33a. Comparison between the film and reconstructed dose for the same H&N planned delivery is shown in Figure 35. Refer to Appendix A, Appendix B and Appendix C for additional dose distribution comparisons of the H&N, prostate and lung study, respectively.

For each film, a gamma distribution histogram was computed for all points contained within the selected region of interest. An example of the histogram is shown in Figure 37, which displays the computed cumulative gamma distribution. This graph plots the percentage of dose

points within the selected region (y-axis) which exceed a given gamma value (x-axis). An ideal cumulative histogram would have 100% at a gamma of 0, with 0% for all other points. In Figure 37, the percentage of points which fail the given criteria (i.e., $\gamma < 1$) is seen to be about 2% from the graph. Since the TomoTherapy TPS did not have the ability to export the gamma distribution, important points on the curve were recorded for each comparison. In addition to the percentage of points passing the criteria, the gamma index for which 90% and 95% of the measured points selected were recorded in order to get a sense of the shape of the curve in Figure 37 without having to display a figure for every gamma distribution.

Tables 15, 16 and 17 contain data that were taken from gamma distribution histograms of the H&N, prostate and lung plans, respectively. In general, the tables show that the DVPA software accurately predicts the dose distribution both for unmodified and modified deliveries. The percentage of points which pass the criteria exceeds 96% for all measured plans for both the H&N and lung deliveries. The agreements for the prostate treatment plan deliveries were not as good, in one case being as low as 72.74%.

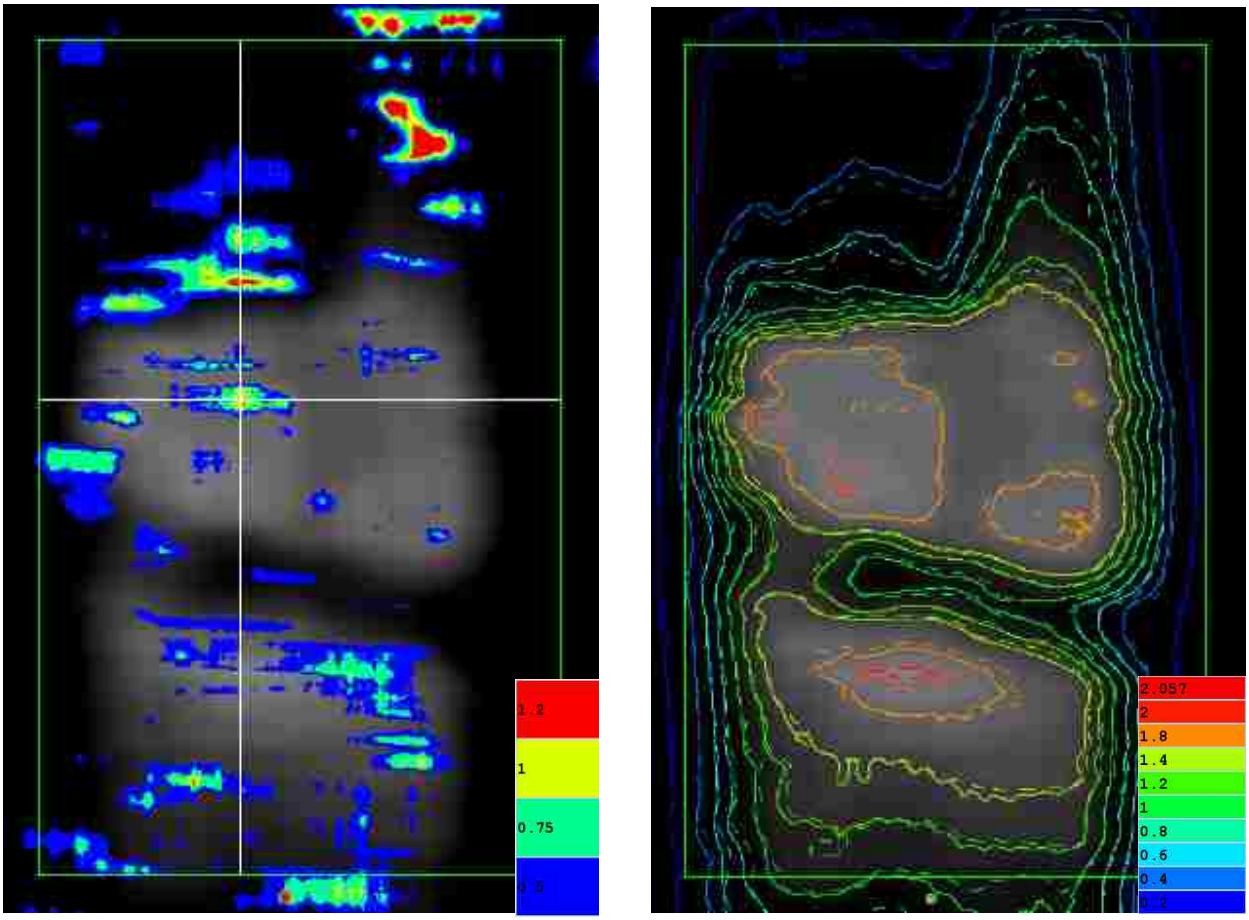

(a) (b)

Figure 33. (a) Gamma display and (b) isodose distribution of a film (solid) vs. planned (dashed) doses from the H&N plan delivery with no intentional offset

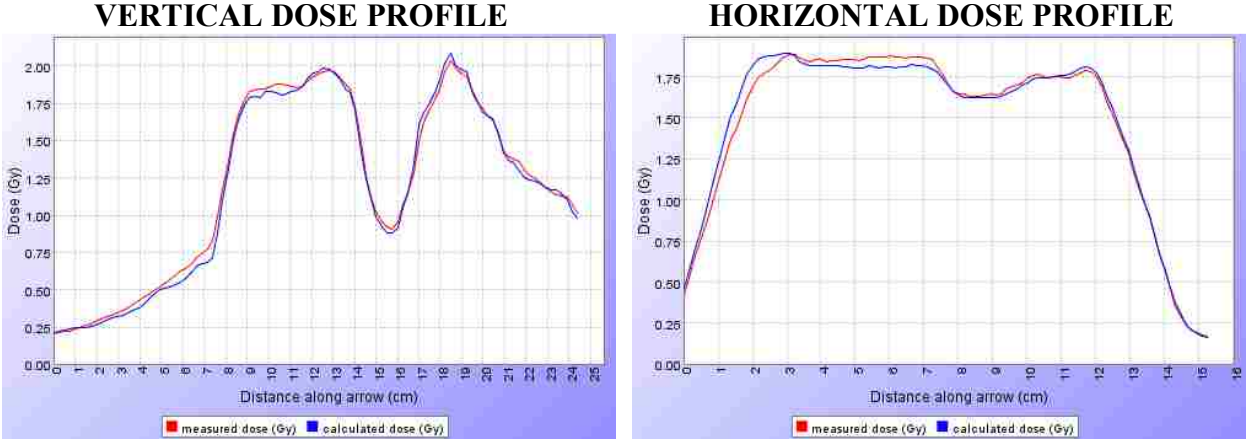

Figure 34. Dose profiles of the film (red) and planned (blue) in reference to the white crosshair in Figure 33a

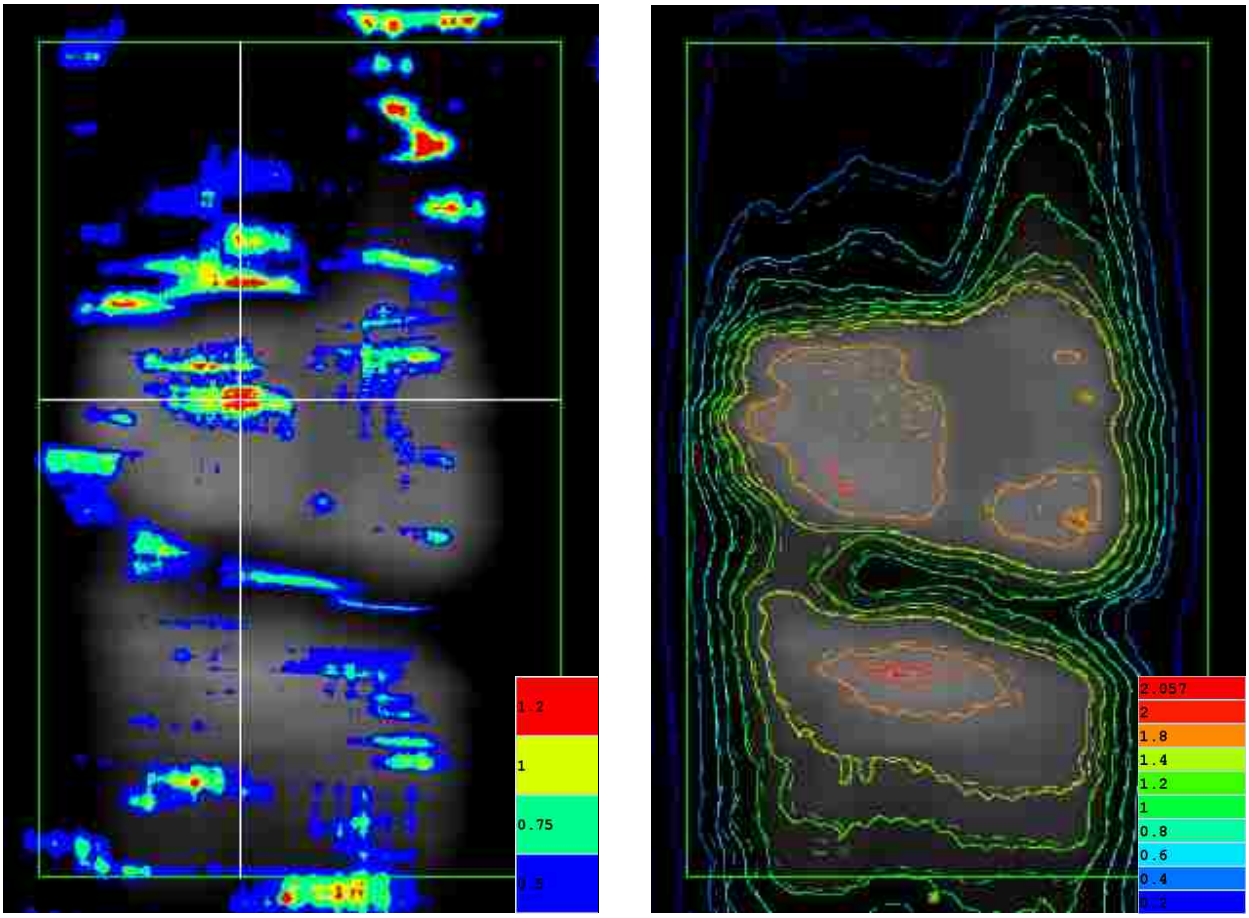

(a) (b)

Figure 35. (a) Gamma display and (b) isodose distribution of a film (solid) vs. reconstructed (dashed) doses from the H&N plan delivery with no intentional offset

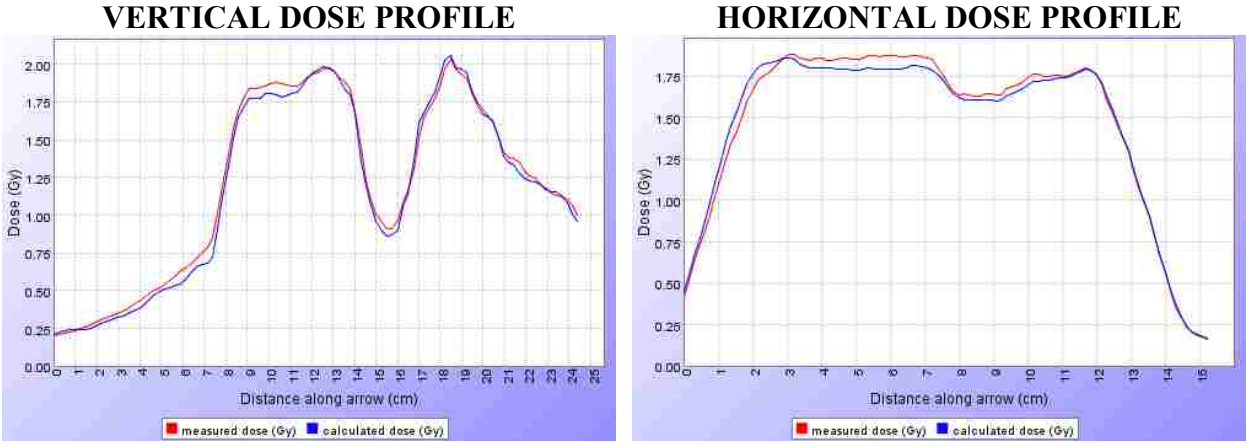

Figure 36. Dose profiles of the film (red) and reconstructed (blue) comparison in reference to the white crosshair in Figure 35a

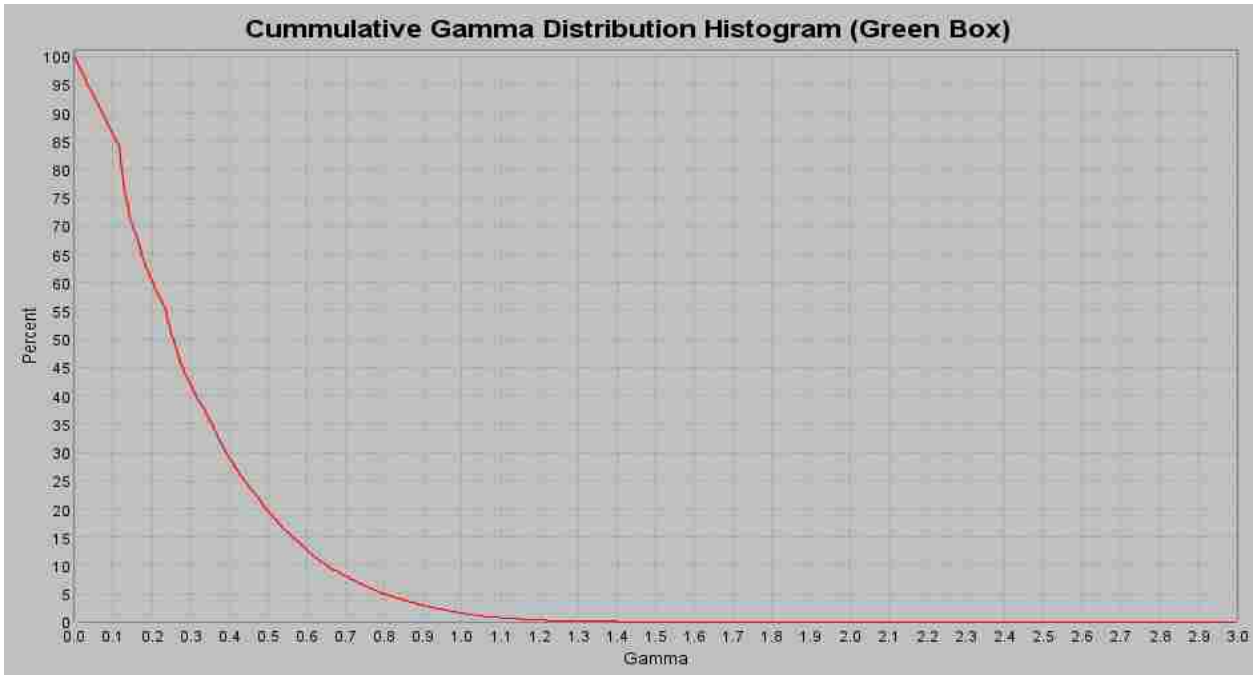

Figure 37. Illustration of the gamma distribution histogram taken over a selected region of interest

Table 15. Summary of the gamma distribution from film versus reconstructed doses for the H&N plan

Delivered Plan	% of pixel with Gamma < 1	Gamma index @ 10%	Gamma index @ 5%
Normal - Day 1	97.9%	0.63	0.80
Normal - Day 2	97.9%	0.62	0.80
Normal - Day 3	99.0%	0.60	0.73
Normal - Day 4	96.4%	0.68	0.90
Normal - Day 5	98.3%	0.66	0.80
All leaves -10 ms	97.1%	0.65	0.85
All leaves +10 ms	98.5%	0.65	0.80
Leaf #27 -10 ms	98.4%	0.67	0.81
Leaf #27 +10 ms	97.8%	0.71	0.85

Table 16. Summary of the gamma distribution from film versus reconstructed doses for the prostate plan

Delivered Plan	% of pixel with Gamma < 1	Gamma index @ 10%	Gamma index @ 5%
Prostate - Day 1 (#1)	91.1%	0.97	1.10
Prostate - Day 1 (#2)	90.9%	0.98	1.09
Prostate - Day 2 (#1)	95.4%	0.86	0.99
Prostate - Day 2 (#2)	97.5%	0.76	0.89
Prostate - Day 3 (#1)	89.1%	1.01	1.14
Prostate - Day 3 (#2)	92.0%	0.96	1.08
Prostate - Day 4 (#1)	87.8%	1.04	1.17
Prostate - Day 4 (#2)	89.8%	1.00	1.13
All leaves +10 ms (#1)	95.7%	0.84	0.97
All leaves +10 ms (#2)	95.4%	0.84	0.98
All leaves -10 ms (#1)	93.2%	0.92	1.06
All leaves -10 ms (#2)	96.9%	0.83	0.94
All leaves +30 ms (#1)	96.1%	0.79	0.94
All leaves +30 ms (#2)	94.5%	0.89	1.01
All leaves -30 ms (#1)	90.1%	1.00	1.09
All leaves -30 ms (#2)	89.5%	1.01	1.11
Leaf 32-33 +10 ms (#1)	94.2%	0.88	1.03
Leaf 32-33 +10 ms (#2)	92.4%	0.95	1.07
Leaf 32-33 -10 ms (#1)	95.1%	0.87	0.99
Leaf 32-33 -10 ms (#2)	96.7%	0.82	0.93
Leaf 32-33 +30 ms (#1)	91.0%	0.97	1.12
Leaf 32-33 +30 ms (#2)	90.8%	0.98	1.13
Leaf 32-33 -30 ms (#2)	89.4%	1.01	1.14

Table 17. Summary of the gamma distribution from film versus reconstructed doses for the prostate plan

Delivered Plan	% of pixel with Gamma < 1	Gamma index @ 90%	Gamma index @ 95%
Lung - Day 1 (#1)	99.9%	0.50	0.58
Lung - Day 1 (#2)	100.0%	0.47	0.54
Lung - Day 2 (#1)	99.8%	0.55	0.64
Lung - Day 2 (#2)	99.9%	0.63	0.71
Lung - Day 3 (#1)	99.4%	0.53	0.62
Lung - Day 4 (#1)	98.6%	0.66	0.78
All leaves -10 ms (#1)	100.0%	0.44	0.50
All leaves -10 ms (#2)	100.0%	0.37	0.42
All leaves +10 ms (#1)	100.0%	0.46	0.52
All leaves +10 ms (#2)	99.9%	0.44	0.50
All leaves -30 ms (#1)	100.0%	0.38	0.45
All leaves -30 ms (#2)	100.0%	0.34	0.41
All leaves +30 ms (#1)	100.0%	0.49	0.56
All leaves +30 ms (#2)	98.6%	0.75	0.84
Leaf 32-33 -10 ms (#1)	99.9%	0.56	0.63
Leaf 32-33 -10 ms (#2)	99.8%	0.58	0.65
Leaf 32-33 +10 ms (#1)	99.4%	0.67	0.76
Leaf 32-33 +10 ms (#2)	99.7%	0.60	0.69
Leaf 32-33 -30 ms (#1)	99.8%	0.57	0.65
Leaf 32-33 -30 ms (#2)	99.8%	0.56	0.64
Leaf 32-33 +30 ms (#1)	97.0%	0.76	0.90
Leaf 32-33 +30 ms (#2)	96.6%	0.77	0.90

CHAPTER 4. CONCLUSIONS

4.1 Conclusions

The purpose of this study was to verify that the method used for DV can determine the actual dose delivered during treatment to within 2% for point dose measurements in the PTV and a gamma of less than 1.0 to at least 90% of a selected region for planar dose distribution measurements. The investigated method accounted for variations in machine delivery due to beam output and/or leaf open time errors to determine the effective leaf open times for a given treatment delivery. A DR is then computed using the energy fluence determined by the effective leaf open times.

The following aims were used to determine the accuracy of the investigated method. For Aim 1, three treatment plans were generated using a homogenous cylindrical phantom (TomoPhantom). Contours from a H&N, prostate and lung patients were copied onto the phantom. Planning parameters and optimization used standard clinical protocols. The results for each plan resembled those of clinical patient plans.

In Aim 2, plans were delivered and measured twice per day for several days to observe the statistical variations in the delivery. In addition to the planned delivery, each plan were delivered with intentional offsets in the leaf open times and beam output. Detector data were extracted after each delivery to be used to determine the effective leaf open times.

Aim 3 consisted of using the effective leaf open times to generate the reconstructed dose of a delivery. It was shown that the method of dose reconstruction based on DV was able to account for changes in the delivery due to intentional offsets in leaf open times and/or beam output. Increasing the leaf open time to all leaves, for an entire delivery, lead to a reconstructed dose that has a higher dose to all structures relative to the planned dose. Similarly, decreasing

the leaf open time of the center two leaves lead to a lower reconstructed dose along the central axis of the phantom relative to the planned dose.

In Aim 4, comparisons were made between all measured dose and reconstructed dose. For point dose comparisons, differences between ion chamber measurements and reconstructed doses of all deliveries ranged from -2.1% to 0.9%. With the exception of one measurement having a difference of greater than 2% from the reconstructed dose, a majority of the differences were approximately -1%. For dose distribution comparisons, differences between film measurements and reconstructed doses for nearly all deliveries had a gamma index of less than 1 for over 90% of the region of interest.

The results from this study showed that the DV method employed by TomoTherapy DVPA software was able to reconstruct the delivered dose to within 2% of the measured point dose (using an ionization chamber) for the three plans with and without intentional delivery errors. Dose distribution comparison between the film and DVPA reconstructed dose showed significant improvements in agreement when compared to that between the film and planned dose. Gamma index distribution between the film and DVPA dose showed that over 85% of the dose distribution within the selected region for the three plans had a gamma value of less than 1.0.

4.2 Recommendation

This study did not include MVCT images acquired prior to deliveries for dose reconstruction. For actual patient treatments, daily variations in setup and anatomical position and/or shape exist. Therefore, use of the daily MVCT image is needed along with DV to properly reconstruct dose that was delivered. This requires that the IVDTs for both the kVCT and MVCT be accurate such that scans of the same object using either modality will result in the

same image (in terms of image value). Monthly quality assurance should be put in place to keep both IVDTs up-to-date. This would involve scanning a heterogeneous phantom, with known densities, on both a kVCT (used for diagnostic and treatment planning) and MVCT (treatment machine) scanner.

4.3 Future Study

This study showed that DV and DR can be used to accurately determine the delivered dose to a typical clinical treatment delivery. These tools provide the option to implement adaptive radiotherapy into a patient's treatment plan during the course of treatment to correct for any deviations from the planned dose. However, to properly utilize the full potential of adaptive radiotherapy, it is important to reconstruct the delivered dose based on the image of the patient during treatment (IGRT). A deformable registration will need to be applied to this current image in order to get an accurate idea of the dose delivered to the targets and critical structures.

By using the recommendation mentioned previously along with a system capable of deformable registration, DV and DR, one could perform clinical patient study to determine the importance of adaptive radiotherapy for helical tomotherapy. This would require a DR for every delivery of a patient's treatment. After the final treatment, a cumulative dose can be computed by summing the DRs for each delivery and comparing it to the planned dose.

REFERENCES

1. International Commission on Radiation Units and Measurements., *Prescribing, Recording, and Reporting Photon Beam Therapy*. (International Commission on Radiations Units and Measurements, Bethesda, 1993).

2. International Commission on Radiation Units and Measurements., *Prescribing, Recording, and Reporting Photon Beam Therapy (Supplement of ICRU Report 50)*. (International Commission on Radiations Units and Measurements, Bethesda, 1993).

3. G. A. Ezzell, J. M. Galvin, D. Low, J. R. Palta, I. Rosen, M. B. Sharpe, P. Xia, Y. Xiao, L. Xing and C. X. Yu, "Guidance document on delivery, treatment planning, and clinical implementation of IMRT: report of the IMRT Subcommittee of the AAPM Radiation Therapy Committee", Med Phys **30** (8), 2089-2115 (2003).

4. J. M. Galvin, G. Ezzell, A. Eisbrauch, C. Yu, B. Butler, Y. Xiao, I. Rosen, J. Rosenman, M. Sharpe, L. Xing, P. Xia, T. Lomax, D. A. Low and J. Palta, "Implementing IMRT in clinical practice: a joint document of the American Society for Therapeutic Radiology and Oncology and the American Association of Physicists in Medicine", Int J Radiat Oncol Biol Phys **58** (5), 1616-1634 (2004).

5. S. L. Meeks, W. Tome, L. G. Bouchet, A. C. Hass, J. M. Buatti and F. J. Bova, "Patient Positioning Using Optical and Ultrasound Techniques",in *Intensity-Modulated Radiation Therapy - The State of The Art*, edited by J. Palta and R. Mackie (Medical Physics Publishing, Madison, 2003), pp. 888.

6. D. A. Jaffray, "X-Ray-Guided IMRT",in *Intensity-Modulated Radiation Therapy - The State of The Art: American Association of Physicists in Medicine 2003 Summer School Proceedings*, edited by J. Palta and R. Mackie (Medical Physics Publishing, Madison, 2003), pp. 703-726.

7. D. A. Jaffray, "Kilovoltage volumetric imaging in the treatment room", Front Radiat Ther Oncol **40**, 116-131 (2007).

8. C. B. Saw, Y. Yang, F. Li, N. J. Yue, C. Ding, K. Komanduri, S. Huq and D. E. Heron, "Performance characteristics and quality assurance aspects of kilovoltage cone-beam CT on medical linear accelerator", Med Dosim **32** (2), 80-85 (2007).

9. J. Pouliot, A. Bani-Hashemi, J. Chen, M. Svatos, F. Ghelmansarai, M. Mitschke, M. Aubin, P. Xia, O. Morin, K. Bucci, M. Roach, 3rd, P. Hernandez, Z. Zheng, D. Hristov and L. Verhey, "Low-dose megavoltage cone-beam CT for radiation therapy", Int J Radiat Oncol Biol Phys **61** (2), 552-560 (2005).

10. R. Mackie, G. Olivera, J. Kapatoes, K. Ruchala, J. Balog, W. Tome, S. Hui, M. W. Kissick, C. Wu, R. Jeraj, P. Reckwerdt, P. Harari, M. Ritter, L. Forrest, J. Welsh and M. Mehta, "Helical Tomotherapy",in *Intensity-Modulated Radiation Therapy - The State of*

The Art: American Association of Physicists in Medicine 2003 Summer School Proceedings, edited by J. Palta and R. Mackie (Medical Physics Publishing, Madison, 2003), pp. 247-284.

11. J. M. Kapatoes, G. H. Olivera, P. J. Reckwerdt, E. E. Fitchard, E. A. Schloesser and T. R. Mackie, "Delivery verification in sequential and helical tomotherapy", Phys Med Biol **44** (7), 1815-1841 (1999).

12. R. M. Seibert, C. R. Ramsey, D. R. Garvey, J. W. Hines, B. H. Robison and S. S. Outten, "Verification of helical tomotherapy delivery using autoassociative kernel regression", Med Phys **34** (8), 3249-3262 (2007).

13. Q. Chen, "Delivery verification using exit detector data", Submitted to 2008 AAPM Annual Meeting (2008).

14. D. Yan, F. Vicini, J. Wong and A. Martinez, "Adaptive radiation therapy", Phys Med Biol **42** (1), 123-132 (1997).

15. K. M. Langen, S. L. Meeks, D. O. Poole, T. H. Wagner, T. R. Willoughby, P. A. Kupelian, K. J. Ruchala, J. Haimerl and G. H. Olivera, "The use of megavoltage CT (MVCT) images for dose recomputations", Phys Med Biol **50** (18), 4259-4276 (2005).

16. W. Lu, G. H. Olivera, Q. Chen, K. J. Ruchala, J. Haimerl, S. L. Meeks, K. M. Langen and P. A. Kupelian, "Deformable registration of the planning image (kVCT) and the daily images (MVCT) for adaptive radiation therapy", Phys Med Biol **51** (17), 4357-4374 (2006).

17. J. M. Kapatoes, G. H. Olivera, K. J. Ruchala, J. B. Smilowitz, P. J. Reckwerdt and T. R. Mackie, "A feasible method for clinical delivery verification and dose reconstruction in tomotherapy", Med Phys **28** (4), 528-542 (2001).

18. J. D. Fenwick, W. A. Tome, H. A. Jaradat, S. K. Hui, J. A. James, J. P. Balog, C. N. DeSouza, D. B. Lucas, G. H. Olivera, T. R. Mackie and B. R. Paliwal, "Quality assurance of a helical tomotherapy machine", Phys Med Biol **49** (13), 2933-2953 (2004).

19. M. R. McEwen and D. Niven, "Characterization of the phantom material virtual water in high-energy photon and electron beams", Med Phys **33** (4), 876-887 (2006).

20. P. R. Almond, P. J. Biggs, B. M. Coursey, W. F. Hanson, M. S. Huq, R. Nath and D. W. Rogers, "AAPM's TG-51 protocol for clinical reference dosimetry of high-energy photon and electron beams", Med Phys **26** (9), 1847-1870 (1999).

21. S. D. Thomas, M. Mackenzie, D. W. Rogers and B. G. Fallone, "A Monte Carlo derived TG-51 equivalent calibration for helical tomotherapy", Med Phys **32** (5), 1346-1353 (2005).

22. N. L. Childress, L. Dong and Rosen, II, "Rapid radiographic film calibration for IMRT verification using automated MLC fields", Med Phys **29** (10), 2384-2390 (2002).

23. N. L. Childress and Rosen, II, "Effect of processing time delay on the dose response of Kodak EDR2 film", Med Phys **31** (8), 2284-2288 (2004).

24. D. A. Low, W. B. Harms, S. Mutic and J. A. Purdy, "A technique for the quantitative evaluation of dose distributions", Med Phys **25** (5), 656-661 (1998).

APPENDIX A: H&N DOSE DISTRIBUTION COMPARISONS

Additional dose distribution comparisons of the H&N plan for various deliveries.

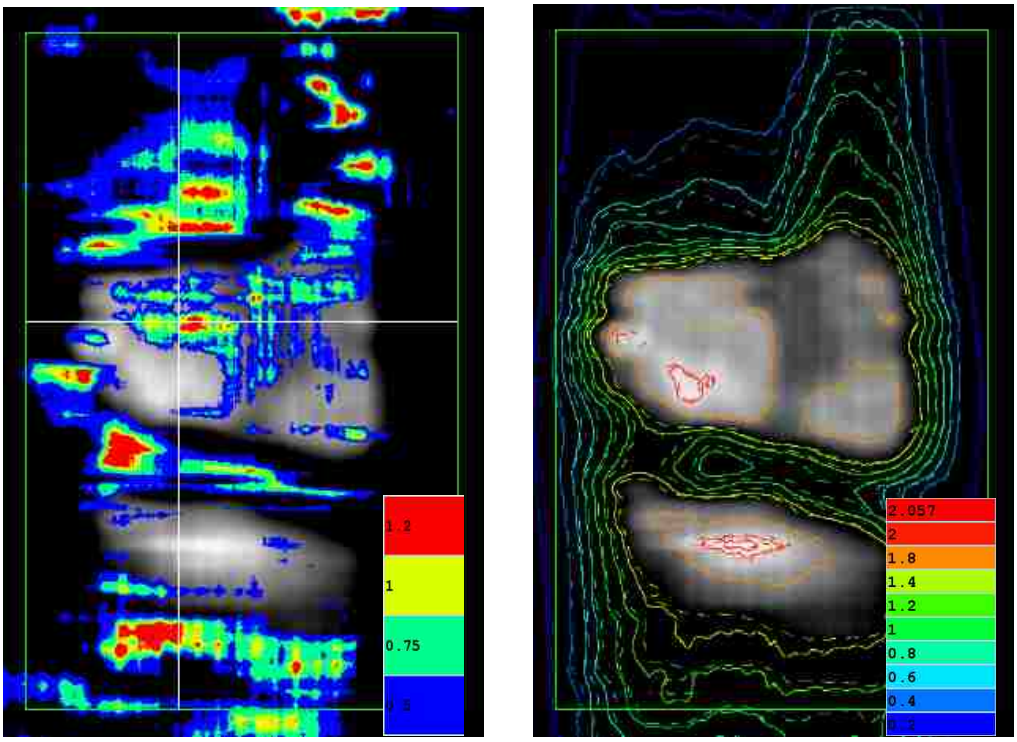

(a) **(b)**

Figure A1. (a) Gamma display and (b) isodose distribution of a film (solid) vs. planned (dashed) dose from the H&N plan delivery with +10 msec center leaf offset

VERTICAL DOSE PROFILE **HORIZONTAL DOSE PROFILE**

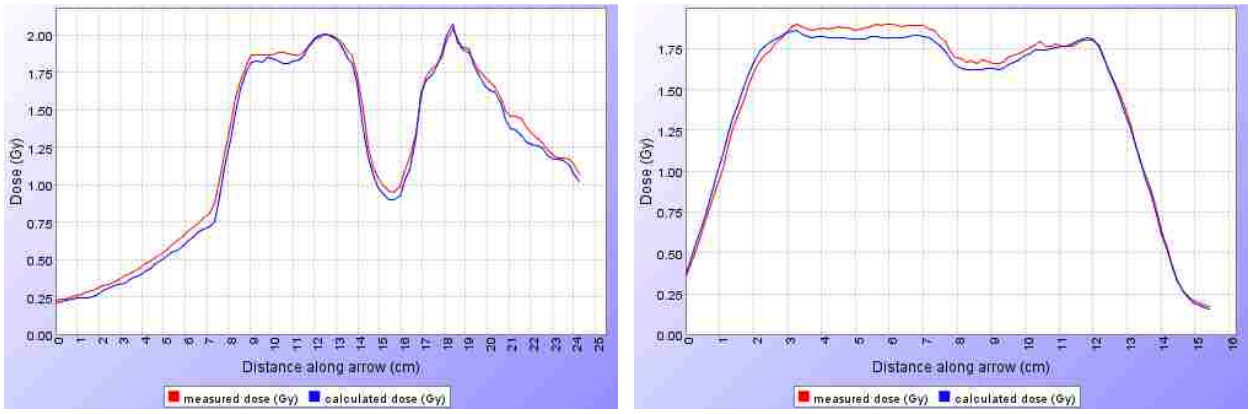

Figure A2. Dose profile of the film (red) and planned (blue) in reference to the white crosshair in Figure A1a

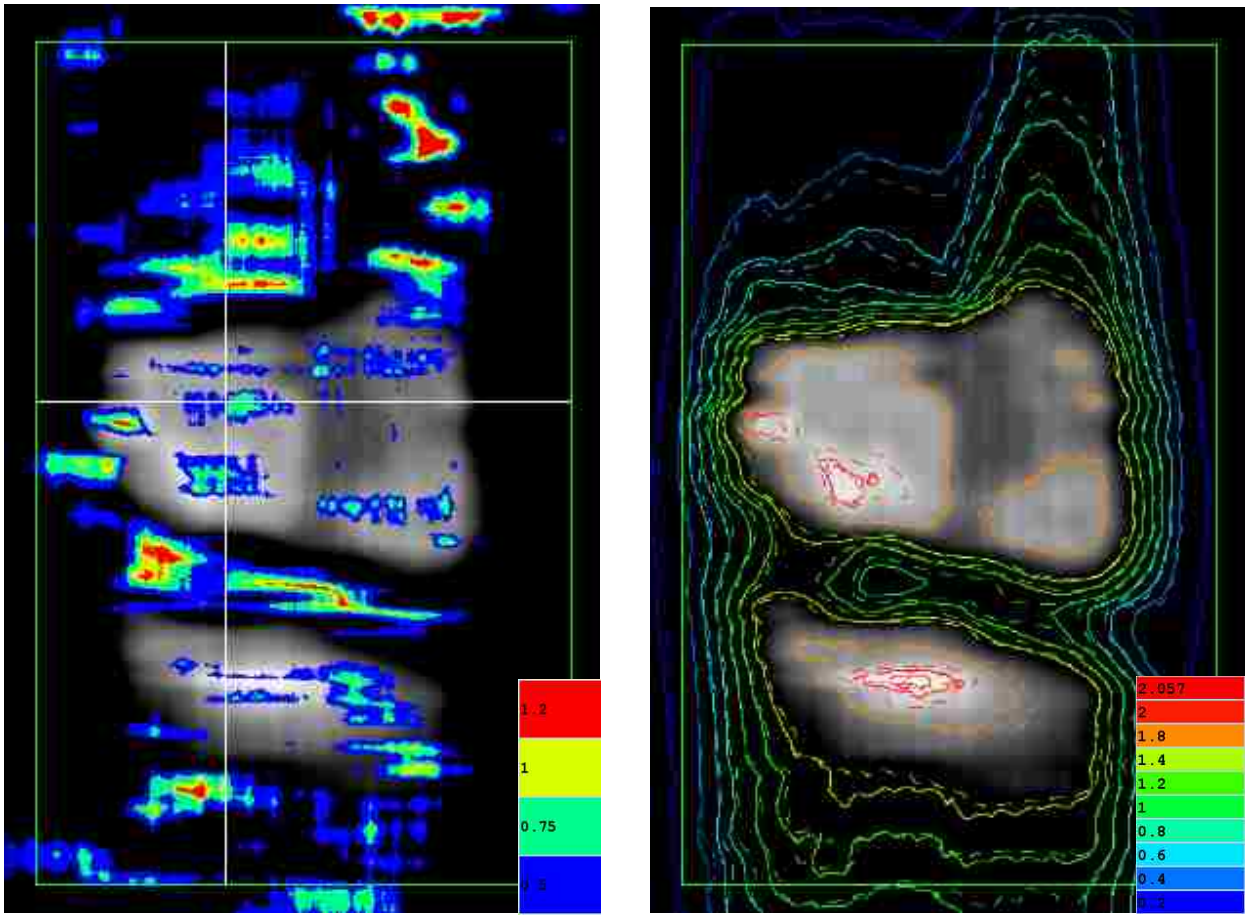

(a) (b)

Figure A3. (a) Gamma display and (b) isodose distribution of a film (solid) vs. reconstructed (dashed) dose from the H&N plan delivery with +10 msec center leaf offset

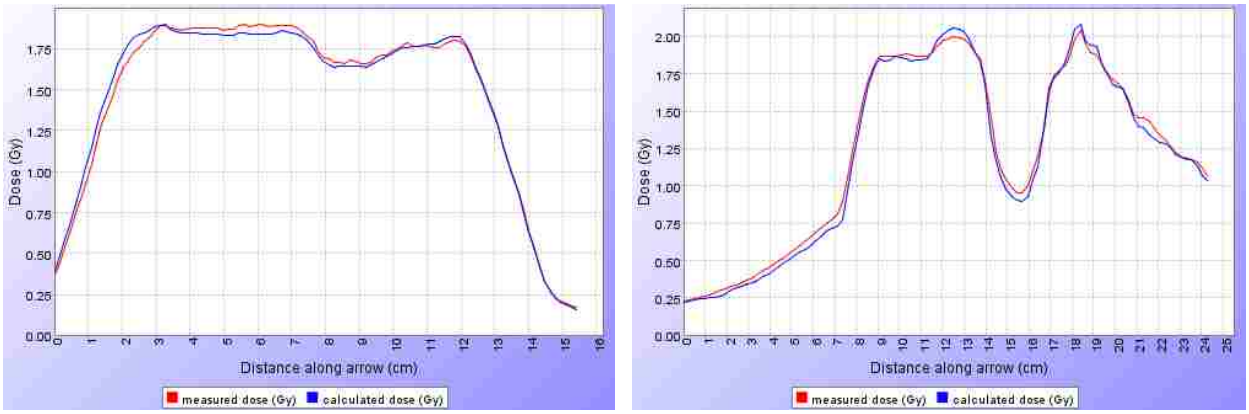

Figure A4. Dose profile of the film (red) and reconstructed (blue) in reference to the white crosshair in Figure A3a

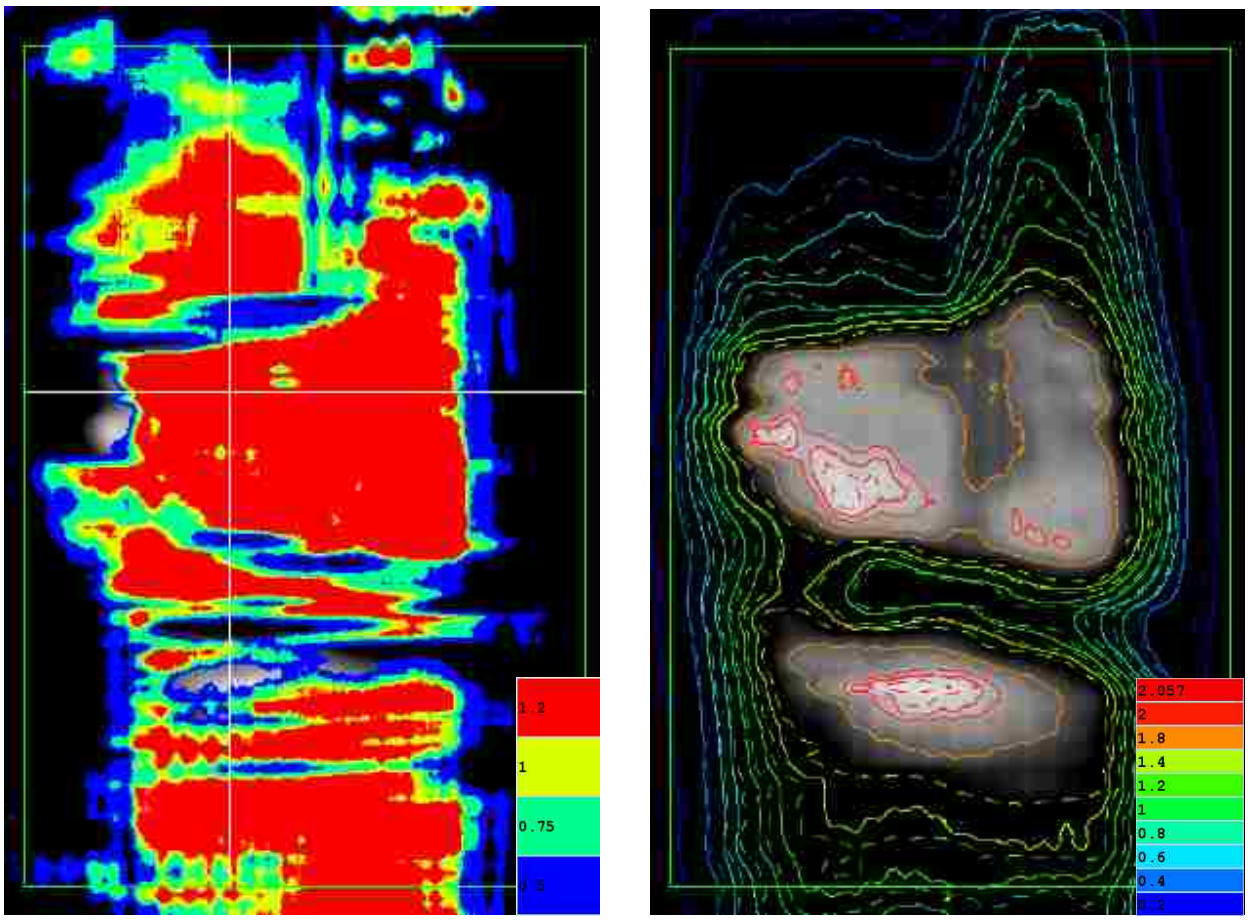

(a) (b)

Figure A5. (a) Gamma display and (b) isodose distribution of a film (solid) vs. planned (dashed) dose from the H&N plan delivery with +10 msec all leaves offset

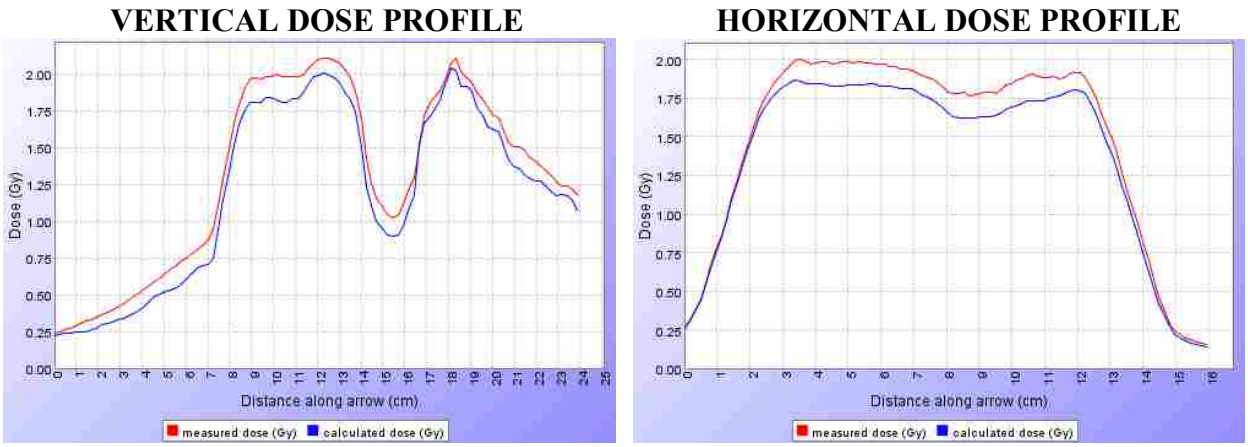

Figure A6. Dose profile of the film (red) and planned (blue) in reference to the white crosshair in Figure A5a

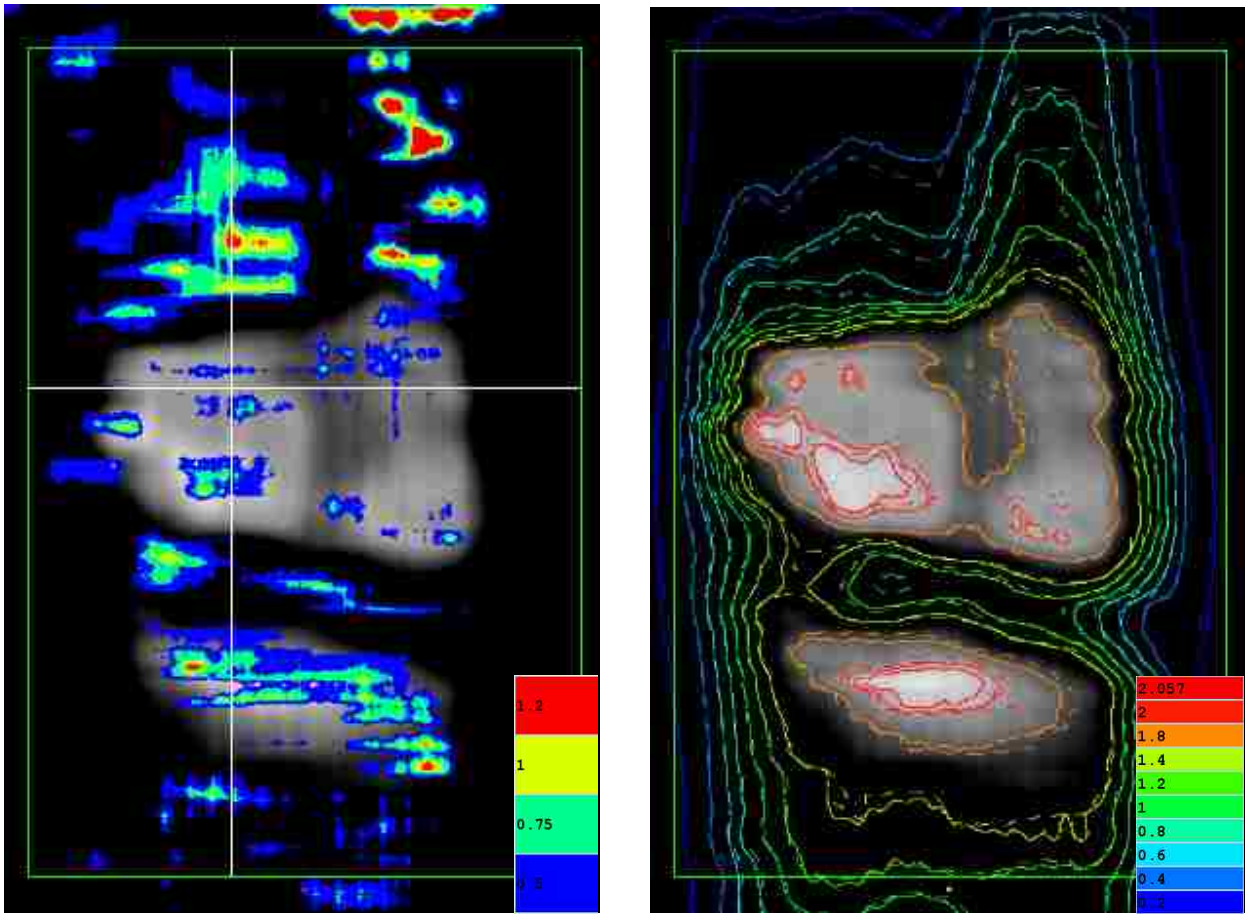

(a) (b)

Figure A7. (a) Gamma display and (b) isodose distribution of a film (solid) vs. reconstructed (dashed) dose from the H&N plan delivery with +10 msec all leaves offset

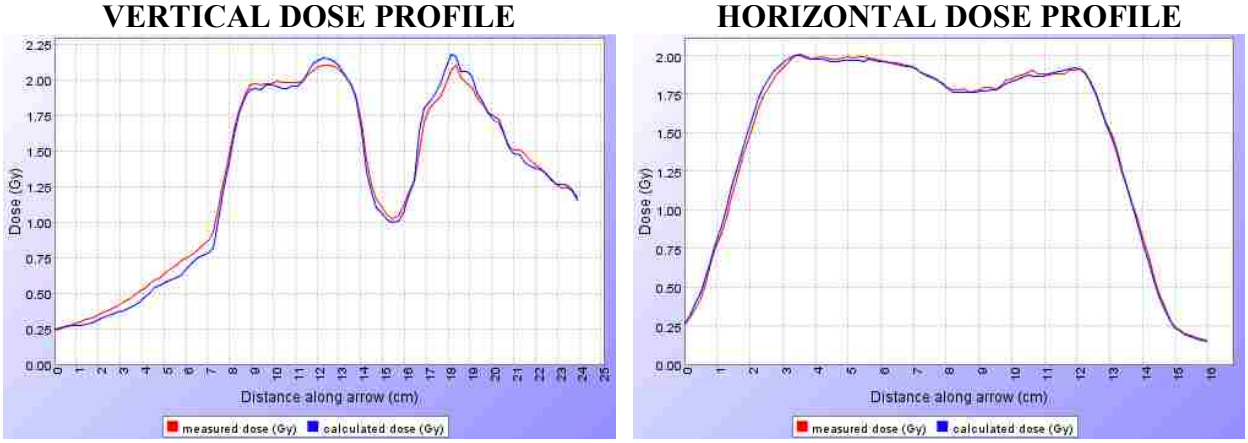

Figure A8. Dose profile of the film (red) and reconstructed (blue) in reference to the white crosshair in Figure A7a

APPENDIX B: PROSTATE DOSE DISTRIBUTION COMPARISONS

Dose distribution comparisons for multiple deliveries of the prostate plan.

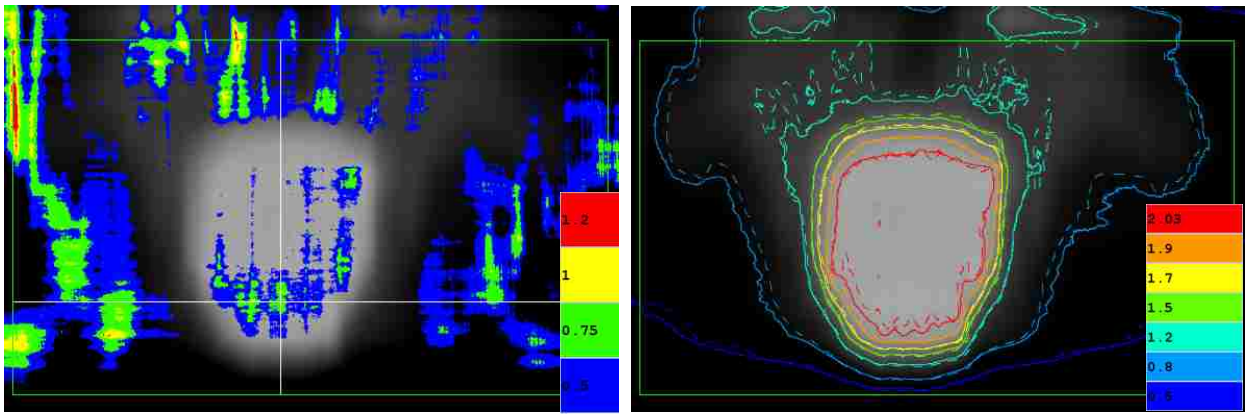

(a) **(b)**

Figure B1. (a) Gamma display and (b) isodose distribution of a film (solid) vs. planned (dashed) dose from the prostate plan delivery with no intentional offset (5/1/08)

VERTICAL DOSE PROFILE **HORIZONTAL DOSE PROFILE**

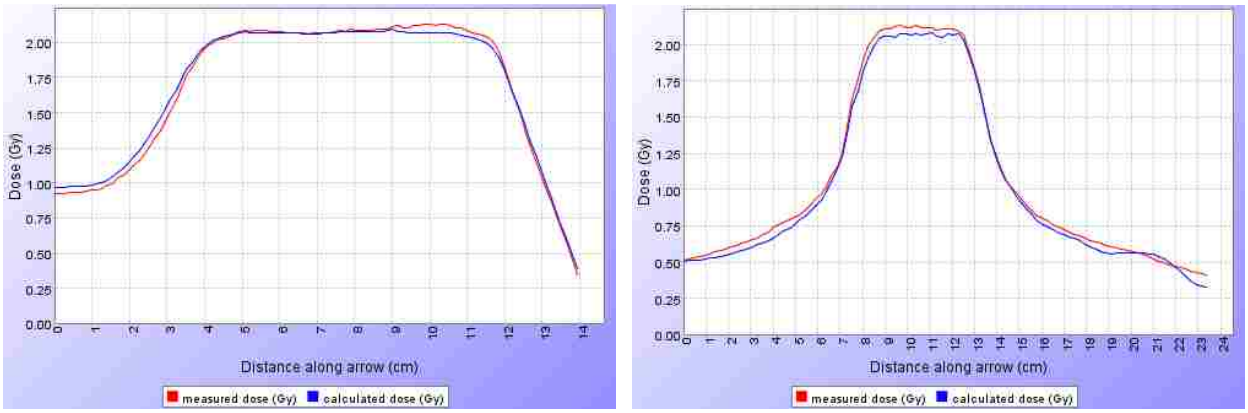

Figure B2. Dose profile of the film (red) and planned (blue) in reference to the white crosshair in Figure B1a

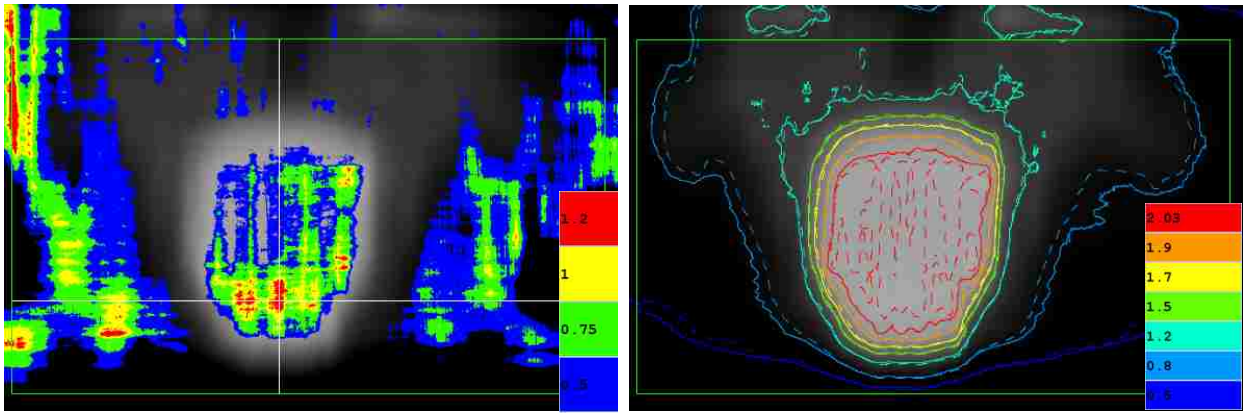

(a) (b)

Figure B3. (a) Gamma display and (b) isodose distribution of a film (solid) vs. reconstructed (dashed) dose from the prostate plan delivery with no intentional offset (5/1/08)

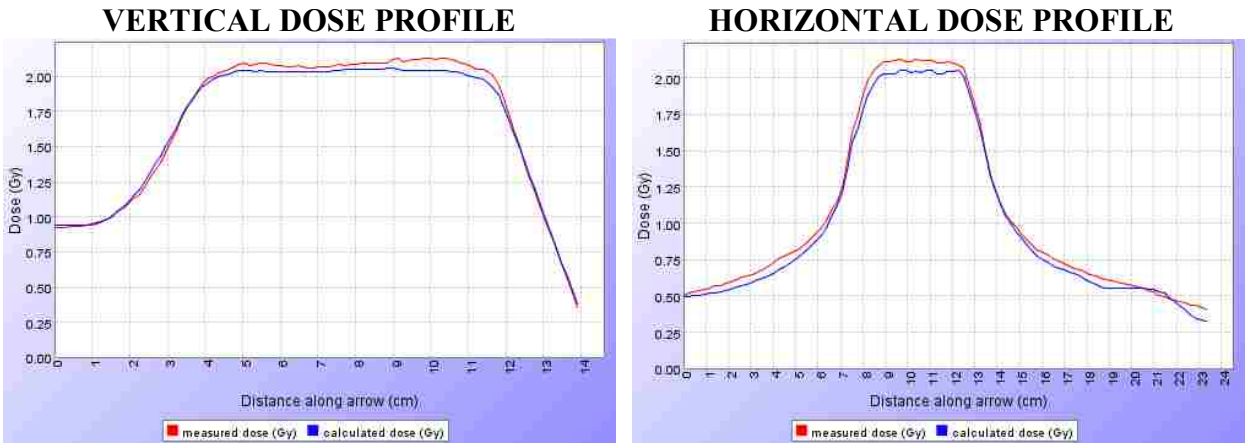

Figure B4. Dose profile of the film (red) and reconstructed (blue) in reference to the white crosshair in Figure B3a

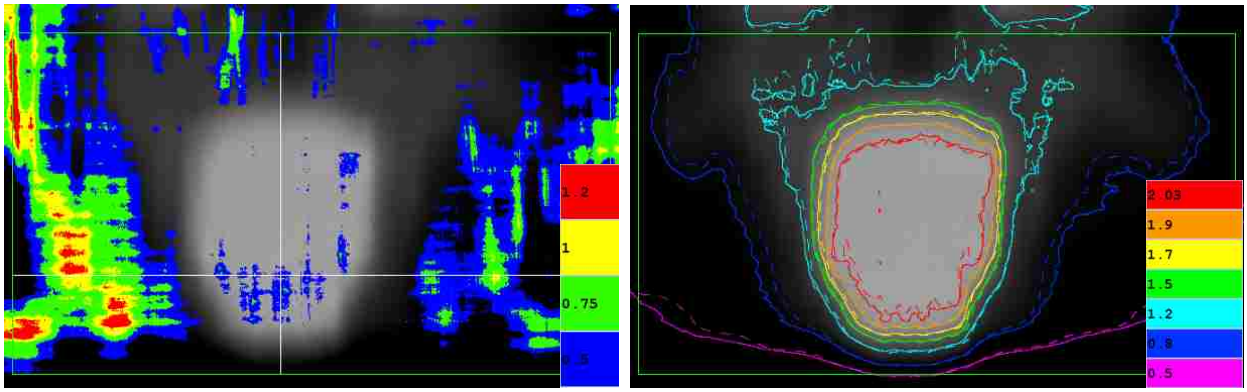

(a) **(b)**

Figure B5. (a) Gamma display and (b) isodose distribution of a film (solid) vs. planned (dashed) dose from the prostate plan delivery with no intentional offset (5/8/08)

VERTICAL DOSE PROFILE **HORIZONTAL DOSE PROFILE**

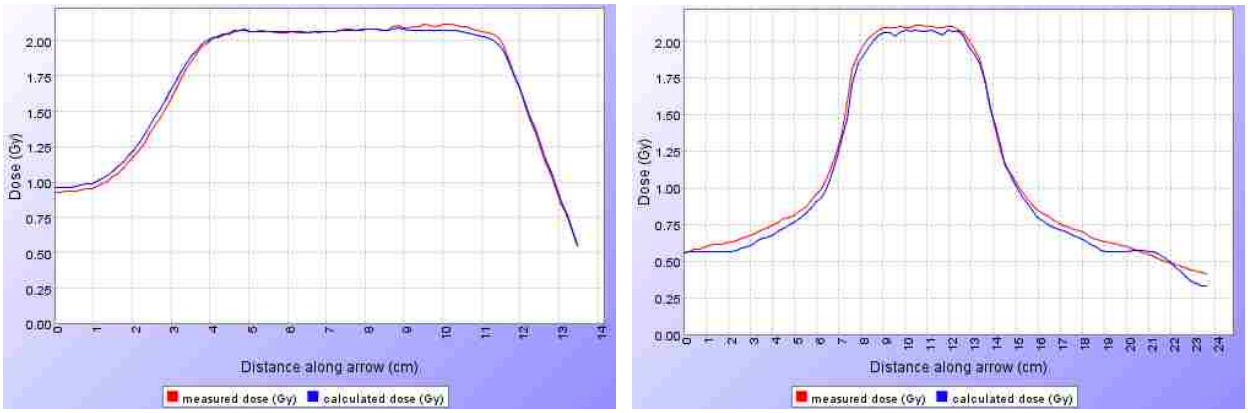

Figure B6. Dose profile of the film (red) and planned (blue) in reference to the white crosshair in Figure B5a

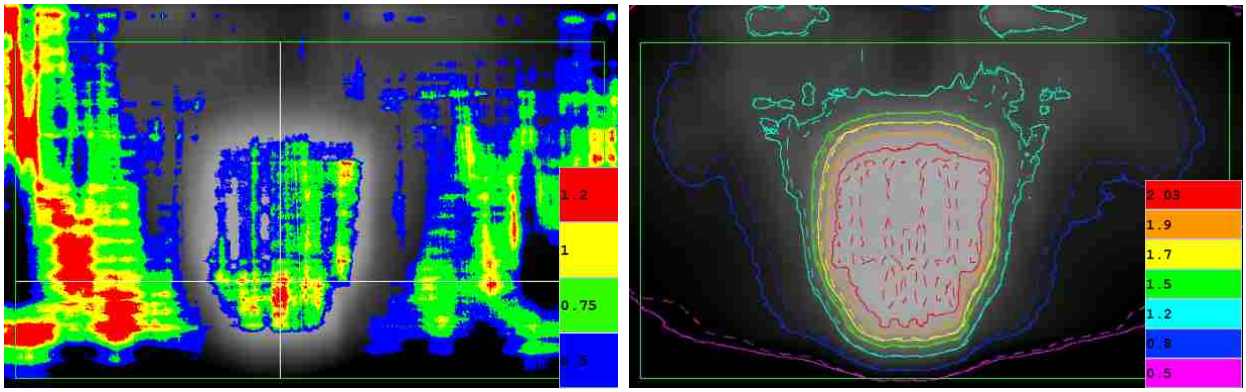

(a) (b)

Figure B7. (a) Gamma display and (b) isodose distribution of a film (solid) vs. reconstructed (dashed) dose from the prostate plan delivery with no intentional offset (5/8/08)

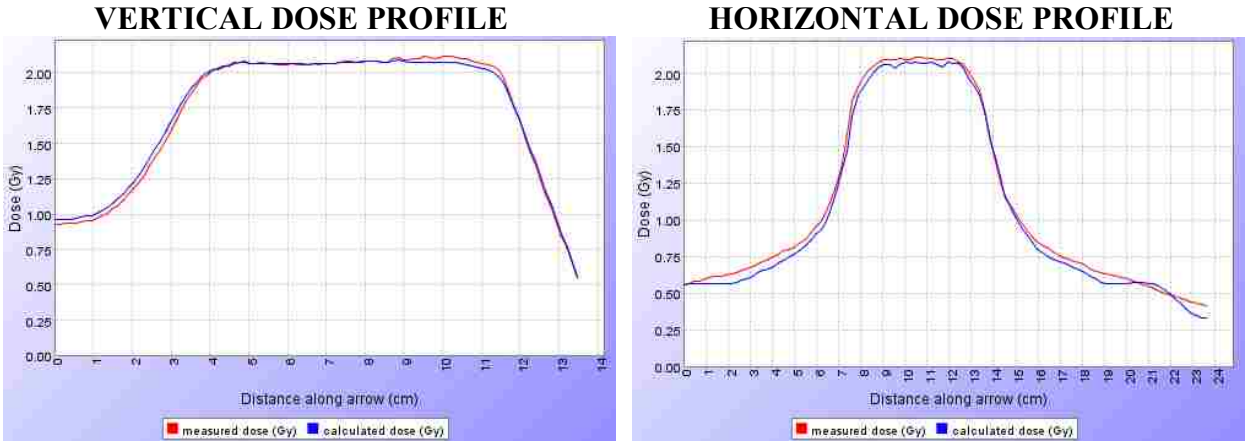

Figure B8. Dose profile of the film (red) and reconstructed (blue) in reference to the white crosshair in Figure B7a

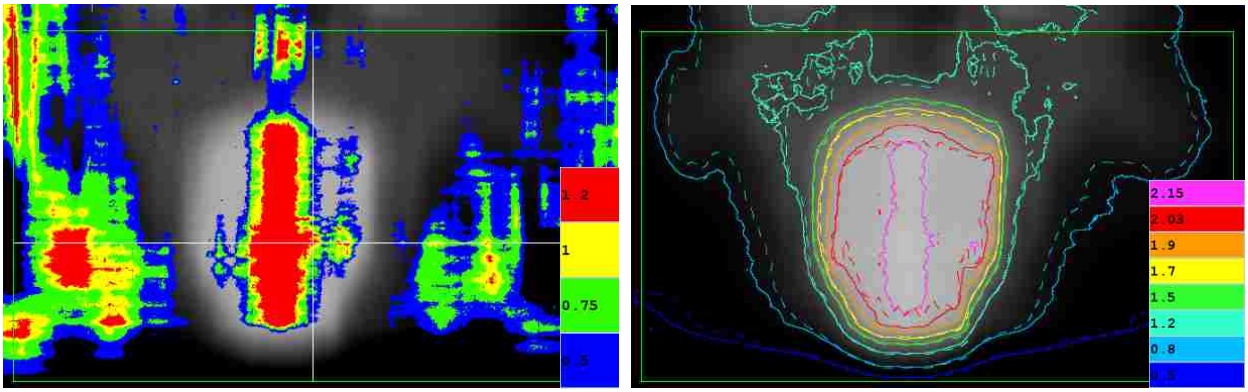

(a) (b)

Figure B9. (a) Gamma display and (b) isodose distribution of a film (solid) vs. planned (dashed) dose from the prostate plan delivery with +30 msec center leaf offset (5/8/08)

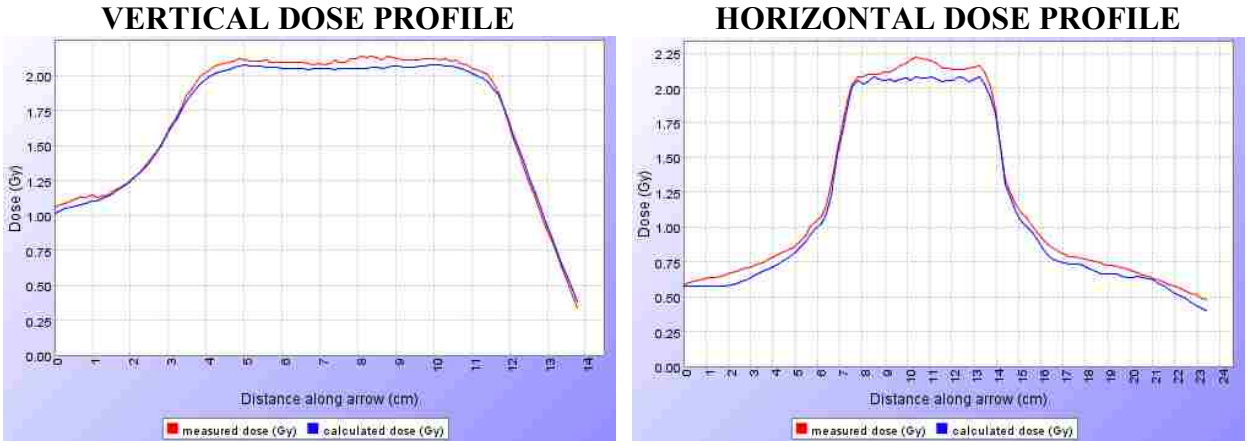

Figure B10. Dose profile of the film (red) and planned (blue) in reference to the white crosshair in Figure B9a

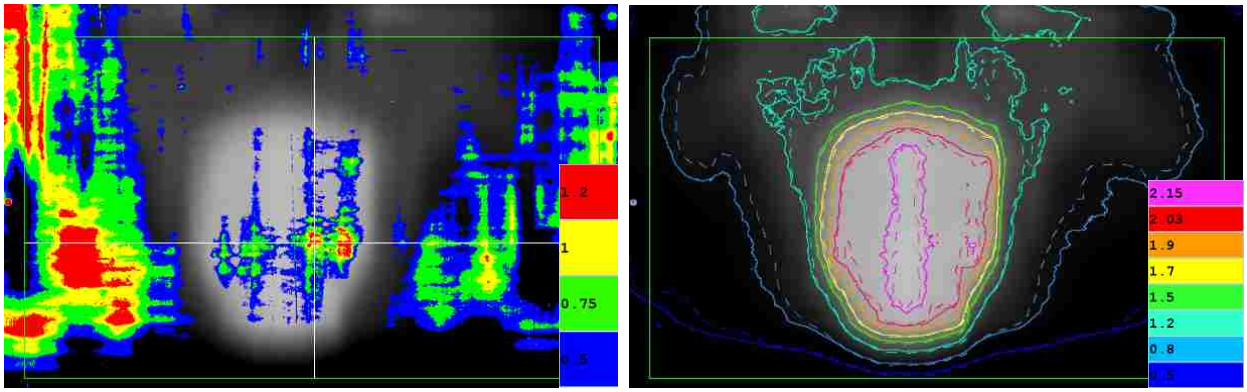

(a) **(b)**

Figure B11. (a) Gamma display and (b) isodose distribution of a film (solid) vs. reconstructed (dashed) dose from the prostate plan delivery with +30 msec center leaf offset (5/8/08)

VERTICAL DOSE PROFILE **HORIZONTAL DOSE PROFILE**

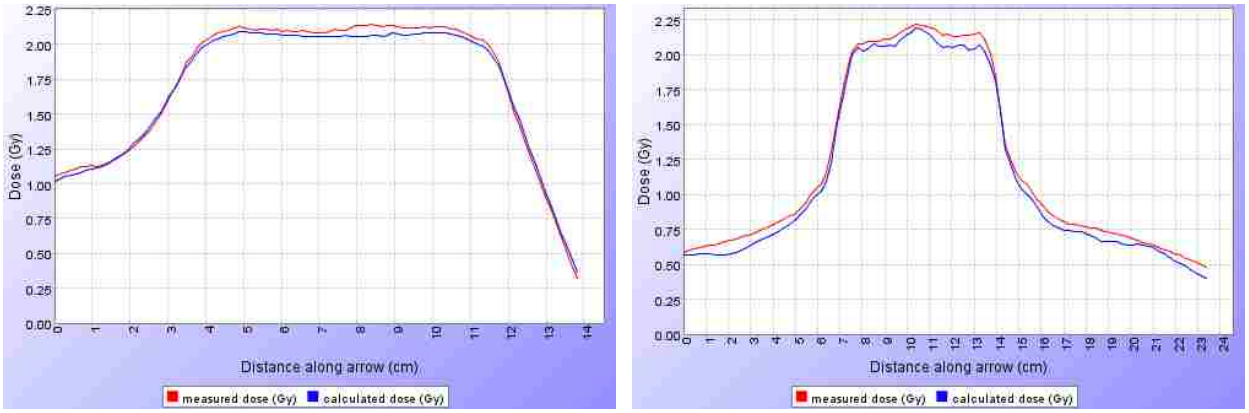

Figure B12. Dose profile of the film (red) and reconstructed (blue) comparison in reference to the white crosshair in Figure B11a

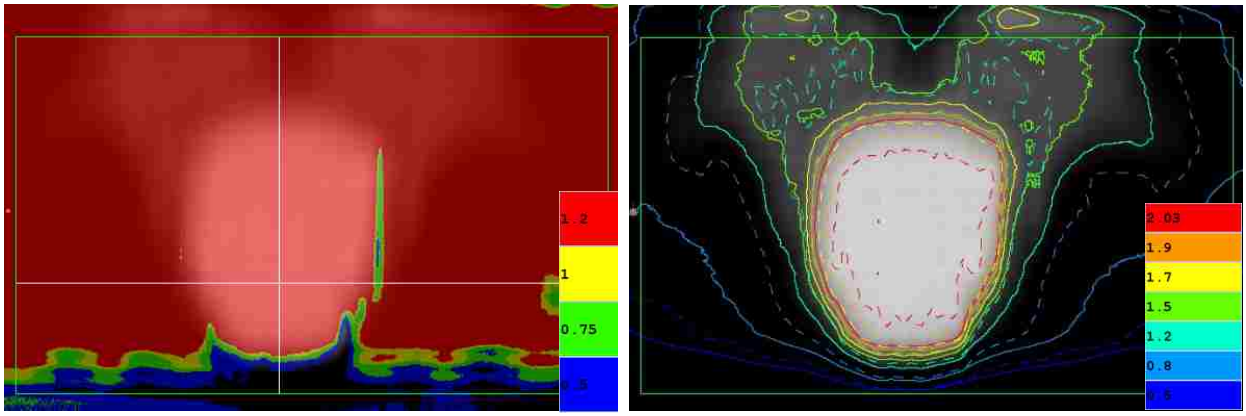

(a) (b)

Figure B13. (a) Gamma display and (b) isodose distribution of a film (solid) vs. planned (dashed) dose from the prostate plan delivery with +30 msec all leaves offset (5/1/08)

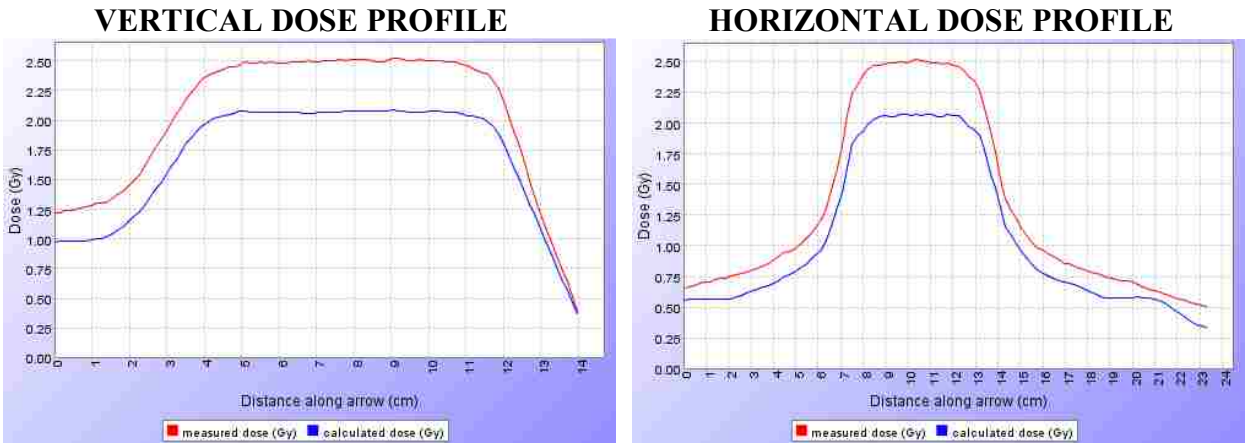

Figure B14. Dose profile of the film (red) and planned (blue) in reference to the white crosshair in Figure B13a

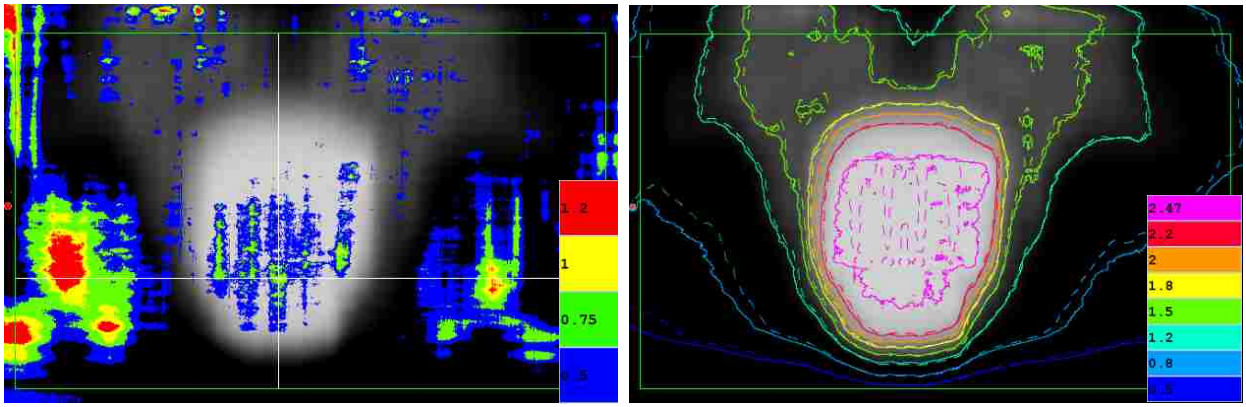

(a) **(b)**

Figure B15. (a) Gamma display and (b) isodose distribution of a film (solid) vs. reconstructed (dashed) dose from the prostate plan delivery with +30 msec all leaves offset (5/1/08)

VERTICAL DOSE PROFILE **HORIZONTAL DOSE PROFILE**

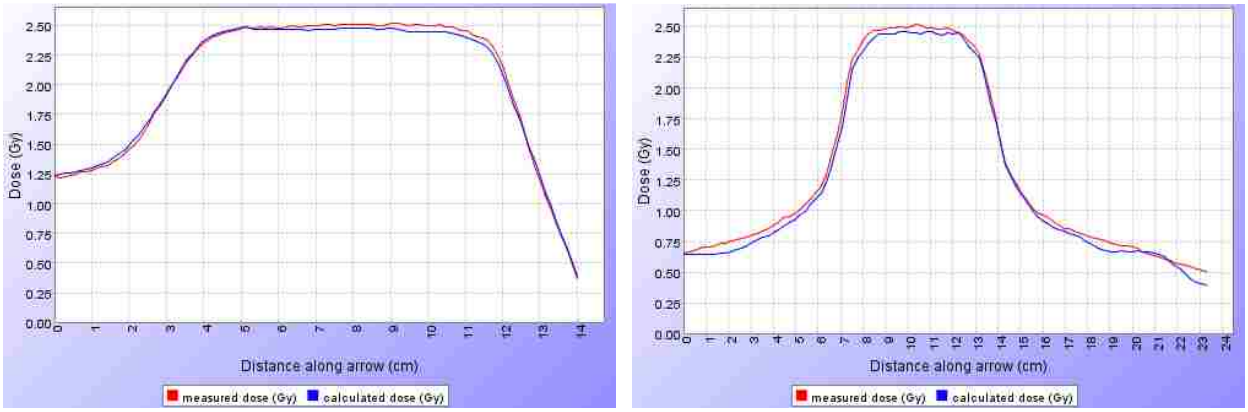

Figure B16. Dose profile of the film (red) and reconstructed (blue) in reference to the white crosshair in Figure B15a

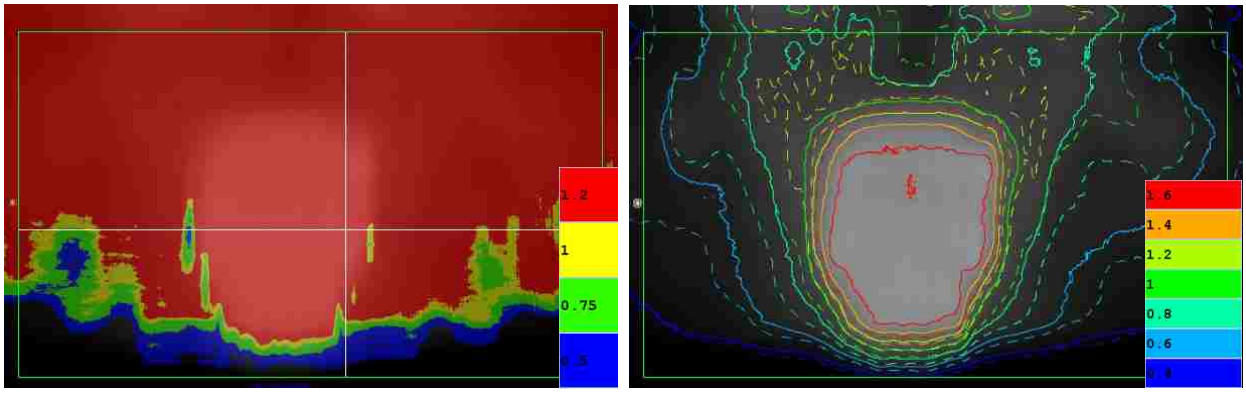

(a) (b)

Figure B17. (a) Gamma display and (b) isodose distribution of a film (solid) vs. planned (dashed) dose from the prostate plan delivery with -30 msec all leaves offset (5/1/08)

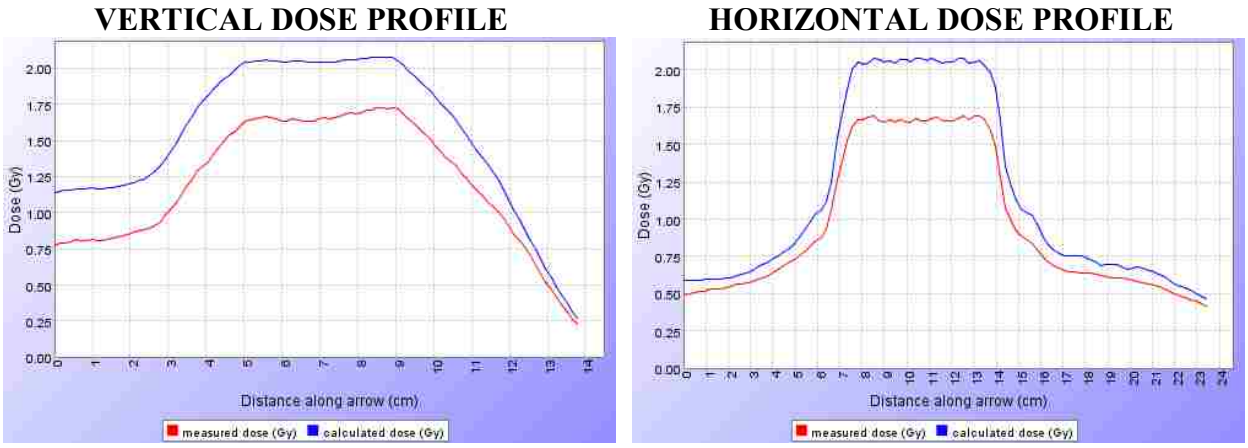

Figure B18. Dose profile of the film (red) and planned (blue) in reference to the white crosshair in Figure B17a

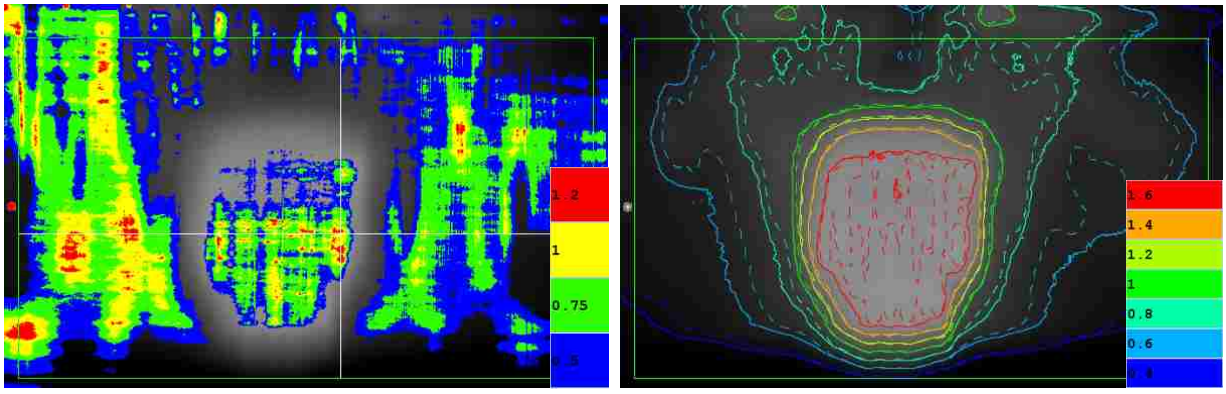

(a) **(b)**

Figure B19. (a) Gamma display and (b) isodose distribution of a film (solid) vs. reconstructed (dashed) dose from the prostate plan delivery with -30 msec all leaves offset (5/1/08)

VERTICAL DOSE PROFILE **HORIZONTAL DOSE PROFILE**

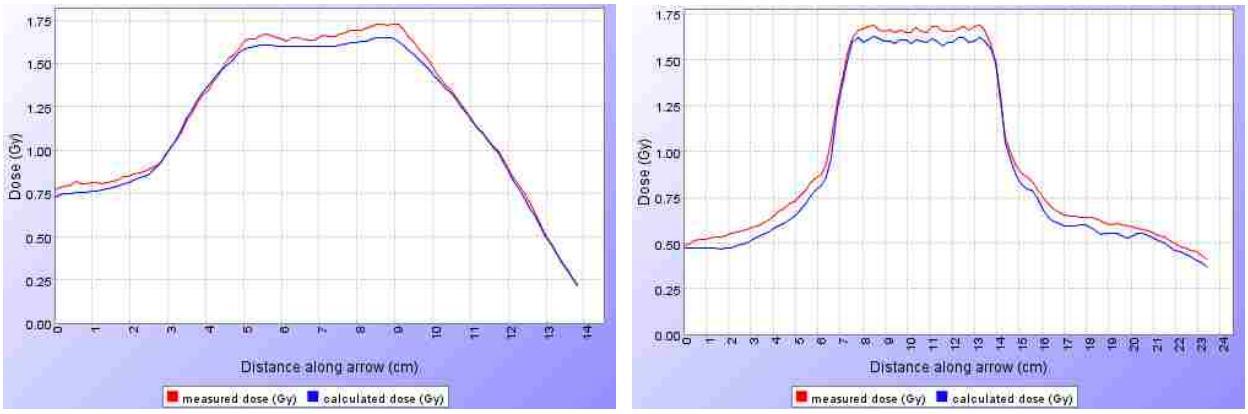

Figure B20. Dose profile of the film (red) and reconstructed (blue) in reference to the white crosshair in Figure B19a

APPENDIX C: LUNG DOSE DISTRIBUTION COMPARISONS

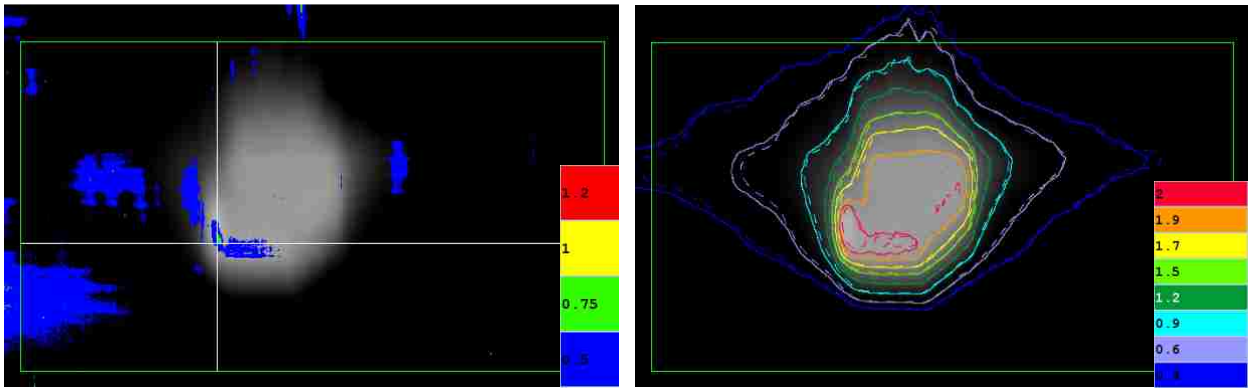

(a) **(b)**

Figure C1. (a) Gamma display and (b) isodose distribution of a film (solid) vs. planned (dashed) dose from the lung plan delivery with no intentional offset (5/30/08)

VERTICAL DOSE PROFILE **HORIZONTAL DOSE PROFILE**

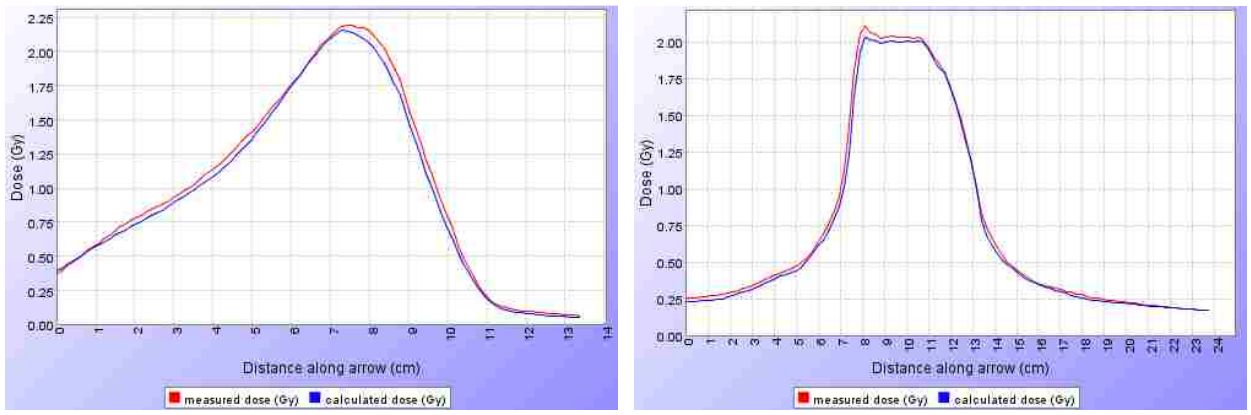

Figure C2. Dose profile of the film (red) and planned (blue) in reference to the white crosshair in Figure C1a

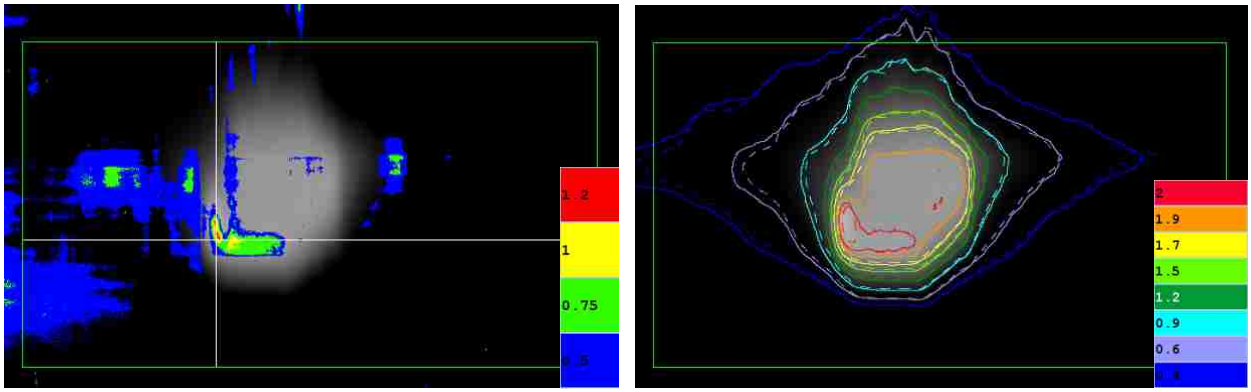

(a) (b)

Figure C3. (a) Gamma display and (b) isodose distribution of a film (solid) vs. reconstructed (dashed) dose from the lung plan delivery with no intentional offset (5/30/08)

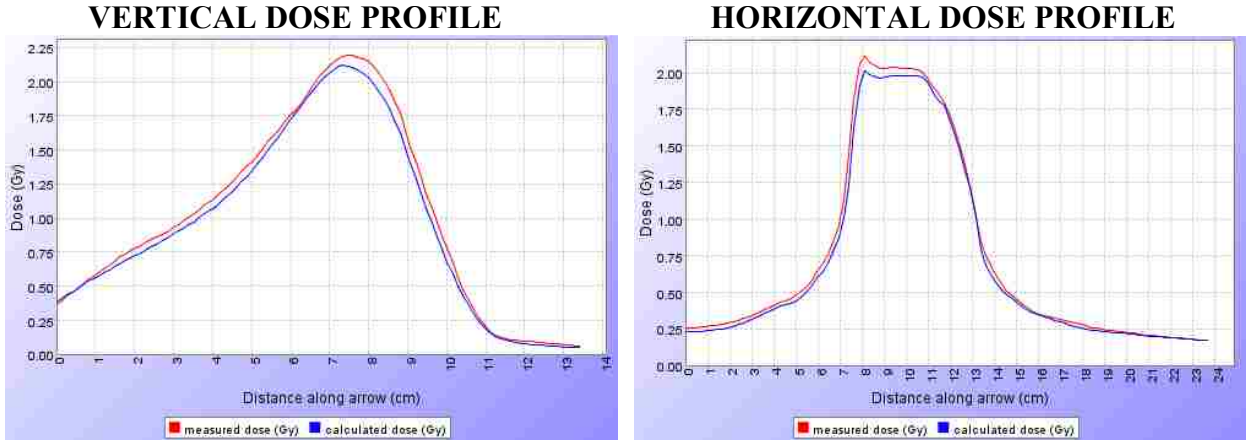

Figure C4. Dose profile of the film (red) and reconstructed (blue) in reference to the white crosshair in Figure C3a

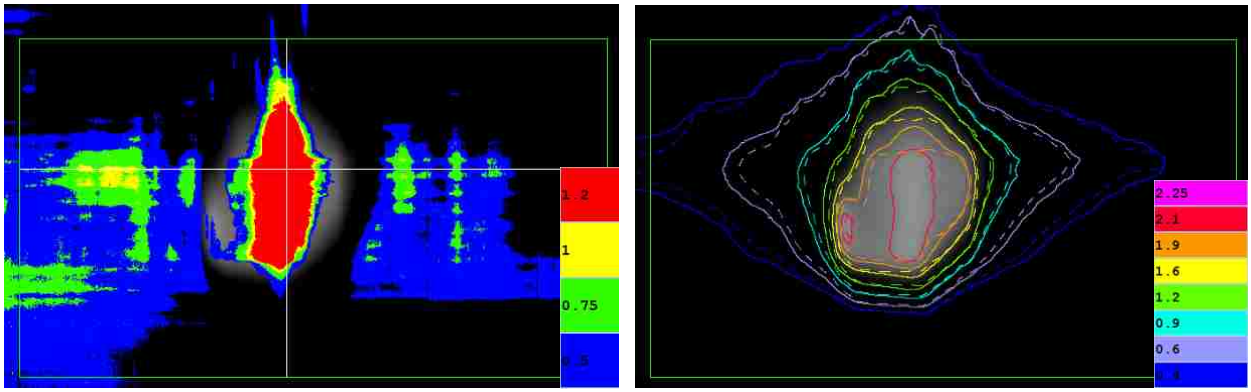

(a) **(b)**

Figure C5. (a) Gamma display and (b) isodose distribution of a film (solid) vs. planned (dashed) dose from the lung plan delivery with +30 msec center leaf offset (6/3/08)

VERTICAL DOSE PROFILE **HORIZONTAL DOSE PROFILE**

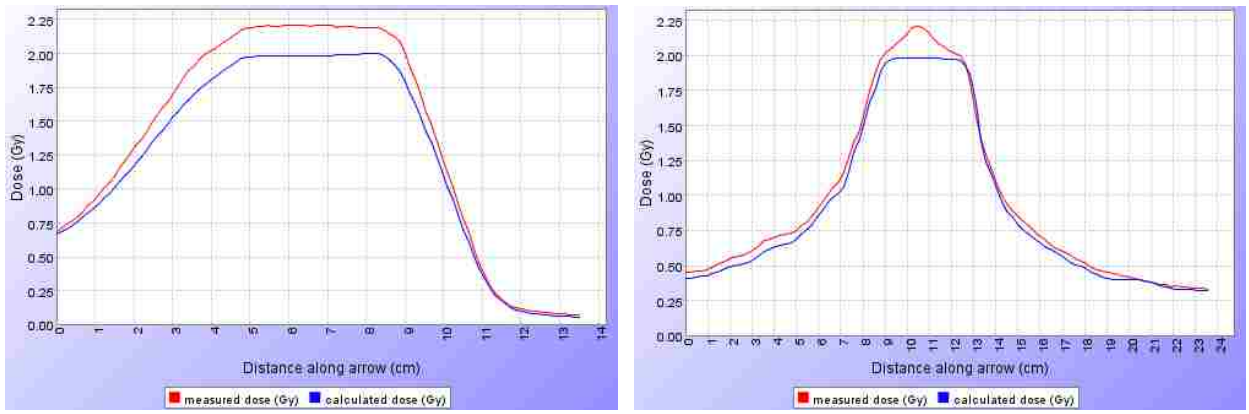

Figure C6. Dose profile of the film (red) and planned (blue) in reference to the white crosshair in Figure C5a

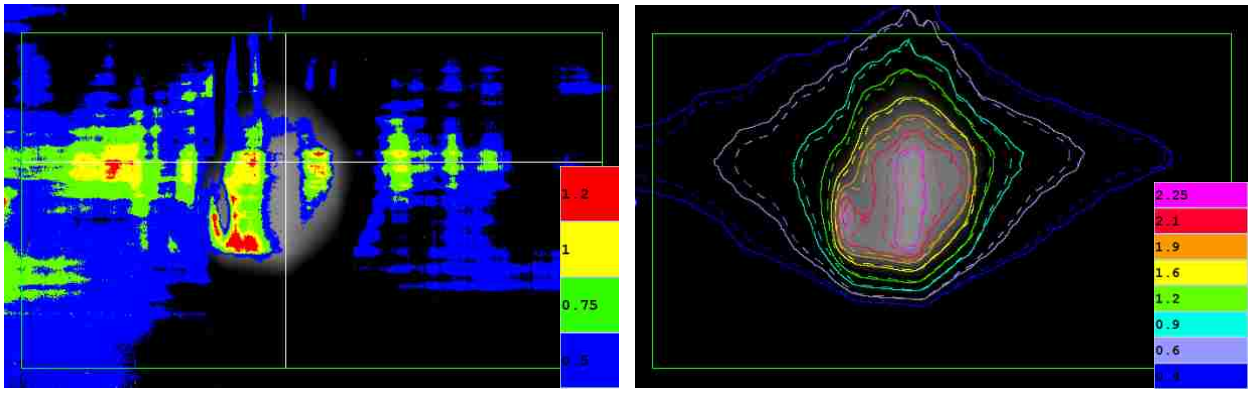

(a) (b)

Figure C7. (a) Gamma display and (b) isodose distribution of a film (solid) vs. reconstructed (dashed) dose from the lung plan delivery with +30 msec center leaf offset (6/3/08)

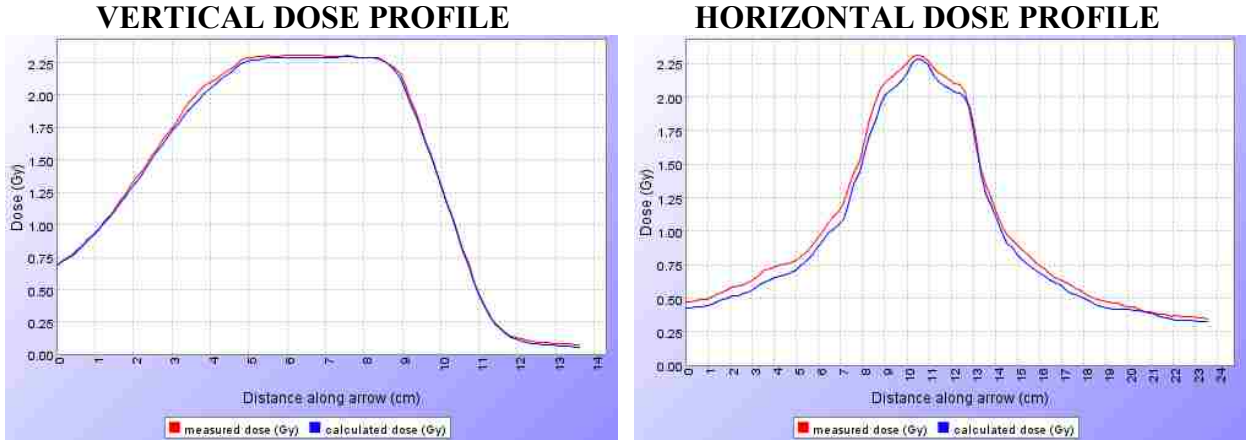

Figure C8. Dose profile of the film (red) and reconstructed (blue) in reference to the white crosshair in Figure C7a

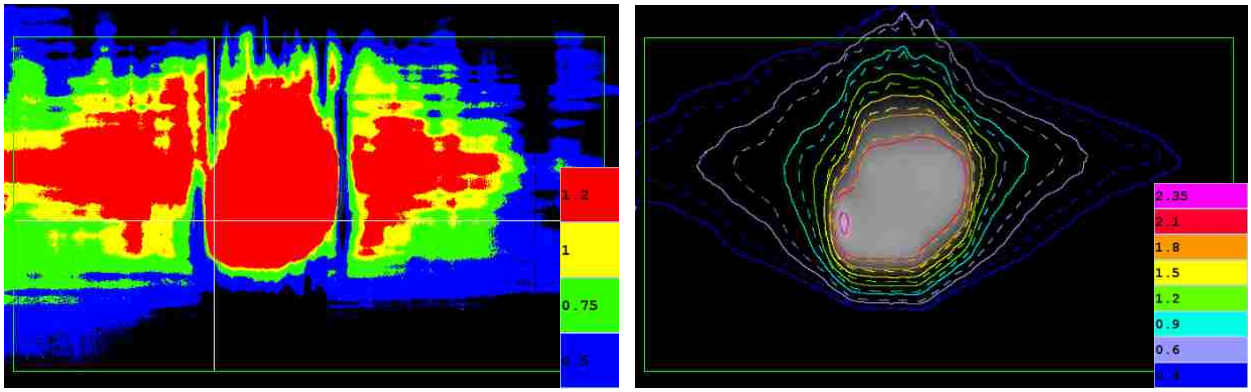

(a) **(b)**

Figure C9. (a) Gamma display and (b) isodose distribution of a film (solid) vs. planned (dashed) dose from the lung plan delivery with +30 msec all leaves offset (5/30/08)

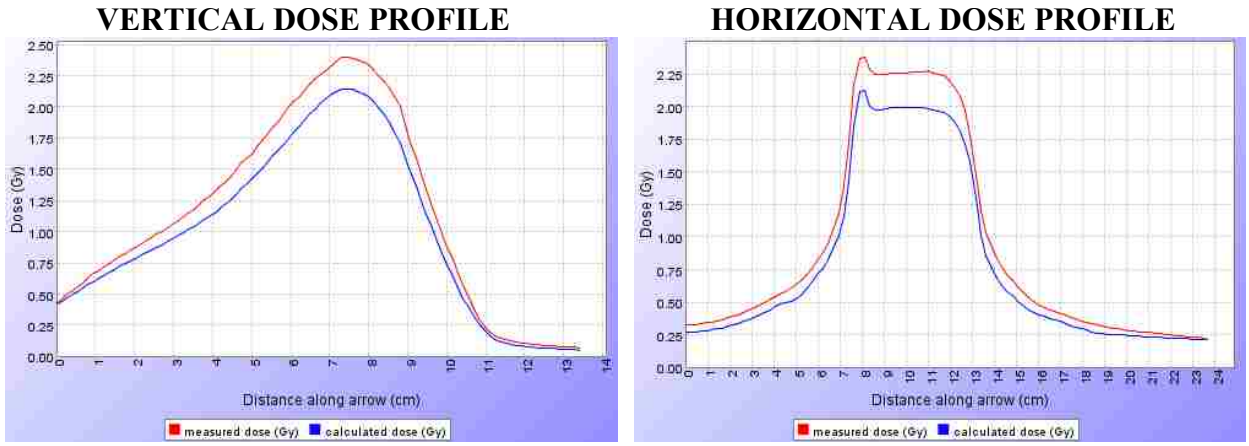

Figure C10. Dose profile of the film (red) and planned (blue) in reference to the white crosshair in Figure C9a

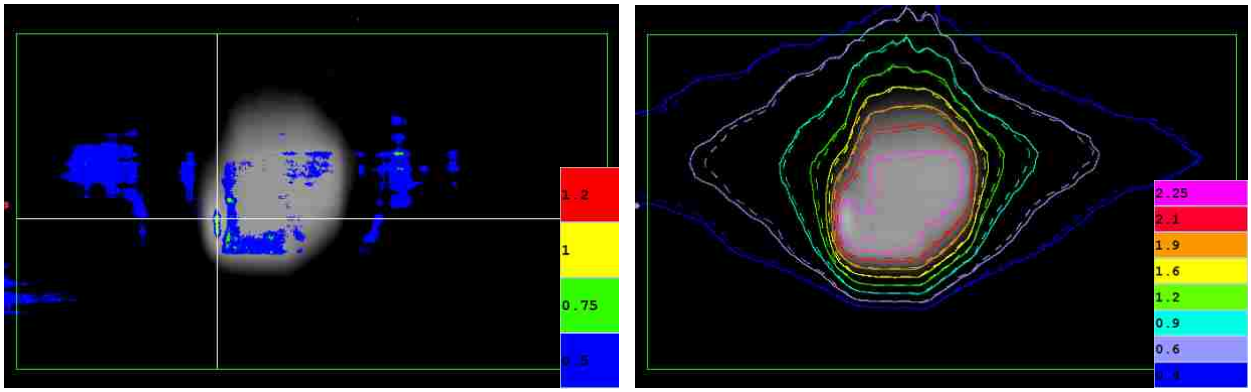

(a) **(b)**

Figure C11. (a) Gamma display and (b) isodose distribution of a film (solid) vs. reconstructed (dashed) dose from the lung plan delivery with +30 msec center leaf offset (6/3/08)

VERTICAL DOSE PROFILE **HORIZONTAL DOSE PROFILE**

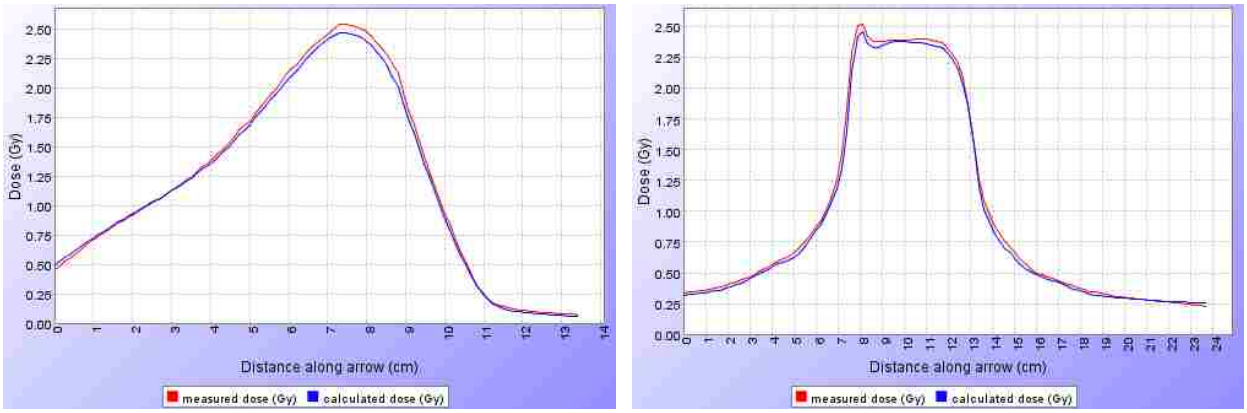

Figure C12. Dose profile of the film (red) and reconstructed (blue) in reference to the white crosshair in Figure C11a

VITA

Ricky Hesston was born as Vu Hong Ky in Saigon, Vietnam, in July 1976, the son of Maurice and Diana Hesston. His family came to the United States in 1979 and grew up in Los Angeles, California, where he completed high school at Grover Cleveland High in 1994. He received his Bachelor of Science with a major in physics and minor in mathematics from Indiana University of Bloomington in May of 1999. In January of 2006, he entered Louisiana State University graduate school and obtained a Master of Science degree in 2009 for medical physics and health physics.